Cranfield University

Cranfield Health

Academic year 2009

Ph.D thesis Henri Knobloch

Serum and urine headspace analysis using electronic nose (e-nose) technology

Supervisor: Dr Claire Turner

Date of presentation: 2nd October 2009

This thesis is submitted in partial fulfilment of the requirements for the degree of a Ph.D.

Abstract

For the last 20 years, several applications of electronic nose (e-nose) have been reported in the area of microbiology, environmental and agricultural monitoring or medical diagnosis. E-noses were used to detect contaminants or for quality control. However, little has been reported about complex methodological problems which are strongly linked to the e-nose performance.

This thesis summarises various e-nose systems and alternatives for gas and headspace analysis, highlights the essential problems associated with e-nose analysis and explains why these devices have a potential for the detection of trace gas molecules but also why a stable and reliable analysis is not possible yet. Methodological weaknesses such as changes in mass flow rates, filter application or sampling methods are addressed. Understanding these enables analysis of serum and urine samples from cattle or badgers either naturally or experimentally infected with the zoonotic diseases caused by *Mycoplasma bovis*, *Mannheimia haemolytica* A1, *Mycobacterium bovis*, *Mycobacterium avium* ssp. *paraTuberculosis* and *Brucella* sp. The circumstances under which meaningful results can be obtained using the ST214 e-nose (Scensive Tech. Ltd., UK) are assessed which show the current limitations for discriminating between samples. Alternative methods for analysing e-nose data are mentioned and reasons are given why under the stated circumstances no straightforward multivariate statistics is possible. However, despite various difficulties, meaningful results at a group level were obtained and could be correlated with other results obtained using alternative analytical methods. This indicates the positive proof-of-principle character of this project.

Acknowledgements

At this point I would like to take the opportunity to acknowledge some persons which have been very important during my Ph.D studentship.

First of all, I would like to thank Mark Chambers and the UK Department for Environment, Food and Rural Affairs (DEFRA) for funding this project (project number SE3221). Even if not all things went as planned before, Mark finished managing this project in a smooth but professional way and never lost key objectives out of his sight. I really appreciated his way of project managing.

Furthermore, I like to thank Heike Köhler and Petra Reinhold from the Institute of Molecular Pathogenesis at the 'Friedrich-Loeffler-Institut' (FLI, Jena, Germany). Both provided a countless number of samples and therefore significantly contributed to the comprehensiveness and validation this Ph.D project. Their personality and scientific competence made the collaboration with the FLI much easier and much more enjoyable.

Beyond that, I really like to thank Claire Turner. I appreciated her 'drys': Preferences for 'dry' wine, preferences for a 'dry' sarcastic type of humour and also her 'dry' scientific perspective focussing on facts and analysing the situation to make a clear and well-thought decision. I learned a lot from her.

Last but not least I like to thank Rosanna Picca for having the opportunity to discuss perspectives, scientific and private ones. Even if we didn't always agree in some topics it was a pleasure sharing opinions.

I gratefully acknowledge Sebastian Hoelters (aka Jean Luc Picard) who gave, pretty much in a captain's manner, guidance in difficult situations. It is an honour still to have him a best friend after a longer time abroad. May be some years still to come!

Finally, I like to thank my parents, my sister and my grandma for supporting me over the last 3 years and for believing in my abilities.

List of contents

Abstract 1

Acknowledgements 2

List of contents 3

List of figures 6

Notations 10

Evaluation of a combination of SIFT-MS and multivariate data analysis for the diagnosis of Mycobacterium bovis in wild badgers. Analyst 134(9), 1922-1927 10

1. Introduction 11

1.1 Biological principles of olfaction – the human nose 14

1.2 Mechanical principles of olfaction – the e-nose 17

1.3 Physical basis of headspace measurement 19

1.4 Types and principles of electronic noses 21
1.4.1 Optical sensors 21
1.4.2 Thermal sensors 23
1.4.3 Chemiresistive sensors 24
(I) Conducting polymer sensors 24
(II) Metal oxide semiconducting (MOS) sensors 28
(III) Conducting polymer e-nose applications 29
1.4.4 Metal oxide field effect transistors (MOSFET) as sensors 29
1.4.5 Amperometric sensors 31
1.4.6 Gravimetric sensor systems 32

1.5. Mass spectrometric methods 36
1.5.1 SIFT- MS principles and applications 36
(I) SIFT- MS principles 36
(II) Application of SIFT-MS techniques 42
1.5.2 Gas chromatographic mass spectrometry (GC-MS) 43
(I) GC-MS principles 44
(II) Problems of GC-MS and sampling systems 45

1.6 Bacteria and infections 47
1.6.1 Mycoplasma bovis 48
1.6.2 Mannheimia haemolytica (Man.haem) 49
1.6.3 Mycobacterium bovis 50
(I) Introduction and impact on the world health status 50
(II) General description and classification 51
(III) Mycobacterium bovis 52
(IV) Special biochemical features and cell wall attributes 53
(V) Detection methods for Mycobacterium bovis and tuberculosis 55
1.6.4 Mycobacterium avium ssp. paratuberculosis (MAP) 59
1.6.5 Brucella ssp. 61

2. Animals, materials and methods 62

2.1 Methodological aspects of e-nose analysis 65
2.1.1 Sampling methods and mass flows 65
2.1.2 Different filters and mass flows using static sampling 67
2.1.3 Conducting polymer e-nose characterisation 68

2.2 Apparatus and applied sampling procedures *68*
2.2.1 CP e-noses application 69
2.2.2 SIFT-MS 70

2.3 Animals, housing, health and savety *71*

2.4 Study designs and experimental challenges *73*
2.4.1 Biological variability of serum samples obtained from healthy cattle 73
(I) Changes in serum samples due to growth or ageing and nutrition 73
(II) Changes in serum samples due to circadian and day to day variability 73
2.4.2 Biological variability of urine samples obtained from healthy cattle 74
2.4.3 Variability of serum samples after Mycoplasma bovis infection 74
2.4.4 Variability of serum samples after Mannheimia heamolytica infection 76
(I) Study design and sample collection 76
(II) Analyses of acute phase proteins (APP) 77
2.4.5 Variability of serum samples from Mycobacterium bovis infected cattle 77
2.4.6 Variability of urine samples from Mycobacerium bovis infected cattle 79

2.5 Samples obtained from naturally infected individuals *80*
2.5.1 Variability of healthy and paraTuberculosis infected serum samples 80
2.5.2 Variability of healthy and Brucella infected serum samples 81
2.5.3 Variability of healthy and Mycobacterium bovis infected serum samples from badgers 81
2.5.4 Variability of healthy and paraTuberculosis infected urine samples 82
2.5.5 Comparison of serum and urine samples 82

2.6 Serum and urine collection and preparation *83*

2.7 Data analysis *84*

3. Results **89**

3.1 Methodological aspects of e-nose analysis *89*
3.1.1 Sampling methods and mass flows 89
3.1.2 Different filters and mass flow rates using static sampling 90
3.1.3 Conducting polymer e-nose characterisation 93

3.2 Healthy and experimentally challenged individuals *96*
3.2.1 Biological variability of serum samples obtained from healthy cattle 96
(I) Changes in serum samples due to growth and nutrition 96
(II) Changes in serum samples due to circadian and day to day variability 100
3.2.2 Biological variability of urine samples obtained from healthy cattle 102
3.2.3 Variability of serum samples after Mycoplasma bovis infection 105
3.2.4 Variability of serum samples after Mannheimia heamolytica infection 107
(I) Analyses of e-nose responses 108
(II) Analyses of acute phase proteins (APP) 110
(III) Correlations between e-nose and clinical results 112
3.2.5 Variability of serum samples from Mycobacterium bovis infected cattle 114
3.2.6 Variability of urine samples from Mycobacerium bovis infected cattle 120

3.3 Naturally infected individuals *124*
3.3.1 Variability of healthy- and paraTuberculosis infected serum samples 124
3.3.2 Variability of healthy and Brucella infected serum samples 125
3.3.3 Variability of healthy and Mycobacterium bovis infected serum samples from badgers 127
3.3.4 Variability of urine samples from healthy and paraTuberculosis infected cattle 131
3.3.5 Comparison of serum and urine samples 133
(I) Comparison of experimentally obtained serum samples 133
(II) Comparison of samples obtained from naturally infected individuals 134
(III) Comparison of experimentally and naturally obtained serum samples 136
(IV) Comparison of experimentally and naturally obtained urine samples 142

4. Discussion **144**

4.1 Methodological aspects of e-nose analysis *144*
4.1.1 Sampling methods and mass flows 144
4.1.2 Different filters and mass flow rates using static sampling 145
4.1.3 CP e-nose characterisation 146

4.2 Healthy and experimentally challenged individuals *147*
4.2.1 Biological variability of serum samples obtained from healthy cattle 147
(I) Changes in serum samples due to growth and nutrition 147
(II) Changes in serum samples due to circadian and day to day variability 149
4.2.2 Biological variability of urine samples obtained from healthy cattle 150
4.2.3 Variability of serum samples after Mycoplasma bovis infection 152
4.2.4 Variability of serum samples after Mannheimia heamolytica infection 154
4.2.5 Variability of serum samples from Mycobacterium bovis infected cattle 157
4.2.6 Variability of urine samples from Mycobacerium bovis infected cattle 160

4.3 Naturally infected individuals *162*
4.3.1 Variability of healthy- and paraTuberculosis infected serum samples 162
4.3.2 Variability of healthy and Brucella infected serum samples 163
4.3.3 Variability of healthy and Mycobacterium bovis infected serum samples from badgers 164
4.3.4 Variability of healthy and paraTuberculosis infected urine samples 165
4.3.5 Comparison of serum and urine samples 166
(I) Comparison of experimentally obtained serum samples 166
(II) Comparison of samples obtained from naturally infected individuals 167
(III) Comparison of experimentally and naturally obtained serum samples 168
(IV) Comparison of experimentally and naturally obtained urine samples 169

4.6 Statistical analysis *171*

5. Conclusion & future work **174**

Methodological *174*

Biological *175*

Appendices **195**

Uni and multivariate Data analysis *195*
Section A 196
Section B 202

Papers published as a first author *208*

List of figures

Figure 1: Illustration of the olfactory mucosa, the olfactory neurons and the glumeruli-, mitral and granular layers which are the most important location for signal pre- processing [1].

Figure 2: Illustration of the signal separation. Similar molecules have similar retention times in the olfactory epithelium OE (temporal separation in the mucosal layer). Further separation is achieved by for the same type of molecules addressing the same glumeruli receptors in the olfactory bulb (OB). Different glomeruli are spatial separated in the OB. The complex signal is simplified [4].

Figure 3: Overview of the basic types of vapour sensing systems; electronic noses [12].

Figure 4: Polymers and solvatochromic dyes are fixed on a distal dip of an optical fibre. The change in fluorescence indicates the kind of molecules that is bound [18].

Figure 5: Cross section of a silicon based planar pellistor. The complex, nanostuctured design explains its expensive production [23].

Figure 6: Results of the oxidative- (left) and the reductive electrochemical polymerisation method (right). A dopant is also attached to the polymer and bound via ionic forces (centre of positive charge in the monomer ring- and an anion as a dopant, grey arrow) [25].

Figure 7: Schematic configuration of a metal oxide sensor including DRAIN, SOURCE and GATE electrodes. Depending on the analyte adsorbed on the sensitive layer, the potential difference changes and influences the current that is measured [12].

Figure 8: a) In the so-called dynamic mode the absorbance of the analyte causes a change of the resonance frequency. b) In the static mode, the weight of the adsorbed analytes cause mechanical surface stress and bend the cantilever. The change in bending is measured with a laser [51].

Figure 9: Section of the SIFT-MS. Precursor ions ionise molecules from a sample, introduced into the flow tube via a capillary, and generate product ions. Precursor ions can be selected by the upstream quadrupole mass spectrometer and product ions are measured with an ion detector [54].

Figure 10: SIFT-MS spectrum of laboratory air. Volatile compounds are measured in the full scan mode (FSM). The intensity or count rate in counts per second [c/s] is plotted against the mass/ charge ratio [54].

Figure 11: Compound/ product ion concentrations of a breath sample in ppb in the course of time in s. You can easily see the breathing pattern (increased compound concentration during expiration phase [54]).

Figure 12: The structure of the β-hydroxy-α-alkyl branched structures of high molecular weight mycolic acid was elucidated by Asselineau in 1950 (left). The general structure of PIMs are shown on the right; X= 0,1,2,3,4; for PIM2, PIM3, PIM4, PIM5, PIM6, respectively; R' and R''= acyl fatty acids [111].

Figure 13: Figure 5 shows the schematic composition of the mycobacterium's cell wall containing the standard gram positive wall and an additional waxy layer made of mycolic acid [112].

Figure 14: Dynamic (left) and static sampling (right) for e-nose analysis. An incoming air stream (1) causes a pressure difference and a variable flow of headspace reaching the e-nose while for static sampling there is a constant pressure and an equilibrium.

Figure 15: Replicates over all sensors using no filter, a 0.45 µm – and a 0.20 µm filter. Divergences decreased with the pore size of the filter indicating quantitative changes due to filter application.

Figure 16: Normalised sensor responses using no filter, a 0.45 µm – and a 0.20 µm filter. Setting "no filter" as a reference, changes in the relative distribution of sensors were observed.

Figure 17: Principle component analysis of ROW- and 2% (v/v) 2-butanol samples. ROW and 2-butanol samples could be discriminated using no filter (1/2) while applying a 0.45 µm filter both substances appeared the same (3/4). Cluster 5 shows the 2-butanol sample using the 0.20 µm filter.

Figure 18: Principle component analysis of e-nose data. Clear discrimination was found between both ST214 CP e-noses covering most of the variance (84%). The remaining variation (15%) was due to changes in sensors responses over time analysing the same sample. Numbers next to data points indicate the time point.

Figure 19: Responses of all 13 sensors over 4 time points. Divergences at time points 1 were largest and decreased at time point 2. At time points 3 and 4 sensor responses in- and decreased again. There was a declining tendency over all 4 time points.

Figure 20: Sensor responses for sensor 6 over all analysis displayed in a sequence. There was a clear difference between day 1 (analyses 1 to 30) and day 2 (31 to 60). Divergences decreased for day 1 while they remained constant for day 2.

Figure 21: Raw divergences (left) and ID averaged divergences (right) for sensor 3. Responses remained at one level until time point 7, decreased significantly and reached a lower level beginning from time point 15. Between time points 8 and 14 there was variation and this is circled on the graph.

Figure 22: Raw divergences (left) and ID averaged divergences (right) for sensor 3. Responses remained at one level until time point 7, decreased significantly and reached a lower level beginning from time point 15. Between time points 8 and 14 there was variation

Figure 23: Divergences of sensors 8 (left) and 3 (right) over time. There was a general increase in sensor responses over time when exposed to serum headspace from all subjects. A decrease was observed at 10:00 am and 16:00 pm after feeding.

Figure 24: Adult cattle (2) had less negative divergence in comparison to juvenile cattle (1) for sensors 8 (left) using SPSS. Summarising and mean-centring all responses, less negative sensors responses for adult cattle (red) were observed considering MEDIAN (right; Matlab heatmaps).

Figure 25: A significant decline after feeding in the morning was observed for sensors 2 to 8, 12 and 13. Similar tendencies were observed also for sensors 9 to 11 indicated as green and blues sections on the heatmap after feeding in the afternoon.

Figure 26: Divergences of sensors 9 (left, placebo treated) and 8 (right, infected with *Mycoplasma bovis*) over the course of the study. Responses were significantly different from the baseline (red) at the end of the study.

Figure 27: Divergences of sensor 3 over the course of the study. The temporal profile indicated an overall increase over time and identified responses 48 and 3 days post inoculation as the lowest.

Figure 28: Averaged and autoscaled divergences for all experimental days, 7 days before infection (-7) to 5 days after infection (5). Clear discrimination was found for days 2 and 3 indicating the biggest changes in divergence.

Figure 29: Concentrations of lipopolysaccharide binding protein (LBP) in serum samples collected before and after an experimentally induced infection with *Mannheimia haemolytica A1* in calves. After infection, the highest concentrations of acute phase proteins were measured 24 hours p.i. for LBP.

Figure 30: Divergences of sensor 5 over time (left). Lowest divergences were obtained at time point 4 (1 = before infection, 2-4 = after infection) indicated at "a" which remaining time points had significantly higher medians ("b") as also illustrated by the mean-centred medians heatmap (right).

Figure 31: Divergences of sensor 12 (left) and for all sensors over all time points (1 = before infection, 2-4 = after infection). A significant difference was found at time point 3. Similar increases without significant relevance were also found for sensors 8 to 10 and 13.

Figure 32: Divergences for sensor 10 (left) and median divergences for all sensors over time points 1 to 4 (tp, right). Significantly elevated responses were found 4 weeks post infection.

Figure 33: Divergences for sensor 11 (left) and the medians for all sensors (right). Group 4 was found to have the highest divergences while group 2 had lowest divergences (group 1 = before infection, groups 2-4 = after infection with no vaccination, BCG vaccination and Ad85a vaccination, respectively).

Figure 34: Optical densities (OD) at 450nm wavelength measured for all subjects and displayed as averages. The unvaccinated control group had a significantly higher γ-interferon concentration at experimental week 18 (time point 4) compared to both, the BCG- and BCG/Ad85a vaccinated group.

Figure 35: Divergences of sensors 9 (left) and median divergences for all sensors as a heatmap (right). Lowest divergences were found for non-vaccinated at time point 1 while highest responses were observed at time point 3 (light grey/ a = non-vaccinated, dark grey/ b = BCG vaccinated, left; dark blue and green-yellow, right).

Figure 36: Responses of sensors 9 (left) and 10 (right) averaged at time points 1 and 2 (pre-infection) and time point 4. The averaged responses are split up into vaccinated and non-vaccinated. Responses for pre-infection and vaccinated sample at time point 4 are at a similar level while

Figure 37: Divergence of sensor 9 over infection groups (left) and 4 over clinical groups (right). Responses decreased from non-infected to infected. Samples with no clinical symptoms had higher divergences than those with latent or clinically evident symptoms.

Figure 38: Divergences of sensors 4 (left) and 13 (right). Responses increased from non-infected to infected.

Figure 39: Clustering of values of naturally infected badger sera. Three clusters were found representing data from 05.01.07 (A), 17.01.07 (B) and all remaining data (C). The day of analysis covered more 95.34% of all variance represented by principle components 1 and 2. Single data points represent variance of a sample in comparison to other samples.

Figure 40: PCA on serum sample analysed 2006. No discrimination was found between naturally infected (A) and uninfected samples (B). Scattering of data was due to methodological factors and covered 91.41% of all variance. Single data points represent variance of a sample in comparison to other samples.

Figure 41: PCA on naturally infected serum samples. A systematic change in the distribution of the values was found. Starting on the left hand side, the values shifted over the course of time to the lower right corner and finally to the upper right corner.

Figure 42: Divergences of sensors 9 (left) and 11 (right) over the infection status. Responses became significantly lower comparing samples from paraTB non-infected and infected individuals.

Figure 43: Divergences of sensors 9 (left) and 11 (right). Samples from farms 1 and 2 had a paraTB positive status while from farm 3 samples were paraTB negative. The negatives had a significantly higher sensor response than positives from all locations.

Figure 44: Divergence of sensor 3 (left) and mean-centred medians for all groups over sensors (right). Sensors 2 to 5 were found to group samples from healthy individuals as one and samples from experimentally infected animals as another group. All negative samples are represented by groups 1, 2 and 4.

Figure 45: Divergence of sensor 5 (left) and mean-centred medians for all groups and all sensors (right). ParaTB and brucella negatives were grouped the same or similar while paraTB positives were below- and brucella positives above the negatives' level of responses.

Figure 46: Averaged and auto-scaled divergences analysing serum headspace (paraTB negatives (1), positives (2) Brucella negatives (3) and positives (4)). Non-diseased data clustered in the middle (1, 3) while the cluster for the paraTB positives (2) data located on the left and the Brucella positives were located on the right.

Figure 47: Divergence of sensor 3 (left) and mean-centred medians for all groups and all sensors (right), including the highlighted responses of sensor 3. Responses of groups 3 and 5 were lower comparing the experimental data only. Groups 6 and 8 are close to each other while group 7 is below and group 9 is above.

Figure 48: Mean-centred medians for all groups and all sensors. Grey covered areas represent sensors which do not show changes in divergence form non-infected to infected for the same disease. Different diseases can develop a different pattern as indicated here for two experimentally and two naturally infected cattle groups. The dashed area indicates a sensors which grouped all healthy individuals the same.

Figure 49: Divergence of sensor 3 (left) and mean-centred medians for all groups over sensors (right, 1= infected, 2= non-infected), Almost all sensors showed differences between infected (lower divergence, dark grey) and non-infected samples (upper group, dark grey, grey) independently to the origin of the sample or the way the samples were obtained.

Notations

Some results from this Ph.D thesis have been published in papers as listed below or displayed on posters at several conferences.

Main papers were:

Knobloch, H., Turner, C., Spooner, A., Chambers, M.A., (2009). Methodological variation in headspace analysis of liquid samples using electronic nose. Sensors and Actuators B-Chemical 139, 353-360.

Knobloch, H., Schroedl, W., Turner, C., Chambers, M.A., Reinhold, P., (2009). Electronic nose responses and acute phase proteins correlate in blood using a bovine. Sensors and Actuators B-Chemical [~~in submission progress~~accepted 12.10.2009].

Comment [J1]: paper angeben

Spooner AD, Bessant C, Turner C, Knobloch H, Chambers M (2009). Evaluation of a combination of SIFT-MS and multivariate data analysis for the diagnosis of Mycobacterium bovis in wild badgers. Analyst 134(9), 1922-1927

1. Introduction

From the past, it is well known that a number of infectious or metabolic processes liberate specific odours characteristic of a disease. This indicates that there are significant relationships between diseases and alterations of the airborne chemicals emitted from the body. Based on this ancient knowledge, the diagnosis of infectious diseases due to an altered profile of volatile organic compounds (VOCs) is a new area of clinical biochemistry and can therefore be used for the early detection of infectious diseases in both veterinary and human medicine analysing readily collectable samples (i.e. blood, urine, exhaled breath, swabs).

One possible method of VOC analysis is the use of so-called electronic noses (e-noses). They have been used already for the last two decades to analyse gases in automotive-, environmental and medical areas. However, it remains entirely unclear if e-noses are suitable for analysis of clinical sample headspace for field detection of infections or diseases. This is of high relevance, since e-nose offers a great potential of inexpensive and rapid analysis of gaseous mixtures. Furthermore, e-noses are often very small and therefore, portable. This is particularly important when analysis has to be carried out in the field and not in laboratories for instance in veterinary medicine when field detection of diseases is required. Often the animals cannot be brought to a clinic or the number of animals is just too large for laboratory analysis. In these cases, an e-nose screening test system would be desirable which analyses the headspace of biological samples (e.g. serum or urine) or breath immediately. However, in order to show the e-nose potential

for reliable field detection, factors affecting its output (methodological and biological) need to be assessed.

Methodological variation is the statistical variation which occurs due to systemic errors of the measurement system. In this case, it describes all variation which is caused by the sampling collection (e.g. type of collection, collection time and day) and during analysis (environmental temperature, analysis time and day, desorption on sensor surfaces).

Biological variation is caused by differences between individuals (e.g. different physiologay between individuals, gender, feeding) or changes in VOC composition due to diseases. Only if there is variation due to the disease which is independent from all other variation e-nose can potentially be used as a VOC field detection system. For these reasons, methodological and biological variation was assessed, analysing serum and urine samples from different experimentally- and naturally diseased cattle and control (non-diseased) animals. Both types of variation give an indication if this particular e-nose or e-noses in general can be used for field detection. In addition, gas chromatography mass spectrometry (GC-MS) and Selected Ion Flow Tube mass spectrometry (SIFT-MS) was used in parallel to validate e-nose analysis and to elucidate potential biological markers ('biomarkers') which are specific for certain diseases.

On the following pages, the basics of olfaction, the physical processes behind headspacing and e-nose as well as SIFT-MS and GC-MS techniques and analysis are reviewed to give a better understanding of the studies conducted. Approaches regarding statistical analysis of e-nose sensor array data were undertaken and a Matlab script was developed.

This project was funded by the Department for Environment, Food and Rural Affairs (DEFRA) with the project number SE3221 and under the management of Dr. Mark Chambers from the Veterinary Laboratories Agency, (VLA, Weybridge). Dr. Claire Turner supervised the work of this Ph.D project which was initially to investigate the potential of e-noses to detect tuberculosis and *Mycobacterium bovis* in serum samples from cattle and badger and to elucidate potential biomarkers for tuberculosis infected animals using SIFT-MS. It is a follow-up project also to validate and repeat the results obtained in the past by the VLA and Reinard Fend (Cranfield University) which led to publications in 2005. Due to difficulties in sample acquisition according to the outbreak of food and mouth disease and sample management, additional serum and urine samples from cattle and calves infected with various diseases were provided by the Dr. Petra Reinhold and Dr. Heike Köhler from the 'Friedrich-Loeffler-Institut' (FLI, Jena, Germany) because the number of samples were not sufficient to carry out reliable headspace and data analysis. Accordingly, the topic of this project was changed towards the evaluation of the potential of e-noses to detect and differentiate between different diseases in naturally and experimentally infected subjects and to compare their e-nose headspace results with those from non-diseased samples obtained from badgers and cattle using the ST214 Bloodhound e-nose. Due to the complex and time consuming character of the studies, this Ph.D dealt with the sampling, headspacing, e-nose and SIFT sample analysis and e-nose data analysis, only. The multi-variate statistical analysis of SIFT-MS data was the subject of a separate Ph.D studentship funded by the same project. The elucidation of biomarkers

of a tuberculosis infection was not possible anymore using just e-nose technology and a minimum of samples for analysis. It finally became to a prove-of-principle study for headspace analysis usable for disease detection.

1.1 Biological principles of olfaction – the human nose

The process of smelling different odours in humans and animals has not yet been fully understood. Basically, the olfactory system consists of an olfactory mucosa, the main olfactory bulb and the olfactory cortex. The olfactory mucosa delivers the odour with the inhaled air stream through the anterior nares. Afterwards the odour molecules diffuse through a layer of mucus and bind onto the chemically sensitive layer of the receptor cells.

Molecules with different physical and chemical properties are distributed in different spatiotemporal patterns across the receptor cell sheet similar to the principle of chromatography. The receptor sheet contains receptor cells responsible for the main chemical stimuli (figure 1). After the separation and binding of odour molecules to the receptor cells which are a part of bipolar neurons projecting an axon to the olfactory bulb, the neurons are depolarised differentially according to the attributes of the molecules. A cascade of signal transduction (via G-proteins) events leads to an increase of membrane conductance and an electric signal or action potential is conveyed to the olfactory bulb [1, 2]

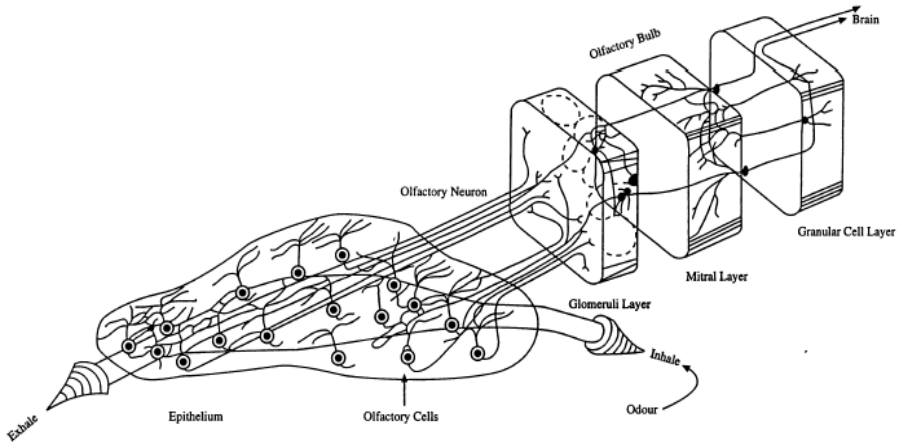

Figure 1: Illustration of the olfactory mucosa, the olfactory neurons and the glumeruli-, mitral and granular layers which are the most important location for signal pre- processing [1].

However, studies suggested that single receptor cells are not highly specific but each receptor responds to a variety of different molecules, especially to their functional groups. This selective and relatively non-specific response seems to be a characteristic feature of olfactory receptors resulting in overlapping receptor responses and the generation of a distinguishable and predictive pattern. This composition of many responses according to the stereochemical attributes of odour compounds determines the molecular deceptive range of smelling [3–6].

However, each olfactory neuron conveys only the signal of one receptor subtype. Similar subtypes of receptors converge to the same axon in the glumeruli layer acting as an “address” [6]. In other words, beside a temporal limitation of the odour generated impulse (retention of molecules in the mucosal layer) there is also a spatial limitation at the glumeruli layer (figure 2). These two processes transform and “simplify” the electrical signal to a smaller

and more specific second order signal that represents a molecular image of the olfactory stimulus [4, 7, 8].

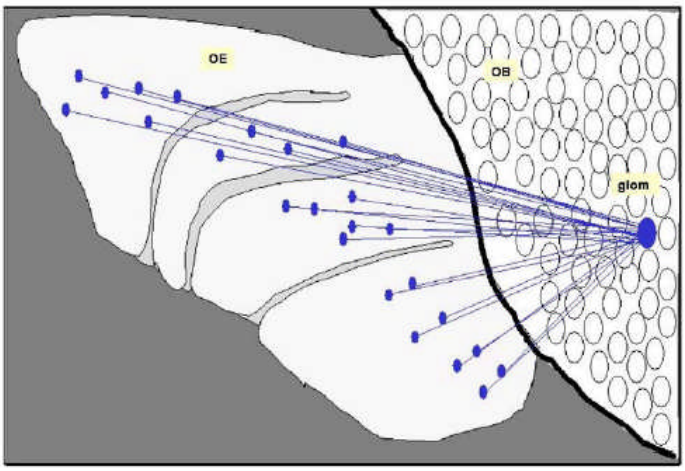

Figure 2: Illustration of the signal separation. Similar molecules have similar retention times in the olfactory epithelium OE (temporal separation in the mucosal layer). Further separation is achieved by for the same type of molecules addressing the same glumeruli receptors in the olfactory bulb (OB). These are linked to the same axons. The complex signal is simplified by a temporal and a spacial separation [4].

This signal is finally transmitted to the periform cortex via the central nerve system where the last stages of processing, the mediation of olfactory memories or “pattern recognition”, takes place [1]. The pattern is the combination of the strength, duration, and quality of the odorant stimuli that are encoded into neuronal signals [4] and is matched to a visual image of what the subject smells.

1.2 Mechanical principles of olfaction – the e-nose

For more than 20 years e-noses have been developed and commercially distributed. The idea behind e-noses is to mimic the human olfactory system (section 1.1) by artificially building and implementing the essential steps contributing to the human odour sensing. The mammalian olfaction system consists of three main subsystems: the olfaction mucosa associated with the odour delivery system, the main olfactory bulb and the olfactory cortex. In an electronic nose there is a similar arrangement. It consists of a sample delivery system (including sample collection, preconditioning and filtration), an array of gas sensors that shows different sensitivities to different classes of compounds (adsorption, signal generation, desorption), a signal collecting unit and pattern recognition software (image recognition, gauging and presentation of the results) [1, 9]. Since odours are often a complex mixture of gaseous compounds, e-noses usually only allow a qualitative analysis of a multi-component matrix [9, 10]. For compound identification, gas chromatography mass- spectrometry (GC-MS) is needed. Later, certain patterns can be associated with certain compounds which may be present in particular concentrations. Since the sensors are unspecific and react to the attributes of the odour compounds, the responses are not quantitative. This partial selectivity is turned into an advantage by detecting overlapping signals, termed virtual fingerprints or multidimensional patterns. In other words, the unavoidable cross sensitivity is exploited by generating these so-called fingerprints [9-11]. There are a lot of different sensing systems which are not understood in detail [10]. Figure 3 summarises the existing systems, which can be classified as optical-, thermal-, electro-chemical- and gravimetric

systems. In the following sections (sections 2.4 and subsections), the basics of the subtypes will be summarised with a focus on conducting polymer based systems used in this project.

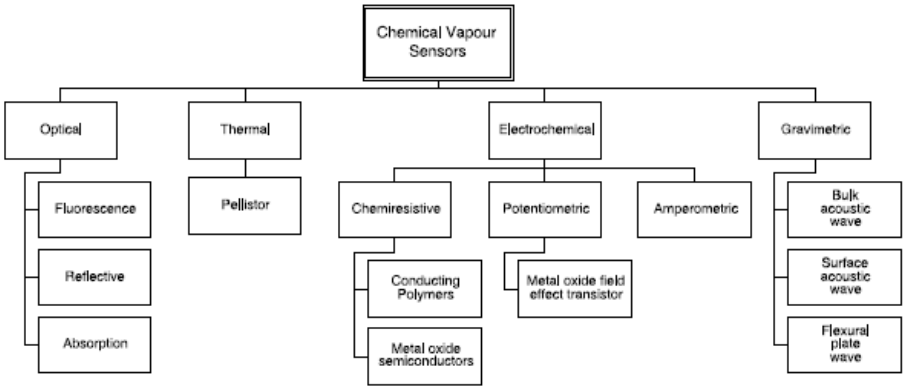

Figure 3: Overview of the basic types of vapour sensing systems; electronic noses [12].

Generally, molecules in the gas phase bind to a sensitive surface by using adsorption, absorption, chemisorption and co-ordination chemistry. As a result, the physical or chemical properties, like wavelength, temperature, conductance or frequency, change. The way of adsorbing the molecule on the sensitive layer determines the strength of binding. A weaker adsorption leads to a better reversibility but, at the same time to a poorer selectivity. Ideally, the sensor should be very reversible and sensitive. During the last few years, e-noses with more than one sensor type have been developed in order to improve discrimination by introducing an additional sensing principle generating another fingerprint based on the changes of different physical properties [12].

Other methods for determining odours like GC-MS, nuclear magnetic resonance (NMR) or infra red (IR) spectroscopy are expensive, non-portable and require trained personnel. The alternative method of panel testing requires trained personnel as well and is not objective. In contrast, e-nose is portable, inexpensive and does not need much operator training. On-line or offsite measurements are possible and the measurement process is less time consuming than most other analytical methods [12, 13]. However, most applications of e-nose are still inferior in performance in comparison to established instruments of analytical chemistry like GC-MS. The main problems are that the individual sensors usually show drift, are not very sensitive, detect only certain classes of molecules and are non-specific, as mentioned above [14].

1.3 Physical basis of headspace measurement

For the measurement of a certain compound in the headspace of a sample, the distribution between the compound in the aqueous- and its vapour in the gaseous phase has to be considered. This relationship is described by Henry's law. The law describes the solubility of a gas in water or its ability to leave the aqueous phase and to establish equilibrium (equation. 1) [15, 16].

Henry's law: $$k_H = \frac{c_a}{p_g} \qquad (1)$$

Where k_H is the Henry constant [mol/L*atm], c_a [mol/L], the gas concentration in the aqueous phase, and p_g [atm] refers to its partial pressure in the

atmosphere over the sample, respectively. Hence, Henry's law constant is a ratio between the distribution of a compound in the liquid and gaseous phases. The equilibrium is strongly influenced by the temperature and a change of just a few degrees can significantly change the concentrations in the phases by changing the compound's solubility and volatility, respectively. That is why the law has to be modified and a temperature dependent Henry's constant appears $k_H(\vartheta)$ (equation 2).

Henry's law (ϑ): $$k_H(\vartheta) = \frac{c_a}{c_g} = k_H \times R \times T \qquad (2)$$

R is the universal gas constant (R = 8.314 J * K^{-1} * mol^{-1}) and T is the temperature in Kelvin. Apart from temperature the standard enthalpy (ΔH) for the compound and the chemical structure determine the Henry coefficient for a particular compound. Henry's law can therefore be described as follows (equation 3) [15, 16].

Henry's law ($\vartheta, \Delta H$): $$k_H(\vartheta, \Delta H) = k_H^0 \times \exp\left(\frac{-\Delta H}{R}\left(\frac{1}{T} - \frac{1}{T^0}\right)\right) \qquad (3)$$

Since k_H^0 is the compound dependent constant that describes the Henry's law under standard conditions at 25°C (298.15 K) $k_H(\vartheta, \Delta H)$ gives the temperature and enthalpy corrected value. Standard Henry coefficient and standard enthalpy have been catalogued for many volatile compounds [16]. By knowing these physical constants and the temperature, one can calculate

the equilibrium's headspace concentration in the gas phase from the compound's liquid concentration with respect to the environmental temperature.

The equilibrium between aqueous and gaseous phase is dependent on the chemical characteristics such as the size of a molecule or the position and nature of its functional groups. [17] Naturally, the equilibrium is also dependent on the transition and transition area of the volatile to the other medium (liquid or gaseous).

1.4 Types and principles of electronic noses

In the following section the most important sensing principles used in electronic noses will be reviewed with a special focus on chemiresistive sensors to which the ST214 belongs.

1.4.1 Optical sensors

Optical sensor systems are based on changes in fluorescence, wavelength absorption or reflection. Like other kinds of biosensors and electronic noses in particular, these sensors exploit the interaction between molecules in the gaseous phase which are adsorbed onto a sensitive layer and result in changes of their optical properties.

One method of detecting molecules uses fluorescent dyes attached to a polymer thin layer [12]. The absorption of molecules changes the fluorescent properties which are then measured with a spectrometer. Alternatively, different solvatochromic dyes are immobilised on polymer matrices on distal

dips of optic fibres as figure 4 suggests. Different fibres with different coated dips consequently lead to a unique pattern [18].

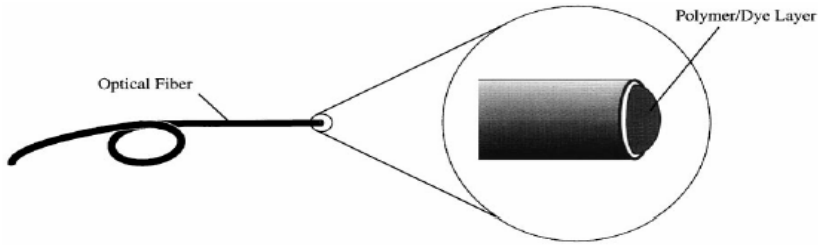

Figure 4: Polymers and solvatochromic dyes are fixed on a distal dip of an optical fibre. The change in fluorescence indicates the kind of molecules that is bound [18].

As an example of an absorptive measurement method, phthalocyanine, a modified porphyrin molecule, can be used for measurement in the UV-Vis spectrum. Phthalocyanine can be modified by binding different metal ions forming a chelat complex. The molecule is then excited with a light source in the UV-vis spectrum and the adsorption can be measured usually within a range of 300 to 800 µm. The absorption wavelength depends on the molecules adsorbed on the sensitive layer and the material, the central metal ion and the peripheral functional groups. A number of different sensor configurations applied to one array produces a fingerprint-like absorption pattern that gives the absorption at particular wavelengths [12, 19, 20].

A second and often used material is polyaniline which changes colour according to its oxidation state. In recent years many devices have used these macroscopic changes of the sensitive layer in the detection of ammonia because polyanilines are known to undergo a significant optical change in the near infrared spectral region when exposed to ammonia. It can also be used

for pH measurement [21]. Other optical methods like white light interferometry also using porphyrine derived molecules [12], interference, luminescence or holographic techniques have been reviewed [22].

1.4.2 Thermal sensors

Thermal sensors often work like a pellistor, a type of micro-calorimetric sensor first reported in the early 1990's. Pellistors measure temperature changes specific for gases [10]. However, only combustible gases like methane can be detected. The idea of thermal detection assumes that the gas needs to be oxidised or thermally decomposed after which heat will be produced and measured. Pellistors consist of a metal coil (e.g. platinum) that can be encapsulated with aluminium and coated with palladium, as figure 5 suggests. A voltage is applied across the coil which heats it up to 500 or 600°C. The high temperature and the outer palladium layer act as a catalyst, causing the gas to combust. The temperature increase depends on the gas that has been decomposed or oxidised. The change in temperature due to the chemical reaction is measured, transducing the thermal signal into an electrical signal. The silicon or silicon nitride layer around the coil isolates the heating element from side interference. The advantages of this kind of sensor are the fast response times and a high and unique sensitivity to different vapours. The disadvantages are the expensive production, high power consumption (100 - 500 mW per element) and the fact that it is only able to detect combustible gases [23, 24].

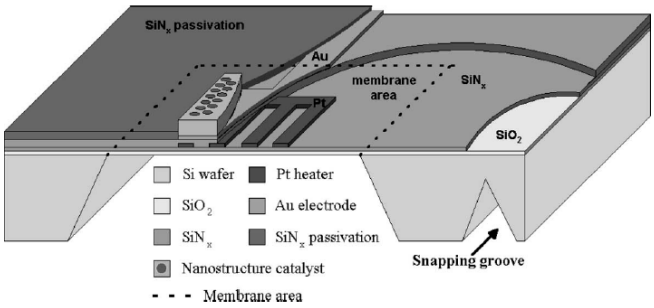

Figure 5: Cross section of a silicon based planar pellistor. The complex, nanostuctured design explains its expensive production [23].

1.4.3 Chemiresistive sensors

Due to the role of conducting polymers as the sensing component in the Bloodhound ST214 electronic nose (Scensive Ltd., UK) used in this project, the characteristics will be explained more in detail.

(I) Conducting polymer sensors

An important group of chemiresistive sensors are conducting polymer (CP) sensor systems. Like metal oxide semiconductors (which are reviewed in the next sub-section) the response of CP sensors is expressed as a change of conductivity because of the adsorption of volatile compounds to a sensitive layer. These polymers are typically made of pyrrole, aniline or other semiconducting aromatic and heteroaromatic materials (black carbon). In an electrochemical process, the monomers are attached to each other. Different functional groups that are bound additionally to the pyrrole or aniline rings change the electrochemical properties of the rings accordingly. This affects the polymerisation process and the application in the devices. The functional groups influence the electron migration during the polymerisation process which leads to a change of the working voltage and to a higher voltage during

the measuring process. Nevertheless, the major impact of the conductivity and semi-specificity of conducting polymers is caused by the dopants. Dopants are anions that are reversibly bound to the monomers via ionic forces because in oxidative- (figure 6, left) or in reductive polymerisation processes (figure 6, right) centres of positive charges are created.

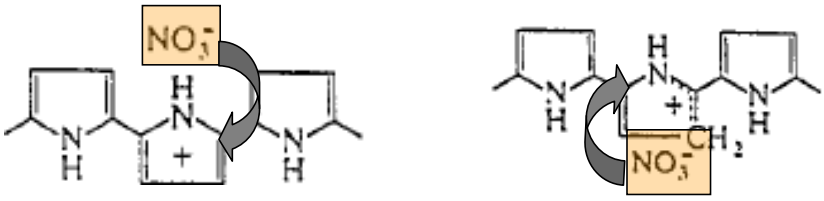

Figure 6: Results of the oxidative- (left) and the reductive electrochemical polymerisation method (right). A dopant is also attached to the polymer and bound via ionic forces (centre of positive charge in the monomer ring- and an anion as a dopant, grey arrow) [25].

The anions lie in suitable cavities between the polymer layers [9, 25-28]. The resulting conducting polymers can be classified into intrinsic and extrinsic polymers. Intrinsic conducting polymers have conjugated π-electron systems along their backbone. The polymerisation is carried out directly on the sensor substrate in an electrochemical cell. There, the polymer precipitates as a thin film onto the working electrode. Furthermore, cyclic oxidation and reduction processes allow the movement of counter ions or dopants in and out of the polymer layer [12, 26, 28, 29].

On the other hand, extrinsic conducting polymers consist of conventionally insulating polymers combined with other conducting polymers or insulating polymers loaded with electrical conductive fillings like carbon black or graphite (so-called co-polymers). When exposed to volatile compounds the volume of

the insulating polymer increases, enlarging the distance between the conducting fraction, the conducting polymer or the conducting particles (carbon black, graphite). This increases the resistance. Both arrangements, intrinsic and extrinsic conducting polymers are composite polymers [12, 27, 29]. The intrinsic and extrinsic polymers form the sensitive layer used in the Bloodhound ST214. In the following table 1 the materials the polymers are composed of and what they respond to are summarised.

Table 1: Polymer and co-polymer materials and sensitivities for all sensors for the ST214 are summarised. The sensors are paired, and each of the pair gives very similar responses [30].

Sensor	Polymer	Specificities		
		High	**Medium**	**Low**
1	Polypyrrole	Alcohols, ketones , water	Organic acids	Amines, esters
2	Polythiophene*	Amines, aldehydes	Alcohols, ketones	Organic acids water, esters
3	Polythiophene*	Amines, aldehydes	Alcohols, ketones	Organic acids, water, esters
4	Polypyrrole	Alcohols, ketones, water	Organic acids	Amines, esters
5	Polypyrrole	Alcohols, ketones, water	Organic acids	Amines, esters
6	Polyaniline	Alcohols	Ketones, water	aldehydes
7	Polyaniline	Alcohols	Ketones, water	aldehydes
8	polypyrrole	Alcohols, ketones, water	Organic acids	Amines, esters
9	polypyrrole	Alcohols, ketones, water	Organic acids	Amines, esters
10	Polythiophene*	Aldehydes	Alcohols, ketones, amines	Organic acids, water
11	Polythiophene*	Aldehydes	Alcohols, ketones, amines	Organic acids, water
12	Polypyrrole*	Alcohols, ketones, water	Organic acids	Amines, esters
13	Polypyrrole*	Alcohols, ketones, water	Organic acids	Amines, esters
14	Internal reference	No response	No response	No response

Legend: Polymers with an "*" are co-polymers (extrinsic sensors) while the other sensors are intrinsic- or intrinsic sensors with substitutes as a sensitive layer.

The selectivity and sensitivity can be modified using different functional groups, polymer structures (length and surface integrity) and but mainly by

selecting different doping ions [27, 31, 32]. As an example, table 2 shows different dopants that are embedded in polypyrrole structures while the conductivity changes [25]. The resistance of the sensor is determined by different attributes of the polymer (material and including the added functional groups) the main influence on the measured signal is caused by the dopants which are embedded between the polymer layers in different concentrations.

Table 2: List of polypyrrole compositions containing prevalent dopants and the changes in conductivity. The indexed numbers of the compositions specify the averaged number of dopants between the polymer layers [25].

Doping anions	PPy composition	σ (S cm^{-1})
TsO^-, NO_3^-	$C_4H_{3.2}N(TsO)_{0.19}(NO_3)_{0.08}$	43
TsO^-, ClO_4^-	$C_4H_{3.09}N_{0.97}(TsO)_{0.23}(ClO_4)_{0.18}$	42
TsO^-, Cl^-	$C_4H_{3.2}N_{0.97}(TsO)_{0.27}Cl_{0.11}$	66
ClO_4^-, NO_3^-	$C_4H_{2.99}N(NO_3)_{0.14}(ClO_4)_{0.13}$	21
Cl^-, NO_3^-	$C_4H_{3.5}NCl_{0.16}(NO_3)_{0.18}$	23
TsO^-	$C_4H_{3.2}N_{0.99}(TsO)_{0.34}$	64
ClO_4^-	$C_4H_{3.1}N_{0.98}(ClO_4)_{0.30}$	11
Cl^-	$C_4H_{3.1}N_{0.99}Cl_{0.28}$	13
NO_3^-	$C_4H_{3.1}N(NO_3)_{0.22}$	8

The advantage of conducting polymer sensors is that they are operated at room temperature which allows the analysis of higher weight molecular compounds without destroying them. Generally, they show fast sensor responses and a base-line recovery or reversibility. The sensitivity is in the ppb and ppm range for alcohols, aldehydes and fatty acids [28].

The disadvantage is that the conducting polymers are very sensitive to water vapour which is an essential constituent of many different samples or its headspaces. Water binds to the polymers because of its strong dipole character and as a result the number of available binding sites decreases or it even may displace doping ions. The sensor becomes less sensitive. Moreover

conducting polymers show a poor reproducibility in the manufacturing process due to the number of influencing factors. This leads to a lack of reproducibility concerning the sensor response at similar conditions [28, 31, 33].

(II) Metal oxide semiconducting (MOS) sensors

A second important group of chemiresistive sensors are metal oxide semiconducting sensors (MOS). They basically consist of a heating coil within a ceramic cylinder. The outer side is coated with metal oxides such as tin dioxide (SnO_2), titanium dioxide (TiO_2), indium (III) dioxide (In_2O_3), tungsten trioxide (WO_3) or nickel oxide (NiO) [11, 27, 34]. The semiconductiong material is doped with traces of different noble metals like platinum (Pt), gold (Au) or palladium (Pd). These dopants affect the properties of the coating properties with respect to reducing and oxidising gases [35]. In a first step oxygen is dissolved in the semiconductor's lattice. This process sets a certain electrical resistance that is equal to the background level. When volatile compounds (predominantly non-polar) are passed over the sensitive layer they are adsorbed by the semiconductor. There, they react with the bound oxygen by trapping or releasing electrons from or to the semiconductor. This causes a proportional change in resistance which can be measured. Noble metal catalysts (e.g. Pt, Pd, Al, Au) enhance the redox reactions. Due to n-type behaviour of tin dioxide ($Sn(IV)O_2$) as a typical semiconductor for instance, the electrical conductivity increases with a reducing gas like carbon monoxide (CO) and decreases in the presence of an oxidising gas like nitric oxide (NO). The sensitivity and selectivity of MOS sensors are determined by the choice of the semiconductor material, the thickness and the arrangement

and size of the metal grains implemented in the polycrystalline sensitive semiconductor layer [9, 12, 23].

However, cross sensitivities, a lack of selectivity and detrimental effects of water vapour are disadvantages of this sensor system. Doped MOS sensors show a better sensitivity to oxygenated volatile organic compounds (e.g alcohols, ketones) [27]. The MOS sensor has a preferred temperature of 300-500°C. The detection limit is in the lower ppb range. Because of the high temperatures, a MOS sensor based device requires high power [9, 12, 36].

(III) Conducting polymer e-nose applications

In human medicine, e-nose technology has been employed in several areas of medical diagnosis, including rapid detection of tuberculosis [37], *Helicobacter pylori* [38], bacterial sinusitis [39] and urinary tract infections [40, 41]. In veterinary medicine, the usefulness of e-nose technology was principally demonstrated for the first time in 2005 by discriminating serum samples obtained from badgers and cattle infected with *Mycobacterium bovis* from those obtained in non-infected controls [42].

1.4.4 Metal oxide field effect transistors (MOSFET) as sensors

MOSFET consists of two n-doped electrodes that are fixed on a silicon substrate. These electrodes are termed DRAIN and SOURCE. Additionally, a third electrode is introduced, the so-called GATE electrode. An insulating layer prevents the transference of charge carriers from the GATE. A heating element provides thermal energy and ensures constant temperatures for the reaction (figure 7) [43].

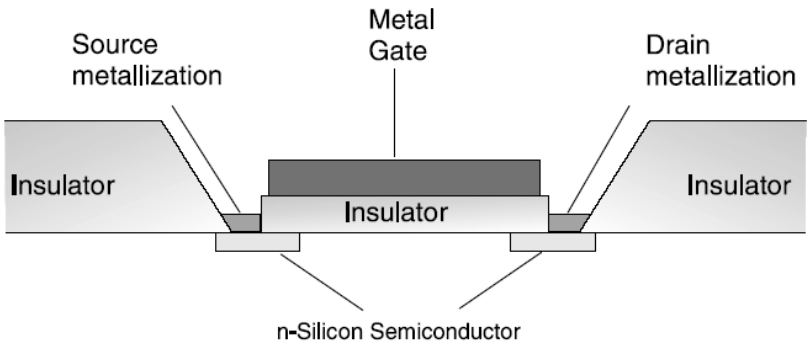

Figure 7: Schematic configuration of a metal oxide sensor including DRAIN, SOURCE and GATE electrodes. Depending on the analyte adsorbed on the sensitive layer, the potential difference changes and influences the current that is measured [12].

Between the DRAIN- and SOURCE electrode a base current flows. This current is influenced by changing the surface potential of the GATE electrode. The GATE electrode is made sensitive to the analyte by introducing catalytic metals like palladium (Pd), platinum (Pt) or iridium (Ir). Vapour molecules are adsorbed onto the sensitive layer. Any reaction between vapour components and the semiconducting layer of the GATE electrode causes a change in the metal GATE properties, notably the potential. This will result in a change in the MOSFET sensor's electrical properties and thus a change in the DRAIN current. The working temperature is usually about 120°C and allows a rapid response to vapour molecules. Other kinds of metal semiconductors may operate at higher temperatures. The sensitivity is in the sub-ppm range [9, 10, 12, 36, 43].

1.4.5 Amperometric sensors

In principle, amperometric gas sensors operate like a classic Clark electrode that is determined by Fick's law and Faraday's law. It consists of an electrochemical cell having a working- and a counter electrode. The cathode usually consists of gold (Au) or platinum (Pt) and the anode typically consists of silver (Ag). Both are in contact via an electrolyte solution. The sample is separated by a semi-permeable membrane. There, the analyte (e.g. oxygen, O_2) diffuses into the electrolyte solution where it is reduced at the cathode. The oxidation takes place at the anode. However, the measured current is proportional to the oxidised and reduced analyte concentration diffusing through the membrane. The membrane can be modified with different coatings to measure different analytes. The coatings are usually enzymes or immobilised bacteria that transform the analyte to produce oxygen, for instance, which can be measured [44].

The advantages of amperometric sensor systems are their insensitivity to water over a wide humidity range, a good sensitivity (ppb-ppm range) and a short response time. Amperometric sensors have a wide linear range and respond, theoretically, to a huge variety of electroactive analytes. They do not respond to saturated hydrocarbons. However, all sensors have to be optimised with respect to polarisation potential, buffered pH, electrode materials and other impact factors. A change of the electrode catalyst or the electrode potential alters and optimises the selectivity to different analytes. This is also a disadvantage because the sensor can only detect the concentration of one analyte. Furthermore, the electrodes are temperature

dependent. Coated sensors are often limited in lifespan because of the immobilised biological material [12, 45].

1.4.6 Gravimetric sensor systems

In 1880 the Curie brothers demonstrated piezoelectricity, a phenomena by which certain anisotropic crystals, when subjected to mechanical stress, generate electric dipoles. Based on this principle, different sensor systems have been established [12].

As one of the most important sensing principles, gravimetric sensor systems are often used for electronic noses. The main subgroups are bulk acoustic wave (BAW), surface- or sound acoustic wave- (SAW) or flexural plate wave- (FPW) or shear horizontal acoustic plate mode sensors (SH-APM). BAW and SH-APM are commonly referred as thickness shear mode (TSM) or quartz crystal microbalance (QMB or QCM) sensors.

QCM sensors basically consist of a gold electrode attached to quartz- or lithium niobate ($LiNbO_3$) crystals [46]. An alternating current forces the crystal to oscillate with a certain frequency (e.g. 10MHz or 30MHz). The crystals are generally coated with a synthetic or a biological material that allows the reversible and semi-specific binding of analytes. The bound molecules change the mass on the surface and cause shear stress. The stress changes the dipole character of the crystal and, hence, the resonance frequency of the system causes a change in the amplitude. The changed wave propagates vertically and horizontally through the bulk [9, 10, 12]. The shift in frequency is detected by an oscillating circuit converting a frequency into a current which can be measured. The proportional relationship of a mass change and a shift

in frequency is expressed by Sauerbrey's equation proposed in 1959 (equation 4):

$$\Delta f = -C \times \Delta m \qquad \text{or} \qquad \Delta f = \frac{F \times \Delta m}{A \times \sigma \times t} \qquad (4)$$

Δ f	[MHz]	= the change in resonance frequency
C		= a constant determined by the bulk properties
F	[MHz]	= the initial resonance frequency in MHz
Δ m	[g]	= the mass adsorbed onto the crystal surface
A	[m^2]	= the total surface area
σ	[g/m^3]	= the density of the crystal
t	[m]	= the thickness of the crystal

The same equation can be used for all sensor systems based on the piezoelectric effect.

Often synthetic or biological materials are immobilised onto the crystal. As a synthetic coating, porphyrins, as for optical applications (section 2.4.1), were used as a sensitive layer for surface acoustic wave sensors. Porphyrins are wide spread ionophores that are able to bind nearly every metal ion as a central atom which determines the selectivity. They also provide various possibilities to bind reversibly vapours to their outer functional groups [46]. That is why different classes of molecules are able to bind volatile compounds by means of different types of interactions, such as electrostatic interaction, coordination- or hydrogen bonding and mimic the human olfaction. The peripheral groups that are substituted on the molecular skeleton of the macrocycle can influence the electronic distribution on the Π-aromatic system of the porphyrin and influence the coordination and the related sensing properties [46, 47, 48].

As an example of a biological coating, isolated olfactory receptor proteins from a bullfrog (*Rana* spp.) were used to mimic human olfaction. A rapid and reversible response to different odorants was observed (e.g. n-caproic acid, isoamyl acetate, n-decyl alcohol, beta-ionone, linalol and ethyl caproate (ethyl hexanoic acid)). The fingerprint was sensitive to the gaseous compounds down to 10^{-6}-10^{-7}g. The long-term stability was determined as up to three months [13]. The detection limit lies in the nanogram range per square centimeter or in the ppbv (part per billion by volume) range at room temperature (25°C) and atmospheric pressure , respectively [12, 46]. Other authors assume only a low ppmv (part per million by volume) range as a detection limit [49].

A second relevant type of gravimetric sensor is the subgroup of surface- or sound acoustic wave (SAW) and bulk acoustic wave sensors (BAW). They exploit the propagation of surface acoustic waves along layered structures or the bulk. On SAW and BAW sensors, the surface generally consists of a piezoelectric substrate and a biological or synthetic coating. Molecules that are present in a gaseous phase bind reversibly at the sensitive surface and cause a change in phase velocity which can be measured as frequency shifts and a propagation loss of the acoustic wave that equals the amplitude of the resulting oscillation.

There are two types of BAW sensors, the delay line oscillator and the single two ports SAW resonator. In delay line sensors the wave travels along a crystal until it reaches an oscillator. The oscillator is coated and interacts with the sample. It delays the wave. This delay in time is measured.

In SAW resonator sensors, the waves are reflected by a ridge in the selective coated substrate. The reflecting wave will be changed due to the properties of the ridge and compared to the original wave. In both cases, frequency shifts or changes of the amplitude of the wave can be related to the added mass of the selective coating. SAW sensors usually operate between 150-400MHz [9, 12]. Sometimes fast chromatography columns can be coupled to SAW sensors to achieve better selectivity and sensitivity due to different retention times of the gas mixture components. The detection limit can be reduced to the ppb level [50].

Additionally, some instruments detect more than just the resonance frequency. For instance a nanometer scale bending caused by mechanical stress of the adsorbed molecules on a cantilever is detected by a laser (figure 8 a, b) [51].

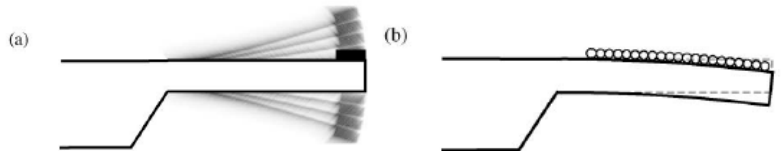

Figure 8: a) In the so-called dynamic mode the absorbance of the analyte causes a change of the resonance frequency. b) In the static mode, the weight of the adsorbed analytes cause mechanical surface stress and bend the cantilever. The change in bending is measured with a laser [51].

In addition, the change in resistance and frequency is measured and plotted versus the known concentration of certain compounds. Later this unique fingerprint can be used to determine the concentration [52].

1.5. Mass spectrometric methods

Due to the objective of the current project the second essential measurement technique is single ion flow tube mass spectrometry (SIFT-MS). The following pages give a brief summary of SIFT-MS. Gas- and liquid chromatographic methods will also be reviewed as they have contributed to the quantification and elucidation of mycobacterial structures and metabolisms.

1.5.1 SIFT- MS principles and applications

(I) SIFT- MS principles

Single ion flow tube mass spectrometry (SIFT-MS) is a method for real time analysis of trace gases and was originally developed and published in 1976 by Adams and Smith. It consists of a microwave resonator, an injection and a detection vacuum pump, two quadrupole mass spectrometers (upstream and downstream), a flow tube with an inlet for a gas carrier stream and the gaseous sample and a channeltron ion detector (figure 9) [53, 54].

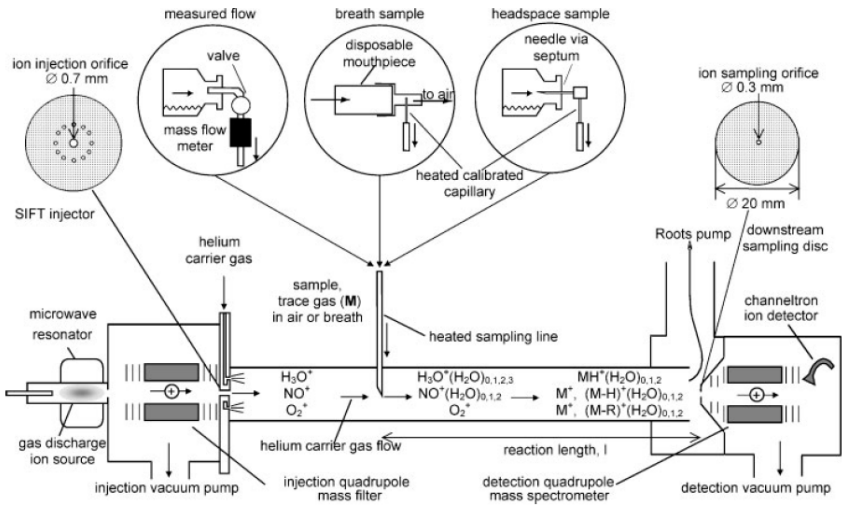

Figure 9: Section of the SIFT-MS. Precursor ions ionise molecules from a sample, introduced into the flow tube via a capillary, and generate product ions. Precursor ions can be selected by the upstream quadrupole mass spectrometer and product ions are measured with an ion detector [54].

In the microwave resonator three so-called precursor ions, H_3O^+, NO^+ and O_2^+ are generated at a sufficient current, at least 10^{-9} A. The ionisation energy is comparatively low assuring non-fragmentation and a defined mass to charge ratio of the precursor ions. This magnetron/cavity arrangement operates in the absence of mechanically adjustable parts and ionises all gas mixtures at a pressure range of 10-100 Pa [55].

The precursor ions are led through an evacuated chamber (p = 100 Pa) with a quadrupole mass spectrometer allowing a selection of precursor ions by setting up a specific electro-magnetic field. These ions are chosen as they react with most trace gases of interest but only react minimally with the main components of air. The precursor ions pass through the injection orifice (0.7 mm i.d.) and are carried along a flow tube by a stream of inert carrier gas

(helium) ($\upsilon = 40 - 80$ m/s). Within the tube the precursor ions ionise the sample molecules that are introduced through a heated sampling capillary. The flow rate through the capillary is measured to provide information essential in determining the concentration of a compound in the trace gas. The temperature within the tube is about 300 K. Finally, the carrier gas, the precursor ions and the ionisation products are led though a sampling orifice (0.3 mm i.d.) into a second evacuated chamber with a quadrupole. There, different product ions can be selected according to their mass charge ratio by changing the quadruple's electro-magnetic field. The channeltron ion detector finally detects the ions [54]. The number of product ions is then calculated taking into account the product ion count rate and the number of precursor ions. The number of the selected precursor ions decrease because they may react with the vapour molecules or, as a result of diffusion processes, they "disappear" onto the tube wall. This time dependent process can be described as (equation 5).

$$[N_i]_t = [N_i]_0 \times e^{(-k \times [E] \times t - \frac{D_i \times N_i}{\Lambda^2})} \qquad (5), [54]$$

While N_i is the number density of precursor ions at different times ($[N_i]_t$ at the time t and $[N_i]_0$ at the beginning), D_i is the diffusion coefficient and Λ is the diffusion length. Furthermore, k is the rate coefficient for the transformation of the sample molecule to a product ion. [E] is the primary molecule density. Since the increase of product ions is directly dependent to the precursor ion concentration and the primary molecule density, the product ion density [P] can simplified be determined as (equation 6).

$$[P]_t = [N_i] \times k \times [E] \times t \times D_e \qquad (6), [15, 53, 54]$$

The simplification assumes that the primary ion concentration is very low so diffusion processes don't seem to be relevant. This is feasible at trace gas concentrations.

SIFT-MS allows the two modes of operation: the Full Scan Mode (FSM) and the Multipe Ion Monitoring (MIM). FSM shows the full spectrum of product and precursor ions that are displayed as count rate or intensity in counts per second versus the mass to charge ratio (figure 10).

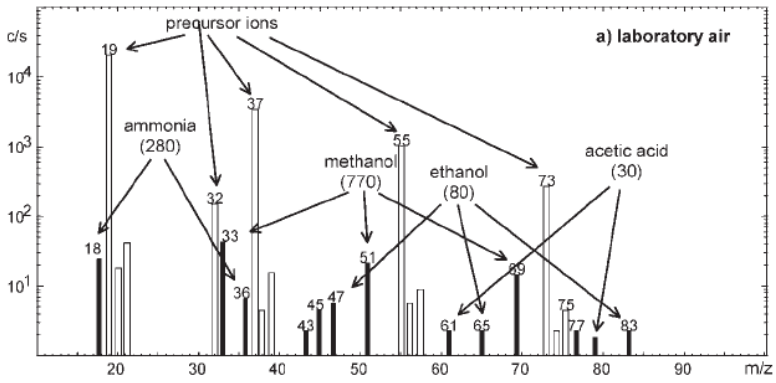

Figure 10: SIFT-MS spectrum of laboratory air. Volatile compounds are measured in the full scan mode (FSM). The intensity or count rate in counts per second [c/s] is plotted against the mass/ charge ratio [54].

The MIM shows only the precursor ions and a selection of product ions. In this mode the detector switches very fast between single mass/charge ratios and detects concentration almost in parallel. The partial pressure can be displayed in real time while the response time is 20 ms. In the maximum 14 ions are detectable separately (figure 11).

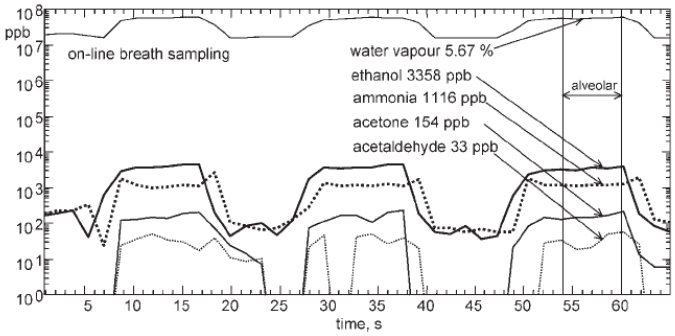

Figure 11: Compound/ product ion concentrations of a breath sample in ppb in the course of time in s. You can easily see the breathing pattern (increased compound concentration during expiration phase [54]).

While SIFT-MS analysis assumes a proportional relationship between number density of the trace gas molecules in the tube and the sum of all signal intensities of the corresponding product ions a consideration of branching product ions is essential. Sometimes there is more than one product ion. The precursor ions react in different ways with the trace molecules. The sample molecules can be protonated by transferring H^+ ions, e.g. by H_3O^+. This exothermic proton transfer occurs in combination with polar molecules with a higher proton affinity (PA in kcal/mol) than that of water (equation 7).

$$H_3O^+ + E \rightarrow P^+ + H_2O \qquad \text{(7), [54]}$$

A clustering of the H_3O^+ and NO^+ precursor ions may appear, especially in presence of a high water vapour concentration in the sample gas phase. This leads to a repeated H_3O^+ or NO^+ precursor ion signal in the mass/charge spectrum as a multi hydrated hydronium ion (equation 8) [15, 56].

$$e.g.: H_3O^{+}{}_{[19g/mol]} + n \times H_2O_{[18g/mol]} = H_3O^{+}(H_2O)_{n[37g/mol+(n-1)\times 18g/mol]} \quad (8)$$

The NO^+ precursor ions primarily react with organic molecules such as aromatic hydrocarbons and organo-sulphur molecules. NO^+ ionises the trace molecules if the ionisation energy is less than the precursor ion ionisation energy (9.26 eV). The main process is a non-dissociative charge transfer which produces organic radical ions. If the ionisation energies of the trace molecule and the precursor ions are almost similar a second product ion appears which is an associated ion of the precursor ion and the trace molecule (equation 9).

$$\begin{aligned} NO^+ + M &= M^{+\bullet} + NO^{\bullet} \\ NO^+ + M &= (NO + M) \end{aligned} \quad (9), [54]$$

O_2^+ precursor ions have a much greater capability (12.06 eV) to ionise than NO^+. That is why O_2^+ is able to initialise a non-dissociative charge transfer with the result of a radical cation P^+, similar to NO^+, or a dissociative reaction with the trace molecule. The result of the latter reaction is the occurrence of two or more fragment ions. O_2^+ reacts with organic compounds and small molecules like NO, or ammonia that are not detected by H_3O^+ or NO^+. The combination of spectra from all three precursor ions and product ions is the key strategy of component identification but for most of the volatile compounds where its identity is known, one of the three precursors is suitable [57]. Looking at reactions with more than one precursor ion enables

the identification of compounds whose ions overlap. For instance, hydrated compounds can be distinguished from another compound e.g. hydrated methanol with two water hydrates may be distinguished from isoprene using H_3O^+ and NO^+. Both give an ion at m/z 69 using H_3O^+, but only isoprene reacts with NO^+ to give an ion at m/z 68 [58].

All hydrated product ions of one trace compound are added to the final signal. Studies on hydroxylated, methylated and oxidised aromatic compounds with different ionisation energies confirmed the necessity to use different precursor ions depending on the trace molecule for correct results [59, 60].

The detection limit for most of the molecules is in the lower ppb range.

Unfortunately, the exploitation of the excellent performance of this device requires an advanced knowledge of ion chemistry. Analysis of multiple samples also requires excellent knowledge in multivariate data analysis. Because of the size, weight, and a lack of robustness, the instrument is not portable. The high power consumption also has to be taken into consideration [15, 53, 54].

(II) Application of SIFT-MS techniques

Since the invention of SIFT-MS the device has been improved significantly. The major drive of this development is its application in several different fields. Breath analysis is potentially very important as it may play a role in non-invasive disease diagnosis. For instance, methanol concentration in breath that may be correlated with the ingestion of fruits or fruit products, ethanol or the artificial sweetener Aspartame, was determined using SIFT-MS [58]. In connection with the latter extensive longitudinal study, isoprene (2-methyl-1,3-butadiene) concentration in breath was also determined. The study didn't

support a positive correlation between blood cholesterol and isoprene [61]. However, other investigations using similar techniques (e.g. proton transfer reaction mass spectrometry, PTR-MS) found a positive correlation that seems to indicate that isoprene may be a surrogate parameter in breath for the blood cholesterol level [62]. Other studies investigated the status of psychological, physical and biochemical stress by breath analysis with isoprene as a representative marker [63]. Further investigations of gas mixtures of different origin (e.g. headspace of blood or urine) [64] were accomplished including headspace analysis of bacteria [53, 65, 66] and fungi [67]. However, comparative measurements using gas chromatography mass spectrometry (GC-MS) needed to be undertaken in parallel [68] since GC-MS is still the internationally accepted gold standard and since it allows the identification of potential 'biomarkers'. A recent study analysing cultures from different Mycobacteria strains (*M. tuberculosis, M. bovis, M. bovis BCG, M. avium complex, M. fortuitum, M. chelonae* and *M. abcsessus*) demonstrated the importance of GC-MS as an essential method for biomarker identification [69].

1.5.2 Gas chromatographic mass spectrometry (GC-MS)

Gas chromatographic systems are appropriate methods for headspace analysis especially with the addition of a mass detector (mass spectrometry). It is considered as the "Gold Standard" for the analysis of volatile compounds and vapours and is applied in many routine laboratories with different configurations.

(I) GC-MS principles

A gas chromatographic system consists of a sample trap, a heated GC column and a detection system. The specific components are selected according to the characteristics of the sample. Since a vapour is a mixture of different molecules rather than a single compound the column generally needs to be a compromise.

Generally, the sample is trapped and flushed by a carrier gas stream (mobile phase) at high temperature. This mobile phase is led through the column that has a coating of compounds (stationary phase) which are optimised to adsorb the target compound or the compound class. The stationary phase binds the mixture of volatile molecules reversibly due to the physical and chemical attributes (hydrogen bonds, van-der-Waals forces, electrostatic interaction). Usually, a temperature gradient within the separation assists the process. Molecules interacting less strongly with the stationary phase are migrating faster through it. A separation takes place that is expressed by different retention times according to the strength of the interactions. Mathematically, separation can be described in a simple way by the van-Deemter equation.

Finally, after elution a detection system analyses the compounds as they come off the column. The analyser can take many forms but a mass detector is commonly used as it is capable of identifying unknown compounds. Other detectors are used, including the thermal conductivity- or hot wire detector (TCD/ HWD) and the flame ionisation detectors (FID). Both methods require the ionisation of the eluted gases. Furthermore, a couple of other detectors have been developed such as electron capture detectors/ ion traps (ECD) or

photo-ionisation detectors (PID). They work with a similar principle but are not reviewed here.

(II) Problems of GC-MS and sampling systems

Since the 1960's and 70's volatiles as constituents of breath or urine have been investigated with gas chromatographic methods. For instance, a flame ionisation detector was one of the first detectors combined with a gas chromatograph. The rising number of investigations in breath with different contexts and other biological media lead to the optimisation of the gas chromatographic methodology. The application of different carrier gas streams (e.g. nitrogen, hydrogen or helium) at different velocities or the suitable temperature for the adsorption and desorption of samples were just the beginning of the evolution process [70, 71]. Today, the detection of trace molecules in breath is quite common. Despite various improvements concerning materials and methods as an evolution process, there are still problems connected with gas chromatography.

Generally, mixtures of trace gases (e.g. headspaces from liquids and solid samples) should be trapped using different systems. For example, Tenax traps or so called multi-bed sorption traps are widely used. These consist of different modified carbon layers which absorb different compounds with different affinities [72-74]. Unfortunately the traps do not represent the spectrum of gas mixtures because the gaseous compounds do not bind to the adsorbing layer in the same way. Additionally, competitive binding has to be taken into consideration. Some compounds may be underrepresented by the signal intensity which has to be cross-checked by determining the recovery rate with a suitable standard [74-76]. Furthermore, the adsorption and

desorption processes require a thermal treatment which possibly decomposes some of the reactive compounds (e.g. 300°C/ 15mins [72, 75]. Alternatively, solid phase micro extraction (SPME) avoids high temperatures but at the same time also does not fully represent the constituents of the gas mixture.

Tedlar or Nalophan bags have also been applied to sampling processes, replacing the trap system and giving therefore the chance to analyse the gas samples directly [77, 78], although the sensitivity of direct analysis is much lower. However, samples can only be stored in solid phase micro extraction (SPME) fibres or Tenax tubes since the composition in gases changes over time. Both systems are often applied to headspace and trace gas analysis because they significantly increase the sensitivity compared to direct sampling methods. Thermal desorption (of which the sorbent Tenax is an example), has an even greater sensitivity (10 to 100 times) than SPME which on the other hand is more inexpensive compared to thermal desobtion systems and can be routinely used for GC-MS analysis due to its simplicity [79, 80].

The coupling of two columns in series can increase the sensitivity and the separation power. Various volatile organic compounds can be detected down to ppm to ppt (parts per trillion) levels. Unfortunately, a comprehensive spectral library and time consuming multivariate statistics are needed to obtain useful information. Columns are not standardised and need to be adapted according to the chemical attributes of marker compounds. These procedures make GC-MS analyses expensive and time consuming.

1.6 Bacteria and infections

A large number of volatile components emitted by the body after bacterial infection have been identified. These volatiles may come from the bacterial metabolism, the bacterial cell walls or are a result of the host's immune response. Due to the simultaneous appearance of oxidative stress and the disease, a pattern of 'biomarkers' is needed to prove the presence of the disease in breath or headspace of samples [81, 82]. Phillips *et al* [82] found various substances or patterns in breath of tuberculosis infected human patients and stated that these patterns are different due to different subspecies or oxidative stress, generally C_4 to C_{26} fatty acids. However, most of these molecules are hardly evaporated at 37°C. Furthermore, e-noses operate at room temperature which makes the evaporation of large molecules more unlikely compared to thermal desorption traps. There is also the question whether during the thermal desorption process of a tube the molecule was decomposed or not and which coloums were used in this study. Finally, it appears to be unclear if such a low number of samples for each group is suitable to perform pattern recognition analysis. The same points of criticism can be found for Shyre *et al* [69, 83]. There were only minor information about the methodology especially for sampling and analysis. Biological variation such as the health status, age or nutrition of the pations was not considered. In the following section the disease causing bacteria will be briefly reviewed to give an overview.

1.6.1 *Mycoplasma bovis*

Mycoplasma bovis is the main causative agent of mycoplasmal mastitis, arthritis and pneumonia in cattle. It causes inflammation in joints and the udder and may lead to a significant reduction in milk productivity of dairy cattle resulting in considerable economic losses. *Mycoplasma bovis* can also cause pneumonia which may be lethal, especially for calves. Transmission is often via the udder of cattle with mastitis or via semen of infected bulls. Since *Mycoplasma bovis* has no cell wall it is not susceptible to most of the antibiotics. The “Gold Standard” for detection is, as for many other diseases, culturing the bacteria which are routinely used in laboratories. But this is time consuming, expensive and not practical for field testing. Other methods are recently under development such as enzyme-linked immunosorbent assay (ELISA) or fluorescent antibody tests techniques to screen for antibodies or antigens for clinically diseased subjects. Whole-cell protein patterns using sodium dodecyl sulphate-polyacrylamide gel electrophoresis (SDS-PAGE) were generated for field samples. Also polymerase chain reaction (PCR) was used to amplify and analyse *Mycoplasma bovis* in supernatants of cell cultures and milk of infected cattle [84, 85]. However, the latter diagnostic tools are not suitable for rapid field testing. For all these reasons there is an urgent necessity for a fast and reliable detection and screening strategy for this pathogen. The analysis of volatile organic compounds in headspace of biological samples can be one approach.

1.6.2 *Mannheimia haemolytica* (*Man.haem*)

Mannheimia haemolytica (formerly *Pasteurella haemolytica*) is the primary agent of pneumonic pasteurellosis – one of the most important respiratory diseases in cattle. Bovine pneumonic pasteurellosis is mainly caused by the gram negative bacterium *Mannheimmia. haemolytica* serotype A1.

The obligate pathogenicity of *Man. haem.* is proven by the isolation of pure cultures from pneumonic lungs as well as by infection studies. At first, serotype A1 strains colonise the bovine upper respiratory tract, continue colonising the lower respiratory tract and finally enter the alveolar spaces. There, bacteria cause an inflammatory host response, including a strong influx of neutrophils accompanied by accumulation of fibrin which forms lesions. The lesions can block the alveolar space and therefore cause necrosis of the spaces. This leads to pneumonia and in severe cases to the death of the individual [86, 87]. Experimental models of infection have been used for decades and for many reasons, for example to understand the pathogenesis of this particular bacterium in the bovine respiratory system [88-92], to determine the effect of treatments [93-95], or to develop different vaccination protocols [96-99].

The determination plasma proteins, so-called acute phase proteins (APPs), are another diagnostic option that has been widely used. These proteins are mainly synthesised in the liver when stimulated (e.g. via cytokines during the acute phase of inflammatory reaction) [100]. In veterinary medicine, APPs are accepted biomarkers for infection and inflammation in experimental studies to reflect the acute phase response as an integral part of the innate immune system [101]. There is evidence that concentrations of serum APPs are

related to the severity of underlying disease and therefore may act as markers of both the presence and the extent of disease [102].

In this experimental study, calves with *Mannheimia haemolytica* A1 infection were used as a model to assess host response under the defined condition of a gram-negative bacterial infection. The objective of this study was to collect blood samples before and after experimental challenge and to analyse the samples for both (i) the concentration of APPs and (ii) the response characteristics of e-nose sensors due to VOCs present in the headspace. Additionally, studies were carried out to determine whether the measurable e-nose response could be correlated with the acute phase reaction generated in the host, because nothing is currently known about the relationship between the acute phase reaction of the host and the change in its metabolic profile of VOCs.

1.6.3 *Mycobacterium bovis*

Due to the importance of Mycobacteria subspecies in this project, these bacteria will be introduced more in detail to give an overview of their impact on the world health status, the classification and routes of transmission. In the following sections, only the *M. tuberculosis*, *M. bovis* and *M. avium* will be addressed due to their major role in wildlife and human tuberculosis.

(I) Introduction and impact on the world health status

Tuberculosis was and is one of the oldest and most dangerous diseases in the world. In 1882, the German microbiologist Robert Koch discovered the agent that causes tuberculosis, the tubercle bacilli. Since then that point of

time tuberculosis has killed millions of people but without causing a massive epidemic or fulminating outbreak.

The causative agent of tuberculosis is one of the most universal pathogens in the world and progressively affects wildlife animals, domestic animals as well as humans. In fact one third of all diseases causing deaths in European capitals are based on tuberculosis infections [103]. Furthermore, the permanent danger of animal tuberculosis worsens the situation as people in developing countries consume unpasteurised bovine milk or milk products which are main routes for transmission.

Human and animal tuberculosis infection has become an even more severe problem since the 1980's with a simultaneous and massive appearance of HIV infections [104, 105]. Today, more than 40 million are infected with HIV and tuberculosis at the same time [103]. Moreover, it is estimated that two billion people, one third of the world's population, are infected with latent tuberculosis [106]. The presence of wildlife animals as a reservoir of mycobacteria infecting animals of economic interest and the closely connected risk for human health leads to the urgent necessity of controlling tuberculosis in order to prevent a further and amplified spreading. Hence, a cost effective and easy to handle device that is dedicated to precise in-field-diagnosis is desirable.

(II) General description and classification

In general, mycobacteria, occurring in soil and water, are slightly curved or straight rods and sometimes branched indicating the ability forming filaments. They are non-motile and non-spore forming. With a very low doubling rate

(18 h) mycobateria in general grows slowly compared to other bacteria like e.g. E.coli which has a doubling rate of approximately 20 minutes [107]. A more detailed consideration reveals fast growing bacteria (M. smegmatis, M.phlei, M. parafortuitum) and slow growing mycobacteria (M. tuberculosis, M. avium, M. bovis) whereas slowly growing bacteria have more pathogenic attributes [108].

(III) Mycobacterium bovis

Whilst *M. tuberculosis* is mainly a human pathogen, the occasional human pathogen *M. bovis* has a broad host range. In fact, the bacterium causes tuberculosis in a lot of domestic animals. Because of different wildlife animals acting as a natural reservoir, it is not possible to eradicate *M. bovis* in livestock even in industrialised countries. For this reason, infected individuals represent a serious risk of infection for humans. That is why bovine tuberculosis became a major animal health- and, furthermore, a human health problem in the UK. Today, basically three means of transmission are significant in human infection:

a) continued consumption of unpasteurised milk from cows and sheep

b) sales of unpasteurised milk and dairy products of infected animals

c) exposure to infectious aerosols from tuberculous animals and their carcasses

After being infected by wildlife animals e.g. badgers, cattle host *M. bovis*. Humans eating raw or uncooked meat or drinking unpasteurised milk from infected cattle are exposed to a low risk of human infection via ingestion. But,

this is still regarded as the main route of infection [109]. After entering the gastro-intestinal tract, *M. bovis* eventually spreads to the respiratory tract. From here M. bovis develops like other mycobacteria [108].

M. bovis organisms can be easily destroyed by cooking meat or pasteurising dairy products. However, airborne infection continues to occur among meat industry and slaughterhouse workers, in regions where the infection is still prevalent in cattle. But, evidence of person to person transmission is rare [110]. Within the period 1990 to 2003 between 17 and 50 new cases of human M. bovis infection were confirmed every year in the UK. This represents between 0.5% and 1.5% of all the culture-positive confirmed TB cases [109]. *M. bovis* as the cause of human tuberculosis remains low compared to that of M. tuberculosis [110]. However, in agriculture M. bovis infections in animals are quite common and in every continent M.bovis infected cattle were found. The high prevalence in European countries could be due to the intensive monitoring. In Africa the high number of counties with no reports is the result of a lack of nationwide observations.

(IV) Special biochemical features and cell wall attributes

The cell walls of mycobacteria feature special attributes that are typical for this species. Beside the common structures (double phospholipid membrane) and peptidoglycan (1-4 glycolic bound n-acetyl-glucosamine and n-acetyl-muraminic acid molecules), mycobacteria have developed an additional fatty acid layer containing mycolic acids covalently bound to arabinogalactan (AG) or phosphatidylinositol mannosides (PIM) [111]. PIMs are reported to be specific for mycobacteria and represent an important part of the

mycobacterium's cell wall [110, 112]. Mycolic acids are 60-90 carbon chains with a hydroxyl group on the beta carbon and an aliphatic chain attached to the alpha carbon (figure 12) [113].

Figure 12: The structure of the β-hydroxy-α-alkyl branched structures of high molecular weight mycolic acid was elucidated by Asselineau in 1950 (left). The general structure of PIMs are shown on the right; X= 0,1,2,3,4; for PIM2, PIM3, PIM4, PIM5, PIM6, respectively; R' and R''= acyl fatty acids [111].

The entire structure is termed mycolyl-AG-peptidoglycan complexe (MAPc, figure 13) [111, 113].

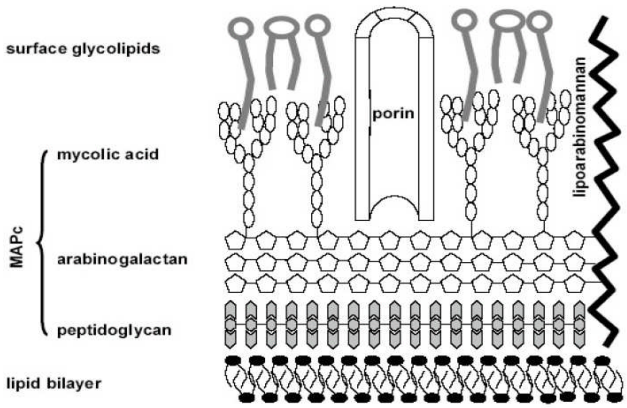

Figure 13: Figure 5 shows the schematic composition of the mycobacterium's cell wall containing the standard gram positive wall and an additional waxy layer made of mycolic acid [114].

MAPc has an extremely hydrophobic character, protects bacteria from destruction by antibiotic agents or macrophages and consequently leads to the evolutionary development of a persistent pathogen in a host organism, which can remain for decades. Apart from constituents like mycolic acids or PIMs, the cell wall of *Mycobacterium bovis* shows some special features. The fatty acids contain ornithine and salicylic acid as well as poly-ol fatty acids at a higher concentration [108, 115].

(V) Detection methods for Mycobacterium bovis and tuberculosis

There are different detection methods for *Mycobacterium bovis* which are based on:

- the cellular response to the agent
- the immunological/ humoral response to the agent
- the detection of the mycobacterium itself or its DNA and the host's pathological response [116].

There are three main tests for TB diagnosis detecting the cellular response. For the tuberculin skin test purified protein derivate (PPD) of mycobacteria is intradermally injected and a swollen and heated area on the skin is observed in case of a positive result. This test is routinely used today [108, 116].

For the γ-interferon (γ-INF) test, PPDs are intradermally injected and the cytokine γ-INF concentration as a consequence of the challenge and an immune response is measured using a sandwich immunoassay while the lymphocyte proliferation assay detects radio labelled lymphocytes (as a consequence of a bacterial challenge) in a flow cytometer [116-119].

For the analysis of the humoral response there are various test kits available. Fluorescence polarisation assays (FPA) detects the change in polarisation when an antibody binds to the surface of bacteria [117, 120]. MAPIA (multi-antigen print immunoassays) uses a mixture of different immobilised antigens on a membrane. The sample incubated on the membrane and the number of occupied binding sites can be measured [117]. ELISA test systems applying a recombinantly engineered antigen (Chembio) or MPB83 (glycosilated lipoprotein) as an antigen (Brock test) are also commercially available. However, all tests are either difficult to apply in the field or give just a poor indication of the actual infection status due to the fact that in many cases there is no immediate immune response. The test systems are simply too slow. For humoral responses there is also the problem of false negatives. For these reasons, culture remains the “gold standard” for tuberculosis detection but is extremely slow.

Mass spectrometric methods can be used to directly detect and identify infections. Using various GC-MS systems, some research groups found that bacteria emit organic derivates of alkanes (e.g. methylated cyclohexanes, heptanes, pentanes or cyclododecane) or aromatics (e.g. methylated benzene) while other C_4 to C_{20} molecules (conjugated dienes, malondialdehyde) have been identified as a product of oxidative stress via a mass spectrometer [81, 82]. Others found methyl-branched fatty acids or secondary alcohols which are breakdown products of the cell wall [121], different fragments of mycocerosic acid, an organic acid specific for mycobacteria cell wall, in sputum samples [122] or free tuberculostearic acid (TSA) in different other biological media (e.g. serum or cerebrospinal

fluid) [123]. Also liquid chromatographic (LC) methods such as thin layer chromatography (TLC) was used to separate and detect keto/- or mycolic acids [124], mycobactins and exochelins [125] and other glycolipids [126].
However, also these methods are highly impractical and not suited for field use. Hence, a cost effective and easy to handle device that is dedicated to precise in-field-diagnosis is highly desirable.

(VI) Pathogenisis and course of the disease

There are three disease states of tuberculosis:
Disseminated tuberculosis- primary tuberculosis, latent-dormant tuberculosis and active tuberculosis.
Disseminated tuberculosis is the result of direct extension of many small tubercles through the body. If untreated, this progressive systemic status will change to latent or active status with severe consequences, mostly in infants or debilitated persons with little or no hypersensitivity.
The latent dormant tuberculosis is the infection status appearing in most cases. The subject remains in this condition for a very long time without suffering any ill effects. Tubercles are observed in many cases. A critical situation appears only with a break down or a weakened immune response.
The active tuberculosis is the most dangerous infection status. After the immune response breaks down and bacteria disseminate into the blood vessels and air passages, necrosis follows and the infected individual acts as a source for further infections. Active tuberculosis has to be treated [108].

The main route of infection for humans and animal tuberculosis is via the respiratory route. *Mycobacteria tuberculosis*. *-bovis* or *–avium*, located in small droplets, are inhaled and access the lungs [127].

Since all mammalian organisms have an innate and an adaptive immune system alveolar macrophages try to phagocytose bacteria being hosted in the lungs. During this process small nodules are formed. After this step two reactions may occur.

Either macrophages are able to destroy the mycobacterium and defend the organism or bacteria survive within the macrophage. The reason for survival of the mycobacterium is the specialised cell membrane with its waxy outer layer that is able to resist the macrophage's antimicrobial defence. Moreover, some mycobacteria (*M. tuberculosis, M. bovis*) that reside in early phagosomes are able to block the phagosome maturation including phagolysosome formation [128-131].

However, in some studies, infected mice showed an increased host response when exposed to Mycobacterium bovis bacillus Calmette Guerin due to PIMs which induced the production of natural killer T-cells [132, 133].

Then, the mycobacteria containing macrophages carry the bacilli to the lymph nodes, trying to present phagocytosed bacterium fragments (antigens) by major histocompatibility complexes (MHC) for the specific immune response. There they present the antigens to the organism's antibodies if the bacteria were destroyed. Usually, the progress ends at this stage and is called disseminated tuberculosis which includes, as mentioned, persistence.

In the course of time, the tubercles may change theire composition in the lymph node basically because of calcification. Then they are called caseous

lesions. The lesions in the lymph nodes form X-ray detectable complexes that are termed Ghon complexes. The infection becomes latent dormant.

If a tubercle liquefies, they form air filled cavities that are the basis for a further spreading through the body, especially to intestines and kidneys [105]. This consequently leads to an infection of other organs and dramatically increases the severity of the disease. This infection status is called active or miliary tuberculosis.

As a consequence of the low doubling rate the disease develops slowly. Over the course of the disease, symptoms like fever, fatigue, and weight loss, in combination with cough or bloody sputum appear. If untreated, tissue destruction causing death follows [107,127]. The parallel appearance of tuberculosis and HIV/ Aids increases the problem for human health.

1.6.4 *Mycobacterium avium* ssp. *paratuberculosis* (MAP)

Mycobacterium avium is in the strict sense an umbrella term for *M. avium* ssp. avium (MAA), *M. avium* ssp. paratuberculosis (MAP) and *M. avium* ssp. intercellulare (MAI). All three subspecies can be termed as M. avium complex (MAC). MACs have a less pathogenic phenotype [112, 134].

Mycobacterium members of MAA cause infections and diseases in a wide range of different animals worldwide. MAA occurs in ruminants, wild and domestic ones, and in birds.

Mycobacterium avium ssp. *paratuberculosis* (MAP) has a less pathogenic phenotype compared to *Mycobacterium bovis* [112, 134]. MAP causes chronic inflammation of the intestinal tract of animals. It is the causative agent of paratuberculosis or Johne's disease that affects ruminants and other

animals. This pathogen causes chronic immedicable gastro-enteritis with the formation of cachexy which can lead to death and because of potential economic losses, Johne's disease is regarded as a serious problem in agriculture. Subclinically, MAP can colonise the gastro intestinal tract at an early stage of the animal's development. In the course of the disease, domestic animals excrete bacteria in their milk or onto pastures. Once there, it can be conveyed in water supplies. That is why it has a high prevalence in dairy cattle and is a bacterial disease of global importance. Because of the similarities of paratuberculosis/ Johne's disease and Crohn's disease and the possible transmission of MAPs to humans, a potential connection between both diseases is currently under debate [112, 134]. Relevant special feature of *Mycobacterium avium* ssp. *paratuberculosis* are the C_2 mycosides as a surface glycopeptides and the absences of any mycobactins [112, 127].

Paratuberculosis can be detected directly proving the presence of the bacterium in faeces or indirectly by culture and polymerase chain reaction (PCR) [135, 136]. However, direct detection requires end-stage subjects which have bacteria already in faeces and indirect methods have a limited sensitivity and specificity (55 % and 99 %, respectively) [137]. A safe diagnostic method is only possible on a group level and therefore not suitable for prevalence estimation. For these reasons, an alternative test would be desirable and one possible approach is the analysis of volatile organic compounds above serum or blood.

1.6.5 *Brucella* ssp.

Brucellosis is similar to MAP in that it is a global zoonotic disease and also causes severe animal and human health problems and economic costs.

Brucellosis is caused by bacteria of the genus *Brucella* and consists primarily of six classical species: *Brucella abortus*, *Brucella melitensis*, *Brucella suis*, *Brucella ovis*, *Brucella canis*, and *Brucella neotomae*. *Brucella abortus*, *Brucella melitensis* and *Brucella suis a*re a serious threat to human health due to the presence of major virulence factors (smooth lipopolysaccarides).

The detection of *Brucella* ssp. is routinely performed using indirect ELISA assays, competitive ELISA and the fluorescent polarisation assay (FPA) screens for antibodies or antigens in milk or meat. The test systems provide a generally good performance of detection of 99 % for both sensitivity and selectivity. However, the usage of *Brucella* ssp. antigens can lead to false positive serological results because there are other antigens showing the same structure such as *Yersinia enterocolitica* [138, 139]. In combination with the fact that a large number of animals need to be tested for surveillance in Europe, an expensive testing program is launched. A new high sample through-put testing method which is inexpensive and does not exploit the detection of *Brucella* ssp. antibodies or antigens is desirable in order to eliminate the 1 % of the false positive test results. One potential approach is the analysis of volatile organic compounds in the headspace of clinical samples.

2. Animals, materials and methods

Methodological and biological variation can significantly change e-nose sensor responses. The biological variation may be caused by a number of factors such as gender, living conditions and the nutrition of animals or changes in their physiology. Methodological variation occurs due to inconsistent sensor responses and non-standardised or non-optimised sampling methods. Therefore, it is necessary to consider both types of variation within a group of clinically healthy individuals and variation between infected and non-infected subjects. In order to elucidate variation caused by the individual, over time and during infection, the following experimental studies were conducted, analysing the headspace of serum and urine:

1) Serum samples from clinically healthy calves and cattle were obtained to elucidate changes in headspace due to ageing, nutrition, feeding and over time (day to day as well as circadian variability).

2) Urine samples from clinically healthy calves and cattle were obtained to investigate the same changes as for 1).

3) Calves were experimentally infected with *Mycoplasma bovis* (a respiratory infection with mild, latent and sub-clinical symptoms). Changes in headspace of serum samples due to infection were assessed.

4) Calves were experimentally infected with *Mannheimia haemolytoca* which is a respiratory infection with severe clinical symptoms. Changes in headspace of serum samples due to infection were investigated.

5) Cattle were experimentally infected with *Mycobacterium bovis* under application of different vaccination strategies (no vaccination, vaccination with

BCG (Bacillus Calmette- Guerin) and a recombinant BCG/Ad85a vaccination). Headspace was analysed to investigate differences between infected and non-infected individuals and between vaccination strategies.

6) Variability of headspace of urine samples from animals experimentally infected with *Mycobacterium bovis;* both unvaccinated and animals given a BCG vaccination were analysed.

Furthermore, serum and urine samples were obtained from naturally infected and healthy individuals as follows:

1) Serum from cattle naturally infected with *Mycobacterium avium* subspecies *paraTuberculosis* (paraTB).

2) Serum from cattle naturally infected with Brucella

3) Serum from badgers naturally infected with *Mycobacterium bovis*

4) Urine samples from cattle naturally infected with paraTB.

The following flowchart illustrates the overall strategy of the e-nose analysis again.

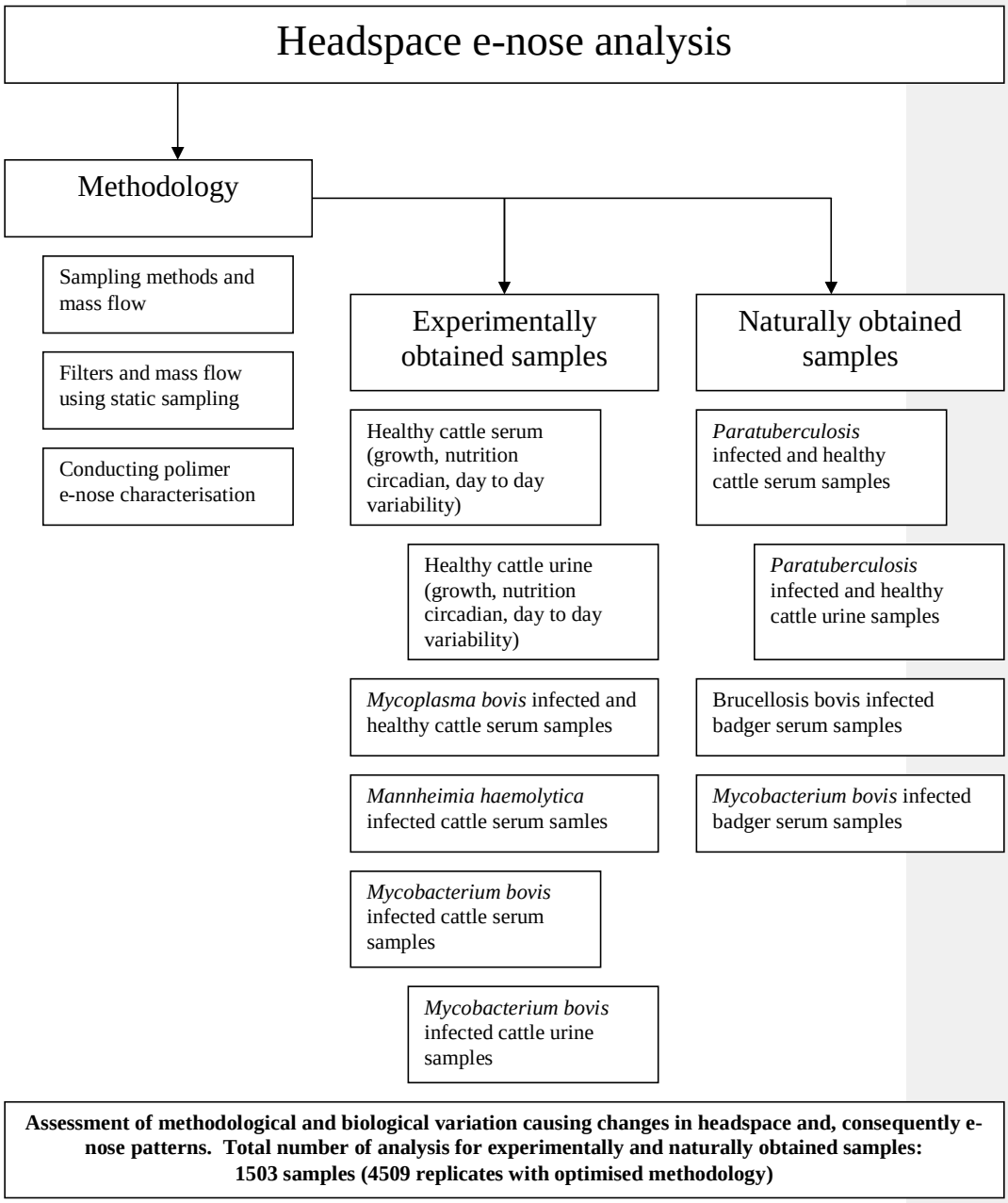
Headspace e-nose analysis
Methodology
Sampling methods and mass flow
Filters and mass flow using static sampling
Conducting polimer e-nose characterisation
Experimentally obtained samples
Healthy cattle serum (growth, nutrition circadian, day to day variability)
Healthy cattle urine (growth, nutrition circadian, day to day variability)
Mycoplasma bovis infected and healthy cattle serum samples
Mannheimia haemolytica infected cattle serum samles
Mycobacterium bovis infected cattle serum samples
Mycobacterium bovis infected cattle urine samples
Naturally obtained samples
Paratuberculosis infected and healthy cattle serum samples
Paratuberculosis infected and healthy cattle urine samples
Brucellosis bovis infected badger serum samples
Mycobacterium bovis infected badger serum samples
Assessment of methodological and biological variation causing changes in headspace and, consequently e-nose patterns. Total number of analysis for experimentally and naturally obtained samples: 1503 samples (4509 replicates with optimised methodology)

2.1 Methodological aspects of e-nose analysis

In order to analyse various samples using the conducting polymer based electronic nose (CP e-nose; Bloodhound ST214 Scensive Tech. Ltd., Leeds, UK) the sampling methodology needed to be investigated. In the following section, the effects of different types of sampling methods, the application of different filters, the stability of mass flows and the sensor response consistency over time are summarised. Further details are described in literature [140]. The CP e-nose contains an array of 14 conducting polymer sensors including an internal reference. The device has a reference- and a sample port as well as an inlet for carbon filtered ambient air which is used during the desorption phase. An integrated pump with a valve system that is piloted by the Bloodhound software controls the different air streams. A typical run consists of an equilibrium- and adsorption phase, a pause, desorption phase and a delay step. Duration of adsorption- and desorption phase and the number of replicates can be changed using the software.

2.1.1 Sampling methods and mass flows

The effect of *dynamic*- (i) and *static sampling* (ii) on the sensor response was investigated.

(i) Using dynamic sampling, a liquid sample (5 ml) was pipetted into a 30 ml duroplastic vial and directly connected to the e-nose sampling port. Two PTFE tubes penetrated the lid of the vial; one is inserted into the liquid (1) the other is the connection to the e-nose and samples the headspace (2) via a device-integrated pump (see figure 14). During the sampling, the headspace was

conveyed through the tube to the 14 sensor array causing a pressure difference in the vial (Δp). An incoming airflow compensated the pressure difference by bubbling environmental air through the sample. There is no controller in the e-nose to adjust mass flows.

(ii) For static sampling, Nalophan bags (KALLE, UK) were used. The material does not emit volatiles detectable by this e-nose and can be adjusted in size to its purpose. The bag is connected to the e-nose via poly-propylene tubes and Swagelok- and Luer fittings and sealed at both ends using plastic ties (Hellermann, Tyton, England). An internal pump delivered the headspace to the sensors array and the bag gradually collapsed. For comparability, the ratios of the liquid sample and the bag volume were calculated (V_{SAMPLE}/ $V_{HEADSPACE}$).

ST214 e-nose dynamic (left) and static sampling (right)

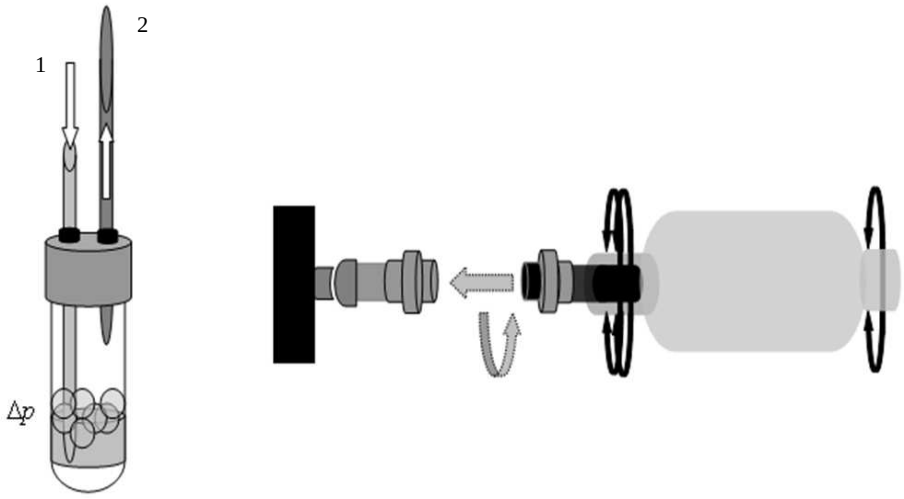

Figure 14: Dynamic (left) and static sampling (right) for e-nose analysis. An incoming air stream (1) causes a pressure difference and a variable flow of headspace reaching the e-nose while for static sampling there is a constant pressure and an equilibrium.

To assess the stability of mass flows and consistency over replicates, different experimental setups were arranged attaching a Luer fitting, an AMW 3300V mass flow controller, a 0.45µm Sartorious Minisart filter and both sampling devices to the e-nose. Changes in mass flow were monitored during the adsorption phase when sampling reverse osmosis water (ROW) at a constant temperature of 25°C.

2.1.2 Different filters and mass flows using static sampling

The mass flows of eight successive replicates were monitored using a similar experimental setup as described above (section 2.1.1). A 2-butanol solution was analysed which gave 10 parts-per-million (ppm) of 2-butanol in the headspace at 25°C. Two different types of filters, a 0.45µm Sartorius Minisart and a 0.20 µm PVDF Whatman Acrodisc, were attached to the ST214 e-noses. The changes to signal intensity (quantitative changes) and signal pattern (qualitative changes) of a CP e-nose (ST214) were studied. For comparison, ROW was also analysed either with no filter or the 0.45 µm filter at a constant temperature of 25°C.

Selected ion flow tube mass spectrometry (SIFT-MS) was also used to investigate quantitative and qualitative changes in samples after passage through a filter. SIFT-MS is a real-time mass spectrometry method that provides quantitative data on compounds present. Full details are given in Smith, D., 2005 [54]. Duplicate sample bags containing 0.5 ml of bovine serum and filled with 0.7 L hydrocarbon-free air were analysed with and without a 0.20 µm PVDF filter (Whatman, Acrodisc LC13). The concentrations

of key marker compounds such as water, acetone, methanol and ammonia were measured.

2.1.3 Conducting polymer e-nose characterisation

Variability of the two CP e-noses from the same production batch (both ST214 e-noses manufactured under the same conditions within the same period of time) across four time points over a day was assessed using bovine serum sampled statically. Small bags (0.8 L) were used for each time point and device. The serum sample volume was 0.9 ml which leads to a corresponding sample to headspace volume ratio of 1.2^{-3}. The temperature was maintained at 25°C. After incubating each bag for 15 mins at 25°C to establish an equilibrium, the bags were subsequently analysed (7 replicates) every two hours on four occasions beginning at 10:00 to assess the following factors:

- Device (describing variance caused by the e-noses)
- Time point (describing variance caused across time)
- Replicates (describing differences due to repetitive sampling across one analysis).

2.2 Apparatus and applied sampling procedures

In order to analyse the headspace of serum and urine samples different devices and sensing principles were applied. Conducting polymer electronic noses (CP e-noses) and Selected Ion Flow Tube Mass Spectrometry (SIFT-MS) were used in parallel to analyse sample headspaces. As a consequence of better stability and repeatability, static sampling was used for headspace analysis, only (see section 2.1). Methodological variations and in particular

temporal inconsistent sensor responses were generally compensated by analysing samples in a random order according to infection status or sampling times. This leads to an equally distributed variation over sampling times or infection status which can be observed as a broad overlapping between groups (e.g. Box and Whisker plots) but, on the other hand, does not allow the consideration of single values within the dataset. This is also the reason why principle component analysis (PCA) cannot be used for capturing variance since it reflects a) methodological variation and b) requires and considers single values rather than datasets of groups (see also section 2.7).

2.2.1 CP e-noses application

As a result of methodological investigations, static sampling was found to be much more reliable with respect to mass flow stability and comparability (see section 2.1). Therefore, only static sampling was applied for analysis. Furthermore, after e-nose analysis, the same bags were also used for SIFT-MS analysis. Thus, identical sampling methods could be used with both methods.

According to the experimental plan, samples were carefully thawed and pipetted into the prepared Nalophan bags (1.6 ml of serum, 2 ml of urine, otherwise stated). The bags (volume of 850 ml) were labelled encoding the origin and infection status of each sample, filled with zero grade air and left for incubation for 15 minutes at 25°C. The room temperature needed to be monitored due to the lack of a temperature controller on the e-nose. After incubation, the bags were attached to the e-nose for headspace analysis as described in section 2.1.1. The times for adsorption and desorption were 20

seconds and the total time for each of the seven replicates was 55 seconds. The divergences (e.g. maximum step response) for each analysis was saved as a text file (*.txt) for replicates 3 to 5 and used for statistical analysis. Data from irregular conditions during the sampling process such as power cuts, damaged bags or any type of device problems were excluded from analysis.

2.2.2 SIFT-MS

Selected ion flow tube mass spectrometry (SIFT-MS) is a method which allows real time analysis of gaseous samples. The sample composition can be quantified analysing multiple ions over time (MIM, multiple ion mode) or mass spectra over replicates (FSM, full scan mode). SIFT-MS was used in the latter mode to analyse the headspace generated from serum and urine samples using the static sampling bags also used for e-nose analysis before. The bags were placed into an incubator for 15 minutes of incubation (SI50, Stuart Scientific, England) at a constant temperature of 40°C and connected to the SIFT-MS capillary. An upstream vacuum leads to an inflow of headspace through the capillary to the flow tube at a constant flow rate and temperature. There, headspace is ionised using one of the three precursor ions (H_3O^+, NO^+, O_2^+). The product ion is flushed through the tube with a carrier gas and conveyed to the mass spectrometer and the detector in a vacuum environment. A quadrupole mass filter separates the ions prior to detection by an electron multiplier, and mass spectra are obtained with a maximum mass to charge ratio (m/z) of 10 to 200. Ten replicates were taken each with a sampling time of 5 seconds. The replicates obtained over the whole m/z range per sample were averaged. Further details have been

described in the literature [54]. Data obtained from the experiments were saved and transferred to a colleague who was undertaking multivariate data analysis of SIFT-MS data.

2.3 Animals, housing, health and savety

All individuals included in experiments were held under controlled conditions according to the guidelines for animal welfare in the European Union. In studies of uninfected control animals and in studies with experimentally induced infections the subjects could be regarded as clinically healthy (symptom free, no fever, diarrhoea, or respiratory symptoms such as cough, nasal discharge or ocular secretions) over the complete period of the study or before infection, respectively.

The studies with clinically healthy individuals and *Mycoplasma bovis* and *Mannheimia haemolytica* were performed in a specialised veterinary institute (Institute of Molecular Pathogenesis at the 'Friedrich–Loeffler–Institut' (FLI; Federal Research Institute of Animal Health), Jena, Germany) under supervision of veterinarians and had ethical approval from the Institutional Commission for the Protection of Animals of the state of Thuringia (registration number: 04-02/03 for the experimental infection with *Mycoplasma bovis* and registration number: 23-51/99 for the experimental infection with *Mannheimia haemolytica*, respectively). The individuals infected with *Mycobacterium bovis* were held at the Veterinary Laboratory Agencies, VLA, Weybridge, UK. Vaccination and infection were also conducted under standardised and controlled conditions and cattle were under daily

supervision of veterinarians. The complete risk assessment can be requested at both institutes.

In both facilities, the FLI and the VLA, environmental conditions such as temperature and humidity were kept constant to ensure reproducibility but may vary from study to study. In general, the calves were fed with commercially available milk substitute and coarse meal. Water and hay were available *ad libitum* (otherwise stated). Cattle were fed with hay and groats.

Mycobacterium bovis is a pathogen which requires a category 3 environment for analysis. Therefore, breath samples were UV sterilised and heated up to 80°C and above before analysis. Blood samples from infected animals were cultured to see whether the bacterium is present in the samples or not and a full risk assessment was carried out to ensure no bacteria leave the safe environment. All animal UK experimentation was undertaken under authority of the UK Animals (Scientific Procedures) Act 1986 following local ethical approval. All laboratory work was conducted after local risk assessment. All work involving ACDP (Advisory Committee on Dangerous Pathogens) class 3 pathogens was additionally approved by the Biological Agents Advisory Committee of the VLA.

Mycoplasma bovis and Mannheimia haemolytica are not transmitted to humans. Cattle and urine samples from subjects infected with paraTuberculosis and Brucellosis were from field subjects.

In contrast to breath samples, the probability for all pathogens for their presence in blood and urine and their number are extremely low.

During all headspace analysis, the Ph.D student worked under GLP (good laboratory practise) condition wearing gloves and a labcoat. A hygene

protocol was followed including cleaning and disinfecting the workspace and autoclaving used and disposable materials. The Ph.D student was vaccinated with BCG in 1980 and against Hepatitis A in 2008.

2.4 Study designs and experimental challenges

2.4.1 Biological variability of serum samples obtained from healthy cattle

(I) Changes in serum samples due to growth or ageing and nutrition

In this trial methodological as well as physiological changes due to growth and nutrition were assessed.

Three conventionally reared calves (breed Holstein) aged four months were held over a period of 40 weeks in stables at the FLI. Serum was obtained and stored as described in section 2.6 and 60 samples were delivered as triplicates (in total 180 samples) to Cranfield University for analysis. The headspace of serum was analysed and changes of e-nose patterns over the complete study were investigated.

(II) Changes in serum samples due to circadian and day to day variability

Furthermore, circadian variation and day to day variation of clinically healthy cattle were investigated. Six conventionally reared calves (breed Holstein) underwent three identical tests, each lasting from 06:00 to 20:00 per day and per calf. The time difference between consecutive tests per subject was 12 ±1 days (mean ±SD). On each sampling day, one individual was separated from the group and venous blood samples were collected in a 2 h interval for eight time points. The calves were fed with a milk substitute three times a day at 7:00, 15:00 and 21:00 in their stables at the FLI.

144 serum samples were obtained as described in section 2.6 and sent to Cranfield University.

2.4.2 Biological variability of urine samples obtained from healthy cattle

Similar to the experiments described above (section 2.4.1), biological variability of urine samples from clinically healthy subjects were investigated. Changes between subjects of different ages (three calves aged 6 to 9 weeks and four cattle aged 47 to 58 weeks) and differences over time (circadian and day to day variation) were determined. Temporal profiles of sensor responses analysing serum headspace were obtained.

The animals were conventionally reared (breed Holstein). Over a period of 16 days, urine samples were obtained from all subjects six times with an averaged interval of three days (3 d ± 1.41, mean ± SD). Samples were taken from each animal at four time points per day; before and 1 h after feeding in the morning (time points 1 and 2) and before and 1 h after feeding in the afternoon (time points 3 and 4). 168 samples were frozen at -80°C and sent to Cranfield University for headspace analysis (also see section 2.6).

2.4.3 Variability of serum samples after *Mycoplasma bovis* infection

As an example of a mild infection of the respiratory tract at a subclinical level, 30 conventionally reared calves were infected with *Mycoplasma bovis* at the FLI, Jena. Each calf inhaled 300 litres of an aerosol generated from 10 ml PBS (phosphate buffered saline) containing 4×10^8 - 1×10^9 cfu / ml (colony forming units per millilitres) of *Mycoplasma bovis* strain Bx 89/97 using a jet nebuliser and a tightly fitting face mask. 2 x 5 ml of culture was also applied

intranasally per animal. Control animals were given the PBS only. Animals were necropsied 3, 7, 10, 14, 21, and 35 days *post infectionem*, respectively (table 3) for pathological studies.

Table 3: Number of individuals sampled over the course of the study. Due to post-mortem investigations the number of challenged and placebo treated individuals decreased at the end of the study.

	ante inoculation	***post inoculation***												
Time points	minus 11 d to 0	1h	6h	1d	2d	3d	5d	7d	10d	14d	17d	21d	28d	35d
Test subjects (challenged)	24	24	24	24	24	24	18	18	12	6	4	4	2	2
Control subjects (placebo)	6	6	6	6	6	6	5	5	4	3	2	2	1	1

ELISA tests, cultures and pathological investigations were performed by the staff of the Friedrich-Loeffler-Institute in Jena.

The objective of this study was to examine differences before and after inoculation as well as between challenged individuals and placebo treated negative control individuals. Temporal profiles of sensor responses analysing serum headspace were obtained.

Therefore, blood samples were taken 11 days, 2 days and directly before challenge (*ante inoculation*, *a.i.*) and on 13 time points after challenge (*post infection*, *p.i.*) as shown in table 3.

329 serum samples were obtained as described under 2.6 and sent to Cranfield University for headspace analysis.

2.4.4 Variability of serum samples after *Mannheimia heamolytica* infection

(I) Study design and sample collection

A total number of 20 conventional cross-bred calves were included in a *Mannheimia heamolytica A1* (*M. haem*. A1) infection study at the FLI, Jena. The subjects were housed in 4 groups and each consisted of 5 calves. The individuals were fed and held as stated in section 3.3. Aged 52 ± 5 days (body weight: 64 ± 6 kg, all means ± SD), all calves were inoculated with *Mannheimia haemolytica* biotype A serotype 1. As described by Schimmel, D., 1987 [141], an 18-hour broth culture of *M. haem.* A1, strain 2353 (P588) was used for the experimental challenge resulting in an acute respiratory infection. Ten ml of the culture containing 1.5 - 2.0 x 10^9 cfu per ml was administered intratracheally per calf and day on two consecutive days (the interval between the two inoculations was 30 hours). Clinical symptoms such as appetite, respiratory rates and body temperature were recorded over the whole study. Surviving calves were euthanised for necropsy five days after the first inoculation of *M. haem.* A1.

For each animal, two jugular venous blood samples were collected before experimental infection (7 days and one hour *ante inoculation*; -7d *a.i*., -1h *a.i.*), and 8 blood samples were obtained *post inoculation* (*p.i.*) as follows: 3h, 6h, 12h, 24h, 48h, 3d, 4d, and 5d after the first bacterial inoculation. Serum was harvested by centrifugation (20 minutes at 1500g) and stored at -80°C until analysis at Cranfield University. Serum headspace of 178 samples was analysed and temporal changes and differences in patterns between pre- and post-inoculation samples were investigated as described in sections 2.2.1 and 2.6.

(II) Analyses of acute phase proteins (APP)

In order to relate the changes of acute phase marker proteins (APPs) to changes in headspace composition, the concentrations of the Lipopolysaccharide binding protein (LBP) and Haptoglobin (Hp) were measured by the staff of the Institute of Bacteriology and Mycology, Veterinary Faculty at the University of Leipzig (Germany) as follows:

Concentrations of LBP in sera were measured using an enzyme-linked immunosorbent assay (ELISA) described elsewhere [142]. Intra- and inter-assay coefficients of variance were below 10 %. The detection limit of the LBP assay was 0.45 ng / ml.

Concentrations of Hp in sera were measured by means of an ELISA as described previously [142, 143]. The coating antibody was IgG (rabbit) anti-human haptoglobin (DAKO, Hamburg, Germany). The same antibody, but conjugated with horseradish peroxidase, was used as the detection reagent. Hp-standard was a calibrated bovine blood plasma. Calibration was done with a colorimetric assay (Tridelta Development Ltds., Greystones, Co., Wicklow, Ireland) and also against purified bovine Hp isolated by affinity chromatography. The detection limit of the bovine haptoglobin ELISA was 0.8 µg/ml and the intra- and interassay coefficients of variance were less than 11 %.

2.4.5 Variability of serum samples from *Mycobacterium bovis* infected cattle

In this study the headspace of blood samples from 15 calves experimentally infected with *Mycobacterim bovis* (*M. bovis*) at the VLA were analysed. All animals were infected with an *M. bovis* field strain from the UK (AF 2122/97)

by intratracheal inoculation of circa 2 x 10^3 cfu per ml as described previously [118, 144, 145]. Furthermore, five individuals were vaccinated with BCG and five with the recombinantly engineered vaccine BCG/Ad85a 14 weeks before and 6 weeks *ad* boost as follows:

BCG was injected subcutaneously in the side of the neck of BCG SSI (BCG Danish Strain 1331, Statens Serum Insitute, Copenhagen, Denmark). 10^6 cfu was suspended in 1 ml of PBS. Ad85a was intradermally injected in the side of the neck with a concentration of 2 x 10^9 pfu (plaque forming units) suspended in 0.5 ml PBS. Five individuals were positive controls.

The status of the infection was confirmed by analysing the collected blood and cultures for γ-INF concentration using the gamma-interferon ELISPOT assay as described [118, 144-147]. Cytokines present in the supernatant of the culture such as γ-INF, IL4, TNFα, IL10, IL17, FoxP3, GAPDH were also determined using cytokine quantitative RT-PCR [148-151]. These analyses carried out by the VLA, Weybridge are intended to support and underline ELISPOT results.

All individuals were sampled for four times: The samples for week 0 (time point 1) were taken immediately prior to infection. Samples from weeks 2 to 4 (time points 2 to 4) were obtained after infection. There were no samples obtained at time point 3 for all individual vaccinated with the recombinate Ad85a. One individual was classified incorrectly regarding its infection satus. Changes in e-nose signal patterns were investigated and referred to the different treatment groups (no vaccination, BCG and BCG/Ad85a vaccination) in order to discriminate between groups and between pre- and

post-inoculation. Also changes in responses for all 49 samples over the course of the study were investigated.

2.4.6 Variability of urine samples from *Mycobacerium bovis* infected cattle

In a second trial, 10 cattle were infected with *M. bovis* as described above. Five individuals were BCG vaccinated and five animals were positive controls as mentioned in section 2.4.5. Each individual was sampled four times, two times before infection and twice after infection over a period of 15 weeks. One urine sample per time point and individual was taken as described and frozen at -80°C. All samples were sent to Cranfield University for analysis to investigate differences in headspace between pre- and post infection samples and between urine from controls and BCG vaccinated individuals. In total 33 samples were used for analysis.

Post mortem examinations and the pathological status of lungs and lymph notes were determined 28 weeks after infection as described [144]. The VLA personnel performing the post mortems and scoring tissues were blinded to the vaccination status of the animals under examination.

For lung tissue a scoring system was established: 0, no visible lesions; 1, no gross lesions, but lesions apparent upon slicing; 2, <5 gross lesions with diameters of <10 mm; 3, >6 gross lesions with diameters of <10 mm, or a single distinct gross lesion with a diameter of >10 mm; 4, >1 distinct gross lesion with diameters of >10 mm; 5, gross coalescing lesions. The scores of the individual lobes were added up to calculate the lung score.

For lymph nodes the scoring was as follows: 0, no necrosis or visible lesions; 1, small focus (1 to 2 mm in diameter); 2, several small foci, or a necrotic area of at least 5 by 5 mm; 3, multiple necrotic areas of at least 5 by 5 mm

distributed throughout the node, or one necrotic area affecting >5% of the node.

Both lymph node and lung pathology scores were added to determine the total pathology score per animal. All scoring was performed by the same operator for all animals to ensure scoring consistency.

2.5 Samples obtained from naturally infected individuals

2.5.1 Variability of healthy and paraTuberculosis infected serum samples

Serum samples from cattle naturally infected with *Mycobacterium avium subspecies paraTuberculosis* (paraTB) were used to investigate differences in headspace due to infection status. The samples came from different farms in Germany. Housing and feeding were not equally standardised. One blood sample per individual was collected at different time points. 43 samples were confirmed paraTB positive and 24 samples were negative. Except for four samples, all positives were found to excrete paraTB as a consequence of the systemic infection. For 12 individuals the clinical and pathological status including the pathological score was determined. A clinical score was introduced as follows: 1 = none, 2 = latent evidence and 3 = clinical evidence. A similar pathological score was applied: 1 = none, 2 = slight, 3 = moderate and 4 = severe. Serum was obtained as described in section 3.6 at the 'Friedrich-Loeffler-Institut', Jena, Germany, frozen at -80°C and sent to Cranfield University for analysis. Gender, nutrition and age were unknown. Headspace was analysed in order to discriminate between paraTB positives

and negatives. Sensor responses were related to clinical and pathological scores.

2.5.2 Variability of healthy and Brucella infected serum samples

Serum samples from cattle naturally infected with *Brucella* were analysed and compared to samples from non-infected animals in order to investigate differences in their in e-nose responses when exposed to their headspace. One sample per individual was collected. 26 samples came from cattle with a confirmed *Brucella* positive infection and 24 samples were obtained from confirmed negatives. The samples with a positive status were free of any co-infection. Animals and housing were not standardised and samples were collected over a long period of time (1983-2004) by the Laboratory Veterinary Agencies, VLA, Weybridge, UK.

Serum samples were frozen at -80°C and sent to Cranfield University for analysis. Gender, nutrition and age were unknown. Headspace was analysed in order to discriminate between Brucella positives and negatives

2.5.3 Variability of healthy and *Mycobacterium bovis* infected serum samples from badgers

In this study, 244 *post-mortem* badger samples were provided by the VLA (Weybridge, UK) for analysis. All samples were tested for a tuberculosis infection by VLA staff using a culture method and commercially available γ-interferon test kit (see section 2.4.5). The samples were classified into 4 groups regarding their culture- and γ-interferon status, respectively (+ +/, + -/,

- + and - -). According to this, the + + and - - samples were selected and analysed in order to minimise the risk including samples with an unclear status. Apart from the culture and γ-INF status no further information such as gender, diet and age were known. The place where they lived, the anaesthetic or the influence of the environment (e.g. their diet, time since last meal etc.) was unknown as well. Differences in headspace between positives and negatives as well as variation between individuals were assessed.

2.5.4 Variability of healthy and paraTuberculosis infected urine samples

Urine samples from 29 cattle were obtained to determine differences in headspace due to *paraTuberculosis* (paraTB) infection. The individuals came from three different farms in Germany. One blood sample per individual was collected. 19 of the samples were confirmed to be paraTB positive and ten samples were classified as negative. All negatives came from one location. The variation between samples coming from the same location was also assessed.

2.5.5 Comparison of serum and urine samples

E-nose data from serum and urine samples were compared in order to see differences caused by different diseases in a complex data matrix. Samples from clinically healthy individuals were compared to healthy control samples and to samples from infected individuals. At first, *experimentally obtained serum samples (I)* were compared to each other followed by a comparison of *all samples obtained from naturally infected individuals (II)*. Finally, all *serum samples (experimental and natural, III)* were compared to each other. Data

from analysis of *experimentally and naturally obtained urine samples (IV)* were also compared to each other (table 4).

Table 4: Overview of samples from experimentally and naturally infected individuals. All serum samples were compared to each other. All urine samples were compared to each other.

Collection	Serum samples	Urine samples
experimentally	Healthy, section 2.4.1 (I/II)	Healthy, section 2.4.2
	*Mycoplasma bovis**, section 2.4.3	
	*Mannheimia haemolytica**, section 2.4.4	
naturally	*Mycobacterium avium subspecies paratuberculosis** (paraTB), section 2.5.1	paraTB *, section 2.5.4
	*Brucella**, section 2.3.2	
	Mycobacterium bovis (badgers), section 2.5.3	

* contain healthy control samples

2.6 Serum and urine collection and preparation

Venous blood samples were obtained following the study design via catheterized vena *jugularis dextra* using serum MONOVETTE (Sarstedt AG & Co, Nuembrecht, Germany). Blood samples were centrifuged (Labofuge 400R; Heraeus, Germany) at 3939 g for 10 minutes otherwise stated.

Urine samples were taken directly from the individual and, if necessary, separated from faeces using a centrifuge. The possibility of bacterial contermination was identical for all samples, infected and uninfected and the probability for bacterial growth has to be considered as low. Serum and urine samples were frozen immediately after collection, stored at -80°C and delivered to Cranfield University for analysis. There, serum and urine headspace were analysed using e-nose and SIFT-MS in parallel under application of static sample analysis as described in section 2.1.1. All samples

were blinded with respect to their infection status and analysed in a random order.

2.7 Data analysis

Since SIFT-MS data analysis is the Ph.D project of another student, the following section will only focus on e-nose data analysis.

When dealing with e-nose data large matrices of data are generated. E-nose responses are generally unspecific which is why a technique is needed to extract the essential information. One approach is to apply Principle Component Analysis (PCA) or Discriminat Function Analysis (DFA). However, the problem with these techniques is that it requires a stable analysis system regarding the sampling process and the e-nose itself (e.g. consistent responses, room temperature independence) which was not the case for this in this project and for this particular e-nose. Furthermore, is appears unlikely, that the e-nose was stable during analysis in the previouse project which led to major publications (e.g. Fend *et al* [47]).

In the past, the signal to noise ration was tried to improve but most of the applications did not consider potential disturbances which are statistically picked up as variance e.g. using PCA. Therefore, it was urgently necessary to go back to uni-variate statistics and to consider the change of each sensor separately in order to elucidate which of the overlapping variances actually influences the sensors to change its response. This enables also the investigation of the impact of all parameters in the sensor panel assuming the environmental conditions are included into the statistic analysis. For this

reason, univariate statistics were applied first and the conditions were investigated under which uni- and multivariate statistical approaches are valid. By separating methodological and biological variation it can be determined which type of variation changes the e-nose pattern.

Before starting e-nose data analysis, data from replicates three to five of all samples were extracted from its text files and unified as one matrix. Those three replicates previously proved to be consistent in their responses [140] (also see section 3.1). The data matrix was then merged with a second matrix containing parameters which encode for sampling time, analysis time, infection status or others to determine exactly the methodological and biological status of each sample. Due to the methodological variation investigated before, univariate data analysis techniques were mostly used to investigate changes in sensor responses due to both, methodological and biological causes. The complete matrix containing parameters and data is used applying different analysis techniques and three different software packages. Linear regression and multifactor ANOVA (mANOVA) were applied to investigate the impact of different factors on the sensor response (e.g. divergence, maximum amplitude of signal in sample analysis) using SPSS (version 11.5, 2002), Statgraphics (version 4.0, 1999) and Matlab 2006b including the PLS toolbox (version 3.5, Eigenvector Research Inc.).

MANOVA is a technique which calculates the total variance (second moment of distribution) as the sum of the squared standard deviations. X is the expected value while μ is the deviation from X.

$$\mathrm{var} = E((X - \mu)^2)$$

It then refers the total variance back to all parameters that are linearly independent and weights the variance of a certain factor.

$$\frac{\mathrm{var}_{total} = n_1 \times \mathrm{var}_1 + n_2 \times \mathrm{var}_2 + ...n_n \times \mathrm{var}_n}{n_1 + n_2 + ...n_n}$$

Skewness and kurtosis of the data are calculated as the third and fourth moment of distribution, respectively.

$$skew = E((X - \mu)^3) \qquad \text{and} \qquad kurt = E((X - \mu)^4)$$

Spearman's rank correlation (Statgraphics) was used to investigate relationships between parameters and data that were not normally distributed. It ranks values from the lowest to the highest and correlates data to each other. Furthermore, the multiple range test (MRT) was applied to investigate significant differences between groups and to check if these groups were homogeneous within the entire dataset. Similar to mANOVA, MRT is focused on certain parameters (e.g. infection status) and does not necessarily reflect the differences of the complete dataset since one factor may not cause the largest variance for all data. However, using this method, also significant differences of factors which cause only little total variation can be assessed.
The level of significance for these analyses was $P \leq 0.05$ and the impact of each factor on the result was given as t-values.
Results were displayed as Box-Whisker plots, tables and heatmaps.

The interquartile range for Box and Whisker plots ranged from 25% to 75% of all data. The median was given as a line in the box. Outlier values (O) are 1.5 to 3 times of the length of a box away from the median and extreme values (*) are further away than 3 times of the length of the box.

Using Matlab, a modularly built programme was written that also performs mANOVA and gives the results as Box-Whisker plots. Furthermore, it displays so-called heatmaps. With this method the averages of each sensor over all groups are calculated and response of a particular group is then referred to the average. Divergences above the average are displayed in red, below the averaged in blue. Raw data, auto-scaled and mean-centred data was used (explanation see below).

The programme displays an overview of means and medians of all sensors and gives the standard deviations. This roughly indicates the variation over replicates and whether data was normally distributed. Normal distribution is also shown as a histogram and as a table including data for skewness and kurtosis for each sensor.

Statistical results were compared with each other using all three programmes.

The only multivariate technique applied was principal component analysis (PCA). Using Matlab, PCA was performed on raw-, auto-scaled- and mean-centred data. Auto-scaling scales all values of a column of the data matrix by its standard deviation which eliminates different ranges or magnitudes of data. Mean-centring eliminates constant offsets by subtracting the column mean from the single values. This data pre-treatment often eliminates instrumental drifts. Principal components which are independent factors of variance are plotted against each other. A so-called SCORE plot which is a scatter plot

describing at least the two principal components (PCs) shows the relationship between samples by displaying the variance of the matrix. Usually PC2 is plotted against PC1 since the first PCs represent the influences that cause the biggest variance. PCs are sorted, beginning with the component with the highest covered variance. With PCs the matrix can be reduced to the most relevant data by showing only differences between samples. The scatter plot may show a certain clustering that is caused by differences (variance) in the matrix values or in the samples, respectively. Discrimination can be observed.

3. Results

3.1 Methodological aspects of e-nose analysis

3.1.1 Sampling methods and mass flows

The Mass flow rate was 200 ml/ minute when the Luer fitting, the flow sensor and the bag fitting were attached. The further attachment of a bag used for static sampling did not change the mass flow rate significantly. However, when attaching the vial for dynamic sampling, flow rate decreased on average by 1/3 to 132 ml/min (see table 5) and was shown to have a large variation during the adsorption phase. The inconsistent mass flow rate was due to the bubbling process. The addition of a 0.45 µm Sartorious Minisart filter led to a reduction in flow rate by 1/3 (to 136 ml/ min) for static and 43% (115 ml/ min) for dynamic sampling compared to the original data.

Table 5: Flow rates in ml/min under different experimental setups

Type of sampling	Luer fitting/ flow sensor	Sampling device	0.45µm filter
Static	200	195	136
Dynamic	200	132	115

Due to the large variation during dynamic sampling, the stability over replicates was analysed for static sampling only. Constant flow rates were found for replicates 2 to 5 (set as 100%) while a minor decrease of 4% was found for replicate 1 and flow rates decreased by 15% afterwards. The

decrease in mass flow occurred with progressive collapse of the bag after approximately 75% of the bag volume was analysed.

3.1.2 Different filters and mass flow rates using static sampling

In this study, the effect of the application of no filter, a 0.45 µm Sartorious filter and a 0.20 µm Whatman filter were assessed comparing the sensor responses of the analysis of a 2-butanol solution giving a 10 ppm headspace at 25 C. The highest sensor responses, expressed as negative divergences (maximum step response), were seen when there was no filter (group 1, replicates 1 to 8). Attaching the 0.45 µm filter, the values became less negative (group 2, replicates 9 to 16); use of the 0.20 µm filter (group 3, replicates 17 to 24; figure 15) led to lowest changes in divergence. The significance of these findings was confirmed using mANOVA (SPSS, $P \leq 0.001$, raw data not shown). Both figures below show the same result but are roteted by 90°.

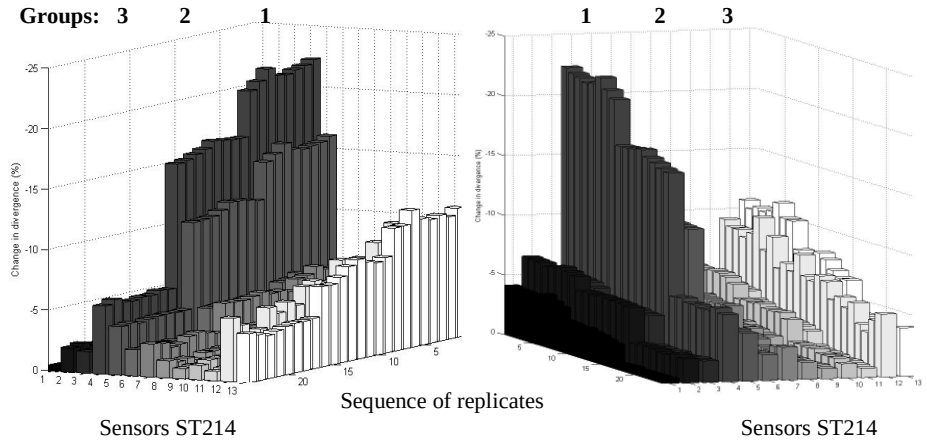

Figure 15: Replicates over all sensors using no filter (group 1), a 0.45 µm (group 2) – and a 0.20 µm filter (group 3). Divergences decreased with the pore size of the filter indicating quantitative changes due to filter application.

Beside the quantitative differences due to filter application, qualitative changes were investigated. Normalising e-nose responses for each type of filter to 100% (no filter, 0.45 µm and 0.20 µm filter, figure 16) shifts in e-nose responses were observed indicating differences in headspace composition after passage through the filters. While only minor changes were observed between no filter and the 0.45 µm filter, major differences in pattern were found between using no filter and the 0.20 µm filter.

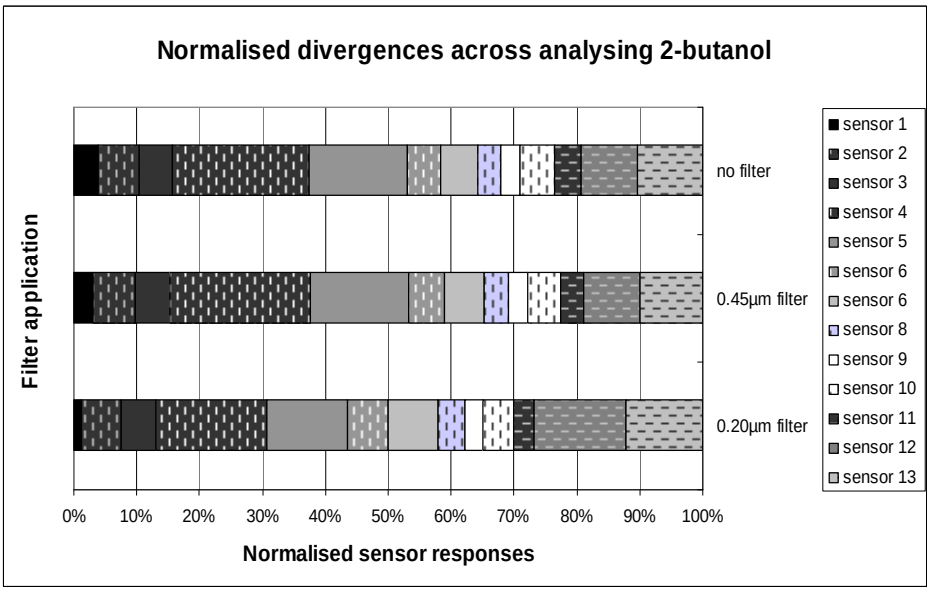

Figure 16: Normalised sensor responses using no filter, a 0.45 µm – and a 0.20 µm filter. Setting "no filter" as a reference, changes in the relative distribution of sensors were observed.

The SIFT-MS analysis of serum samples using no filter and a 0.20 µm Whatman Acrodisc filter revealed a significant reduction in mean concentrations of water by 17% (from 5.15 % for unfiltered samples to 4.26% for filtered samples), of ammonia by 29% (from 771 parts-per-billion (ppb) for

unfiltered and 547 ppb for filtered samples) and a significant increase in the concentration of methanol by 126% (from 424 ppb for unfiltered and 962 ppb for filtered samples).

Using all data for principle component analysis (PCA), the principle components 1 and 2 covered 99.90% of all variance. 2-butanol clusters were found on the left and showed a shift to the right end (figure 17, clusters 2, 4 and 5) under the application of different filters indicating that the main variance was caused by filter application. ROW could be discriminated from 2% (v/v) 2-butanol using no filters (clusters 1 and 2) but overlapped using a 0.45 µm Sartorious Minisart filter (clusters 3 and 4).

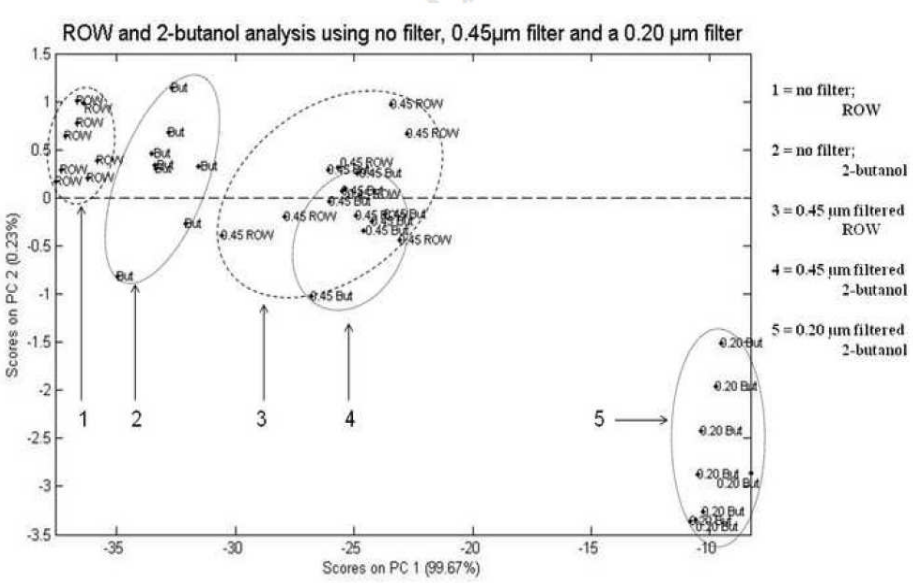

Figure 17: Principle component analysis of ROW- and 2% (v/v) 2-butanol samples. ROW and 2-butanol samples could be discriminated using no filter (1/2) while applying a 0.45 µm filter both substances appeared the same (3/4). Cluster 5 shows the 2-butanol sample using the 0.20 µm filter.

3.1.3 Conducting polymer e-nose characterisation

Sensor responses from all four time points obtained from two CPs of the same type and manufacturer were analysed using PCA. Principal Components 1 and 2 covered 99.10% of all variance (PC 1 covered 84.03%, PC 2 covered 15.07%). A clear discrimination between the e-noses was found using auto-scaled data (figure 18). Without pre-treatment, data could not be interpreted.

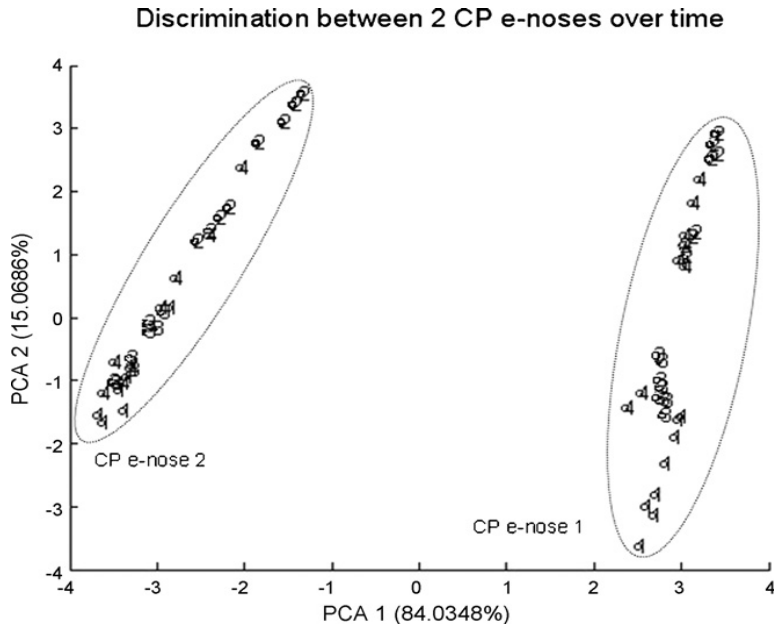

Figure 18: Principle component analysis of e-nose data. Clear discrimination was found between both ST214 CP e-noses covering most of the variance (84%). The remaining variation (15%) was due to changes in sensors responses over time analysing the same sample. Numbers next to data points indicate the time point.

Considering PCA plots in detail, time points 1 and 3 as well as 2 and 4 were grouped together for CP e-nose 1. Similar results were found for e-nose 2 however, responses of time point 4 were more scattered.

SPSS analysis using linear regression and multifactor ANOVA ($P \leq 0.05$) showed that the *device and* the *time points* significantly influenced the results and confirmed the Matlab findings (raw data not shown). Considering the responses over time for each device separately, divergences changed throughout the day for both e-noses (shown for one e-nose in figure 19). Sensor responses were highest at time point 1, decreased at time point 2 increased and decreased again for time points 3 and 4. Responses obtained at time points 1 and 3 were close as were 2 and 4. Results for the other e-nose showed a similar trend.

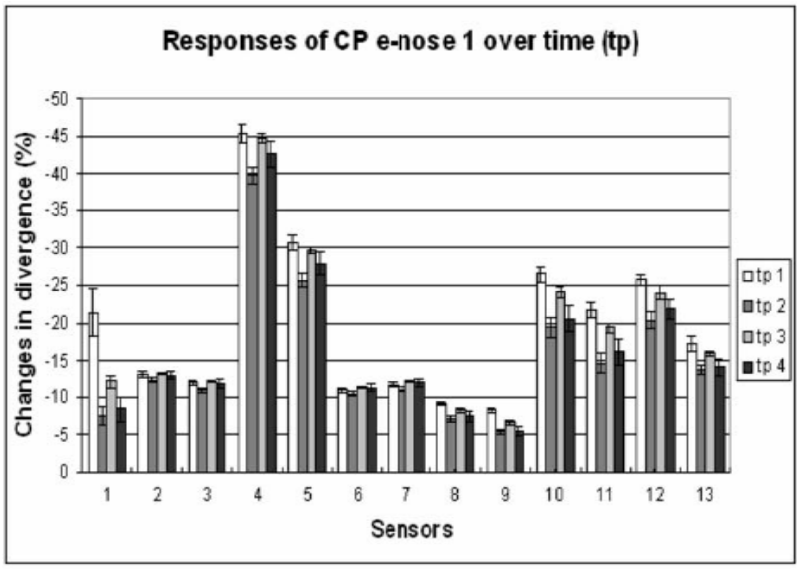

Figure 19: Responses of all 13 sensors over 4 time points. Divergences at time points 1 were largest and decreased at time point 2. At time points 3 and 4 sensor responses in- and decreased again. There was a declining tendency over all 4 time points.

For almost all sensors and both devices the temporal variation appeared sinusoidal, and there was a tendency for responses to decline across all time

points and for both e-noses, demonstrated using SPSS multifactor ANOVA ($P \leq 0.05$). These also confirmed similar PCA results, and in particular for PC 2 which grouped the same time points together. The methodological variation indicated significant changes in sensor responses due to the sampling method, filter application and over time (days and hours). Therefore, only static sampling without using a filter was used in order to reduce methodological variation. Furthermore, all samples were analysed in a random order to distribute the variation on all sub-groups of the dataset. Analysis of single samples was not possible and is not recommended for the studies described here due to the scattering of data. Means and medians of groups were used for statistical analysis instead and also need to be used for differentiating groups. Because of the scattering, ranges of data (groups) which may overlap may be significantly different considering their means or medians.

For the same reason PCA is not a valid approach with these datasets since it captures the methodological variation only and considers the variation (principle component) of the scattered single values representing the variance for each sample in consideration of replicates 3 to 5 and all 13 sensors.

Further details of these experiments may be found in Knobloch *et al*., 2009 [140].

3.2 Healthy and experimentally challenged individuals

3.2.1 Biological variability of serum samples obtained from healthy cattle

Sensor signal divergences of replicates 3 to 5 were used to investigate methodological and biological variation of the dataset as they were the most stable and representative. Three times the same set of 60 samples (in total 180 samples) were analysed to investigate methodological- (sensor long and short term stability) and biological variation (due to growth, nutrition and age).

(I) Changes in serum samples due to growth and nutrition

From the methodology point of view, the analysis sequence was found to be a linear combination of time- and day of analysis and was therefore excluded. The dataset showed significant temporal variation (both between days and from hour to hour) for responses of sensors 2 to 9, 12 and 13 (mANOVA, $P \leq 0.05$). E-nose responses for day one (analyses 1 to 30) were more negative than divergences of day two (analyses 31 to 60). Furthermore, responses obtained at day one showed a negative trend over the day while for day two values remained constant (see figure 20).

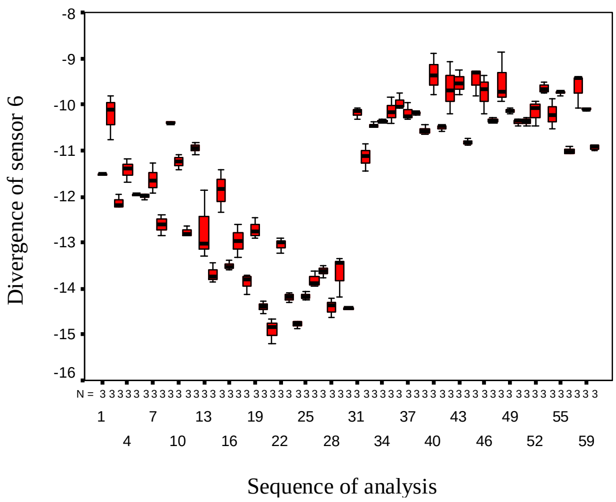

Figure 20: Sensor responses for sensor 6 over all analysis displayed in a sequence. There was a clear difference between day 1 (analyses 1 to 30) and day 2 (31 to 60). Divergences decreased for day 1 while they remained constant for day 2.

Replicate number had no influence on the sensor responses. When the triplicate set of samples was analysed, significant changes were observed (mANOVA, $P \leq 0.001$). For all sensors except for sensors 8 and 9, divergences became more positive (increased) from sets 1 to 3 (raw data not shown). When the identical samples were analysed at each of the two days, the sensor responses were not comparable indicating strong methodological variation.

Considering the first set of samples only, raw data and averaged data from individuals were considered in order to minimise methodological variation and to analyse biological variation. For example, figure 21 shows raw divergences (left) and ID averaged data (right) of sensor 3. From time point 1 to 7 responses remained with some variation at one level and dropped remarkably

at time points 7. For time points 15 to 20 the responses were increased again but remained lower than at the beginning. In the middle section (time points 8 to 14) significant biological variation was found. Results of averaged data were clearer than results from raw data. Like for the other sets, other sensors showed the same profiles.

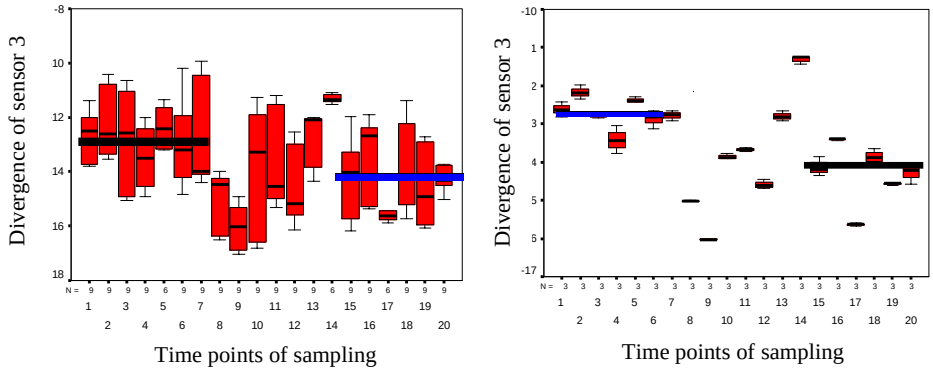

Figure 21: Raw divergences (left) and ID averaged divergences (right) for sensor 3. Responses remained at one level until time point 7, decreased significantly and reached a lower level beginning from time point 15. Between time points 8 and 14 there was variation and this is circled on the graph.

Results for the other two sets consisting of the same samples and analysed under the same conditions showed similar temporal changes over 20 time points.

For the second set, sensors 2, 6 to 9, 12 and 13 showed a decrease in non-averaged responses (figure 22 left) over time while for ID averaged responses, sensors 2, 3, 6 to 8, 12 and 13 significantly declined (figure 22 right). From time points 1 to 7 divergences remained approximately at one level but showed large variation from weeks 8 to 12. For time points 13 until the end divergences stayed (with some variation) at one level which was

below the level at the beginning. Results of averaged data were clearer than results from raw data.

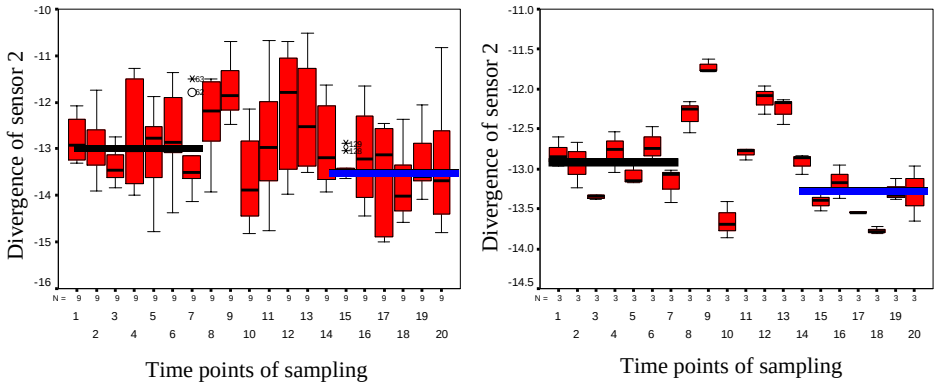

Figure 22: Raw divergences (left) and ID averaged divergences (right) for sensor 3. Responses remained at one level until time point 7, decreased significantly and reached a lower level beginning from time point 15. Between time points 8 and 14 there was variation

For the third set, all responses were inconsistent over 20 time points. No variation larger than the average variation over time (in the middle of the experimental study) was found for this set (mANOVA, $P \leq 0.05$).

Considering data from all three sets (data from all samples analysed for three times) a general decline in divergence over time was found to be statistically significant (mANOVA, $P = 0.01$) for sensors 2 to 9, 12 and 13 regardless of whether data was averaged or not. No variation in the middle section (around time points 8 to 14) was found for raw- and non-averaged data (data not shown). Similar mANOVA results were obtained using SPSS and Statgraphics. Results for Statgraphics and the Matlab programme were identical (see also the following sections).

The variation between weeks 8 and 14 as well as the two plateaus before and after this variable stage, showing a general decrease over time on a group level, indicate changes in headspace composition over a 40 weeks period which was associated with the maturation of calves to young cattle. This may be a result of changing physiology, perhaps due to changing from a predominantly milk based diet to one based on solids.

(II) Changes in serum samples due to circadian and day to day variability

In a second study, circadian variation, day to day variation (intra-individual variation) and inter-individual variation were assessed analysing the headspace of serum samples obtained from six clinically healthy calves eight times per day at three different days (in total 144 samples). Data of six samples were excluded from analysis due to irregularities during sampling process or data saving.

As in the study before, methodological parameters (e.g. day and time of analysis) significantly affected the sensor responses (mANOVA, $P \leq 0.05$, data not shown). Replicates had no influence on the divergences.

Considering biological variation, the effect of the day and time of sampling and the individual (ID) was investigated. Regarding the factor *sampling day*, sensor 1 was found to have more positive divergences at day three while sensors 2 to 8 indicated lowest e-nose responses at day two (multiple range testing, MRT, Statgraphics, $P \leq 0.05$). The remaining sensors were statistically homogeneous.

The influence of the *individual* was found to be significant (mANOVA, $P \leq 0.05$, data not shown) but without any particular trend.

The *sampling time* was found to have general positive tendency over time for sensors 2 to 9, 12 and 13 (figure 23, black dotted line, mANOVA, $P \leq 0.05$). A MRT (Statgraphics) revealed a tendency of a decline at 10:00 (dashed circle, after the first feeding) and a significant decrease of divergences at 16:00 (dashed circle, after the second feeding). The decline in response at 10:00 was significant for sensor 8.

MRT is based on mANOVA focussing on certain parameters (e.g. sampling time) and investiges signicant changes in divergence based at a group level by considering the means of the data, only. The overlapping of Box and Whisker plots arises from all types of variation (e.g. analysis time) but since all samples were analysed in a random order, the variation was distributed equally on all groups. Different letters indicate a 95% probability that the mean divergences are different or in other words, that they are 2 standard deviations away from each other with respect to a certain parameter (sampling time).

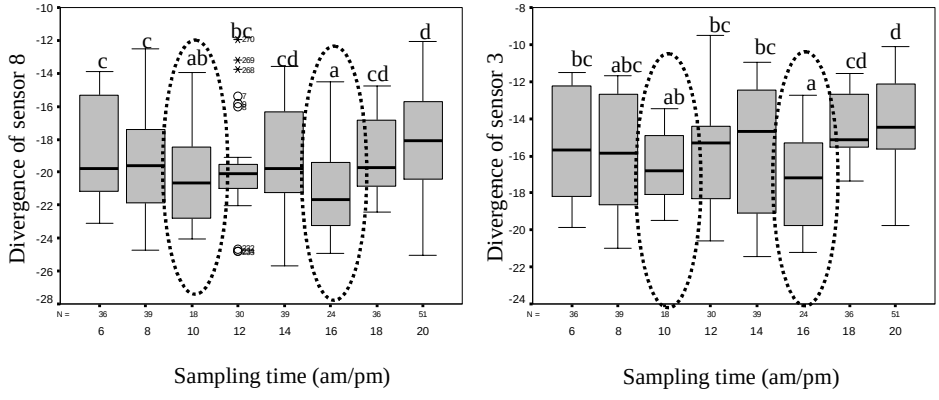

Figure 23: Divergences of sensors 8 (left) and 3 (right) over time. There was a general increase in sensor responses over time when exposed to serum headspace from all subjects. A decrease was observed at 10:00 am and 16:00 pm after feeding.

MANOVA was performed using all three programmes. The results obtained using SPSS were similar while results for Statgraphics and the Matlab programme were identical.

Despite the methodological variation and variation between individuals, an increase in divergence was observed over the day and a decrease in responses at 10:00 and 16:00 was found on a group level. The calves were fed shortly before the decline at 7:00 and 15:00 and this may account for the differences observed.

3.2.2 Biological variability of urine samples obtained from healthy cattle

The headspace of 168 urine samples (see section 2.4.2) obtained from clinically healthy cattle was analysed to investigate methodological and biological variation such as differences between juvenile and adult cattle (age), differences over the period of the trial (day to day variation) and differences over the day including the influence of feeding (circadian variation). Ten samples were not considered for analysis due to irregularities in sampling- or data handling.

Methodological parameters (e.g. time and day of analysis) significantly influenced e-noses responses (mANOVA, $P \leq 0.05$) but were equally distributed on all groups due to randomisation so could be accounted for.

As for biological parameters, the individual (ID), age, the sampling day and sampling time were defined and their influences was assessed. The different *individuals* did not show significant differences between each other (mANOVA, $P \leq 0.05$).

However, comparing *juvenile and adult* cattle, significant differences between the groups were found for the responses of sensors 1, 5 and 8 to 11 using SPSS (mANOVA, $P \leq 0.05$). Adult individuals had more positive divergences. For Statgraphics mANOVA, sensors 4, 5 and 8 to 13 showed significantly different responses due to age. MRT confirmed less negative divergences for adult cattle (Statgraphics, $P \leq 0.05$, data not shown). Spearman's rank correlation found changes in sensor responses due to different ages for sensors 5 to 8 and 11 to 13 and significant differences in sensor responses due to age were found for sensors 4, 5 and 8 to 13 applying the mANOVA with the Matlab programme. As an example, figure 24 (left) illustrates the responses of sensor 8 for juvenile and adult cattle. An overview of all responses including the changes of sensor 8 is displayed as a heatmap (right). Coparable to the results in section 3.2.1, significantly different divergences were found based at a group level regarding the factor age.

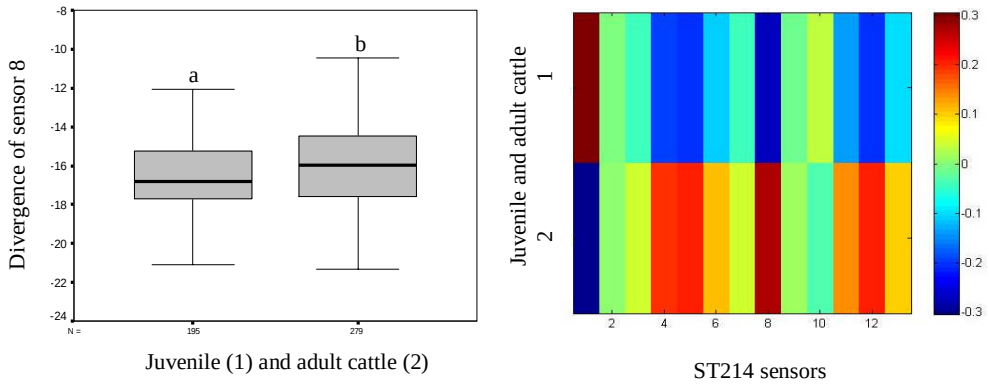

Figure 24: Adult cattle (2) had less negative divergence in comparison to juvenile cattle (1) for sensors 8 (left) using SPSS. Summarising and mean-centring all responses, less negative sensors responses for adult cattle (red) were observed considering MEDIAN (right; Matlab heatmaps).

Considering the *sampling day*, significant decreases over all 6 days were found for sensors 10 and 11 only. The remaining sensors did not show a general trend over time using SPSS while Statgraphics and Matlab found all sensors to be significantly changed over days. Spearman's rank correlation also found significant decreases of divergences for sensors 10 and 11 only. Performing MRT, lowest divergences were found at the last day (day 4) however, trends overall were inconsistent (data not shown).

Investigating the influence of the *sampling time* on e-nose responses, divergences of sensors 1, 2, 6, 7, 9 to 11 and 13 were significantly decreased over the course of the day using SPSS while Statgraphics and Matlab analyses revealed significant changes for sensors 1 to 8 (and in addition sensor 9 for Matlab) and 13.

Spearman's rank correlation found no general trend over time. However, when applying MRT, sensors 2, 6 and 7 showed significantly decreased divergences after both feeding times (time points 2 and 4 compared to time points 1 and 3) while sensors 3 to 5, 8, 9, 12 and 13 showed decreased divergences after the first feeding only. The responses of all sensors are displayed as mean-centred divergences in a heatmap (figure 25). The blue and green sections represent decreased divergences over the day reaching a minimum for sensors 4 to 8 after feeding in the morning, a maximum before feeding in the afternoon and decrease again after feeding reaching a minimum for sensor 9 to 12.

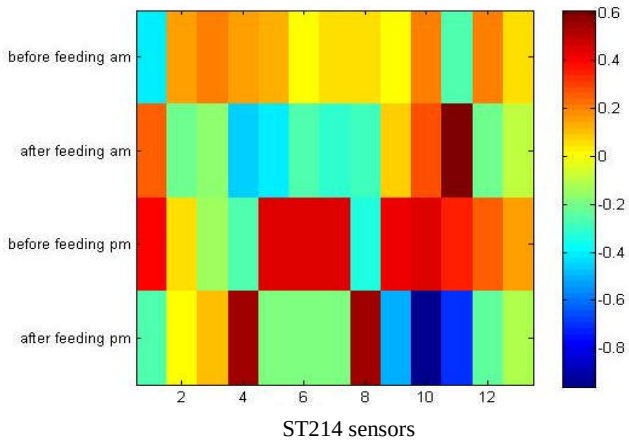

Figure 25: A significant decline after feeding in the morning was observed for sensors 2 to 8, 12 and 13. Similar tendencies were observed also for sensors 9 to 11 indicated as green and blues sections on the heatmap after feeding in the afternoon.

The results indicate that there was a difference in urine headspace composition on the group level comparing calves and cattle (age of individuals), only. Differences were confirmed for a wide range of sensors using all programmes and techniques. Changes in the headspace may represent different metabolic processes between juvenile and adult cattle or differences in feeding. The sampling day had an inconsistent influence on the data and reflects the biological variability which is similar to the individuals of each group. However, there was a decline after feeding in the morning and the afternoon and a general decrease over time indicating circadian variability.

3.2.3 Variability of serum samples after *Mycoplasma bovis* infection

After the analysis of serum samples obtained from *Mycoplasma bovis* infected individuals, three datasets were excluded due to irregularities in the sampling process. For the remaining data (in total 329 samples over all subjects) the

different methodological and biological factors causing variability in the responses were assessed. This study was to investigate whether there were any differences in headspace of serum samples from infected and placebo treated cattle.

As for previous studies, time- and day of analysis caused significant differences for all sensors (mANOVA, $P \leq 0.05$). The sampling day was found to influence the responses of sensors 4 to 9 significantly (see figure 26 left) comparing the pre-infection data and the negative controls only. Responses decreased over time which was mainly due to the later sampling days.

Divergences of placebo (left) and *Mycoplasma bovis* (right) treated serum samples

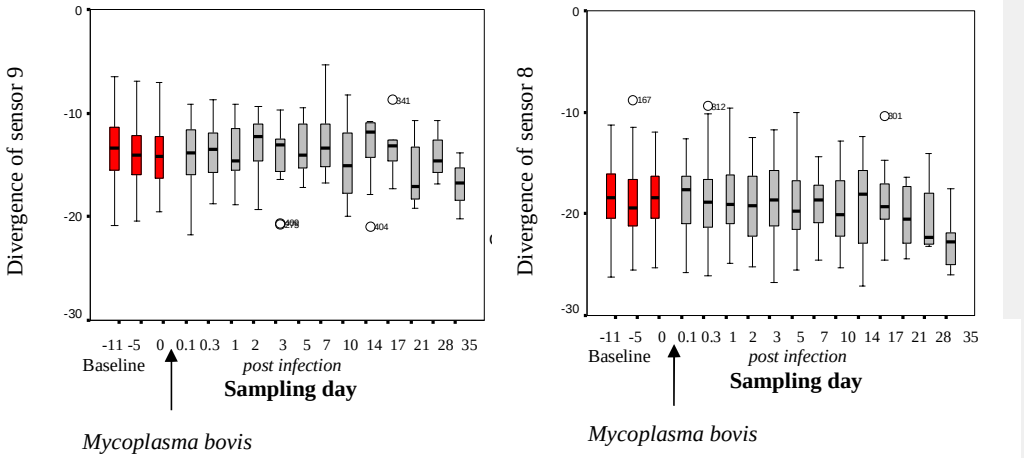

Figure 26: Divergences of sensors 9 (left, placebo treated) and 8 (right, infected with *Mycoplasma bovis*) over the course of the study. Responses were significantly different from the baseline (red) at the end of the study.

Similar observations were made for the divergences of sensors 2 to 9 when analysing the samples from Mycoplasma bovis infected cattle (figure 26, right). However, this result could not be confirmed using the MRTs.

Responses remained the same comparing the pre-infection samples, placebo treated post infection samples and the infected post infection samples for the vast majority of all sensors. Differences between samples from placebo treated and challenged individuals were found to be significantly different only at the last two days but there were data from only one placebo treated and 2 *Mycoplasma bovis* infected individuals, respectively. Nonetheless, these findings may be the detection of early stage sub-clinical symptoms. Other factors, methodological or biological ones, did not influence e-nose responses to a significant extent.

Pathologically, animals exposed to Mycoplasma bovis showed mild clinical symptoms and a significant increase in respiratory rate and rectal temperature starting at 3 days post infection and reaching its maximum 7 days after infection. Antibodies against Mycoplasma bovis were found in all individuals except for one between days 7 and 10 and culture results clearly indicated the presence of the pathogen in the lung tissue. Macroscopically, no lesions were found at necropsy but histological investigations proved mild brochial pneumonia 7 days after infection.

3.2.4 Variability of serum samples after *Mannheimia heamolytica* infection

This is presumably the first study demonstrating that a changed VOC profile of serum headspace correlates with acute phase reactions in the host, following a pathogenic infection in a model organism.

(I) Analyses of e-nose responses

After experimental infection, 6 calves (30 %) died before the end of the study. Four calves died between 24-48 hours, and two died between 48-72 hours after the first challenge with *Mannheimia haemolytica* A1.

In analysing divergences, significant methodological variation (time- and day of analysis) and biological variation were found. The latter were analysed both in terms of changes *due to the infection status* (i.e. responses before and after experimental challenge) and over the *time course of the study*.

Regarding the *infection status*, responses of sensors 2 to 8 significantly increased between all pre- and all post- inoculation samples while sensors 10 and 11 decreased (mANOVA, $P< 0.05$). Divergences of sensitive sensors became more negative after challenge. Having a detailed look at the kinetics of divergences over sampling time using the MRT, lowest responses were found on days 2 and 3 for sensors 2 to 5, 10 and 11. Figure 27 illustrates a typical change in divergence over time for sensor 3. In general, divergences of sensitive e-nose sensors were approximately the same level before and shortly after challenge, then declined and reached a minimum at days 2 and 3 *p.i.*, and increased again until the end of the trial. However, responses of sensors 10 and 11 continued to decrease.

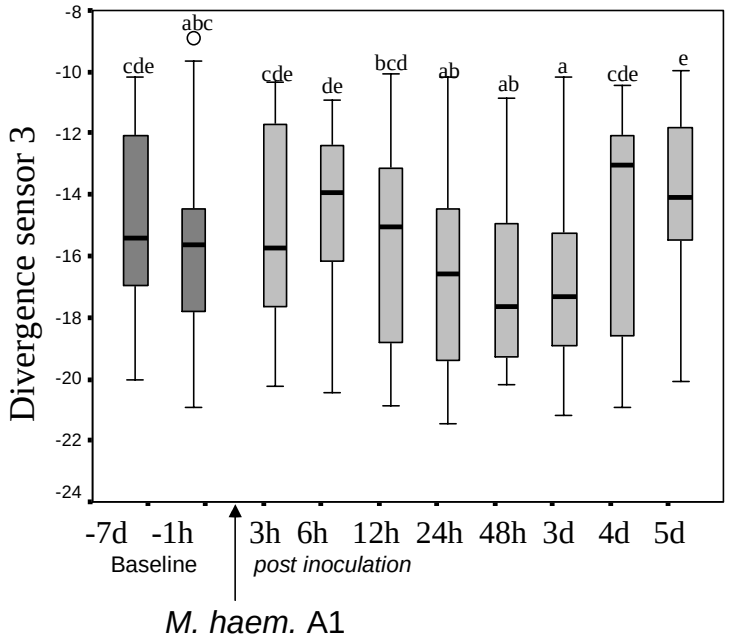

Figure 27: Divergences of sensor 3 over the course of the study. The temporal profile indicated an overall increase over time and identified responses 48 and 3 days post inoculation as the lowest.

Using Statgraphics and Matlab performing mANOVA ($P \leq 0.05$), sensors 1 to 5 and 8 to 13 were found to change significantly in the course of the study. Sensors 3, 6 and 7 were identified to decrease significantly when grouping all samples obtained as pre- and post infection samples.

In surviving calves, the following clinical signs were dominant: Within the first 6 hours after challenge, the appetite dropped markebly and the majority of animals became quiet, dull or depressed. Significant increases in respiratory rates were observed within the first 3 hours and in rectal temperature within the first 6 hours after challenge. The maximum temperature was measured 2 days after challenge. Both rectal temperature and breathing frequency (data

not shown) remained significantly increased in the group until the end of the study.

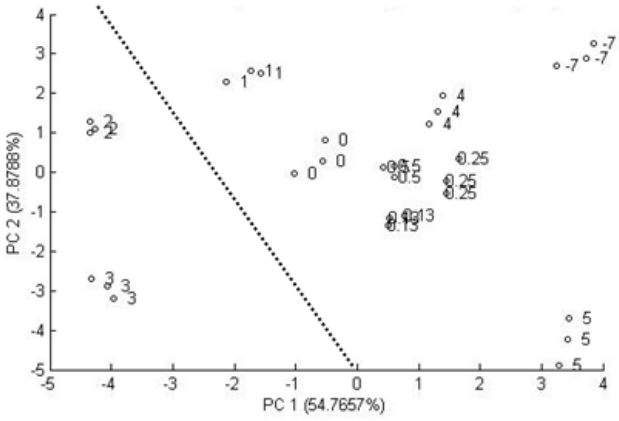

Figure 28: Averaged and autoscaled divergences for all experimental days, 7 days before infection (-7) to 5 days after infection (5). Clear discrimination was found for days 2 and 3 indicating the biggest changes in divergence.

When averaging data due to methodological variation and performing a Principle Component Analysis (self assembled script, Matlab, 2006b) days 2 and 3 could be clearly discriminated from all the remaining days (figure 28). This confirmed the temporal change in divergence found for various sensors before.

(II) Analyses of acute phase proteins (APP)

Analysis of serum samples before infection (n = 40) showed concentrations of LBP of 2.4 ± 2.2 µg/ml (mean ± SD) and 0.02 ± 0.04 mg/ml (mean ± SD) of Hp. After challenge with *M. haem*. A1, APPs increased significantly with the following time kinetics (Figure 29): for both lipopolysaccharide binding protein (LBP) and Haptoglobin (Hp), the first significant increase was observed 12

hours after infection reaching a maximum 24 and 48 hours after infection for LBP (about 600% of baseline data) and 48 hours p.i. for Hp. Significantly elevated concentrations of both APPs were measurable until the end of the observation period (5 days p.i.). A significant relationship was found between LBP and Hp as expressed by the coefficient of Spearman's rank correlation of rsp = 0.73 (P < 0.0001, n = 178).

Rank correlations between rectal temperature and APPs were $r_{sp} = 0.51$ (P < 0.0001, n = 178) for LBP, and $r_{sp} = 0.49$ (P < 0.0001, n = 178) for Hp, both indicating significant relationships between the rise in body temperature and increased concentrations of APPs in the blood.

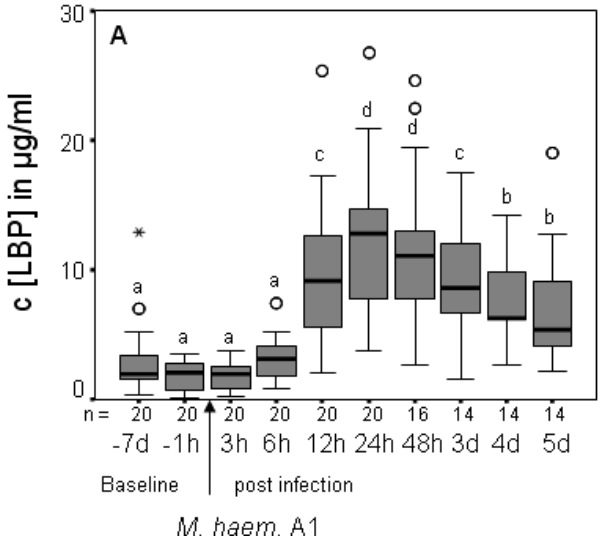

Figure 29: Concentrations of lipopolysaccharide binding protein (LBP) in serum samples collected before and after an experimentally induced infection with *Mannheimia haemolytica A1* in calves. After infection, the highest concentrations of acute phase proteins were measured 24 hours p.i. for LBP.

(III) Correlations between e-nose and clinical results

As shown in table 6, significant correlations were found between responses of e-nose sensors and the severity of the infection expressed by either APP concentrations in the blood or rectal temperature. Strongest correlations were found between e-nose responses and the concentration of both APPs. With increasing concentrations of LBP, sensors 2-4 and 6-8 became more negative and sensors 10 and 11 became more positive. As the concentration of haptoglobin increased, responses of sensors 2 to 8 and sensor 13 became more negative. However, it seems unlikely that sensors respond to the APPs directly. It is more likely that they pick up a molecule, which is easier to evaporate. It furthermore remains unclear why pairs of sensors which are supposed to be sensitive to same classes of compounds (see section 1.4.3, table 1) don't react similarly.

Table 6: Spearman rank correlations rectal temperature and APPs (LBP, Hp). Divergences of sensors 8 and 9 correlated with rectal temperature while there was a correlation between the responses of sensors 2 to 4, 6 to 8, 10 and 11 and LBP concentrations and sensors 2 to 8 and 13 is correlated with Hp concentrations.

Responses of e-nose sensors	Rectal temperature in °C		c [LBP] in µg/ml		c [Haptoglobin] in µg/ml	
	r_{sp}	*P*	r_{sp}	*P*	r_{sp}	*P*
Sensor 01	0.0488	0.2737	0.0220	0.6211	-0.0091	0.8391
Sensor 02	0.0386	0.3871	-0.1255	**0.0049**	-0.1628	**0.0003**
Sensor 03	0.0755	0.0904	-0.1304	**0.0034**	-0.1264	**0.0046**
Sensor 04	0.0411	0.3564	-0.1101	**0.0136**	-0.1660	**0.0002**
Sensor 05	0.0515	0.2477	-0.0723	0.1050	-0.1257	**0.0048**
Sensor 06	0.0262	0.5563	-0.1057	**0.0177**	-0.1288	**0.0039**
Sensor 07	0.0331	0.4576	-0.1069	**0.0165**	-0.1335	**0.0028**
Sensor 08	0.0888	**0.0465**	-0.1059	**0.0176**	-0.1006	**0.0241**
Sensor 09	0.1398	**0.0017**	-0.0093	0.8348	-0.0046	0.9185
Sensor 10	0.0749	0.0930	0.1119	**0.0121**	0.0628	0.1590
Sensor 11	0.0839	0.0597	0.1223	**0.0061**	0.0776	0.0817
Sensor 12	0.0448	0.3148	0.0265	0.5525	-0.0427	0.3385
Sensor 13	0.0047	0.9153	-0.0239	0.5915	-0.1003	**0.0244**

Legend: r_{sp}: coefficient of Spearman rank correlation; $P \leq 0.05$ indicates significant correlations (bold).

The general temporal profile of the sensor responses after infection was inversely proportional to increasing concentrations of APPs.

The most negative responses of e-nose sensors were found 48 hours after challenge which corresponded to the highest peaks of Hp concentrations. In contrast, peaks in LBP concentrations were observed earlier, i.e. 24 hours after infection. Therefore, coefficients of correlation between e-nose sensors and LBP were lower compared to those between e-nose sensors and haptoglobin.

With respect to body temperature, only the responses of sensors 8 and 9 could be correlated showing an increase in divergence with increasing rectal temperature. Coefficients of correlation were very low; ranging between 0.09 and 0.14.

3.2.5 Variability of serum samples from *Mycobacterium bovis* infected cattle

This study was to investigate whether there were differences in headspace of *Mycobacterium bovis* infected cattle. Data was analysed for each group: positive controls, BCG vaccinated subjects and BCG/Ad85a vaccinated subjects. 49 samples were analysed in total and divergences of all sensors over all three treatment groups (positive controls, BCG vaccinated subjects and BCG Ad85a vaccinated subjects) were analysed in terms of methodological and biological variation. *Day and time of analysis* was found for almost all sensors. There was no overall trend over sampling time or according to the treatment group (mANOVA, $P \leq 0.05$).

Considering the *control group* (no vaccination) separately, a significant decrease over all four time points was found for all sensors using SPSS mANOVA. Statgraphics mANOVA identified sensors 1, 5 and 8 to 13 to be significantly changed over time. The MRT revealed that there was a minimum in divergence at time point 4 causing main differences over time, for instance for sensor 5 (approximately 4 weeks after infection, figure 30, left). Furthermore, there was also a minor decrease in responses of sensors 8 and 11 to 13 immediately after challenge at time point 2 (e.g. see mean-centred medians heatmap, sensor 9, figure 30, right).

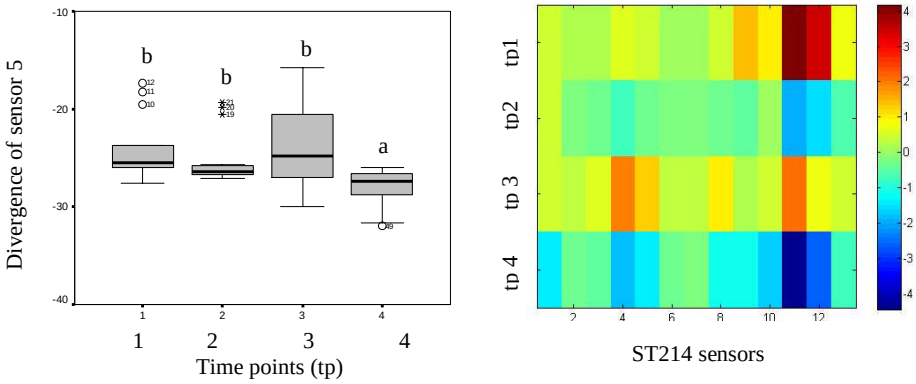

Figure 30: Divergences of sensor 5 over time (left). Lowest divergences were obtained at time point 4 (1 = before infection, 2-4 = after infection) indicated at "a" which remaining time points had significantly higher medians ("b") as also illustrated by the mean-centred medians heatmap (right).

Analysing the sensor array exposed to serum headspace from BCG vaccinated individuals, a significant decrease in divergence over time was found for all sensors (SPSS, mANOVA). Almost all sensors were also influenced by methodological factors such as day and time of analysis. Sensors 1 to 4, 6, 7 and 13 were found to be significantly changed over all four time points using Statgraphics and the Matlab script (figure 31, right). The MRT identified divergences for time point 1 as the lowest (figure 31, left). Most sensors remained constant. Increased responses were only found at time point 3 but without significant relevance (sensors 8 to 10 and 13). Only sensor 12 indicated a significant difference at time point 3 (figure 31, left).

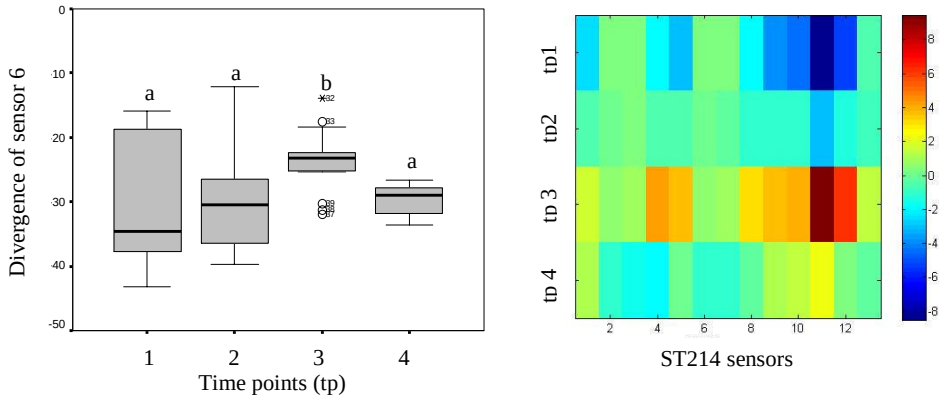

Figure 31: Divergences of sensor 12 (left) and for all sensors over all time points (1 = before infection, 2-4 = after infection). A significant difference was found at time point 3. Similar increases without significant relevance were also found for sensors 8 to 10 and 13.

Divergences of all sensors were significantly increased when serum headspace samples from BCG/Ad85a vaccinated individuals were analysed (SPSS and Statgraphics mANOVA, except for sensor 2; $P \leq 0.05$). As an example, responses of sensor 10 are shown (figure 32, left). The MRT revealed that highest divergences were found at time point 4 (figure 32 left, right).

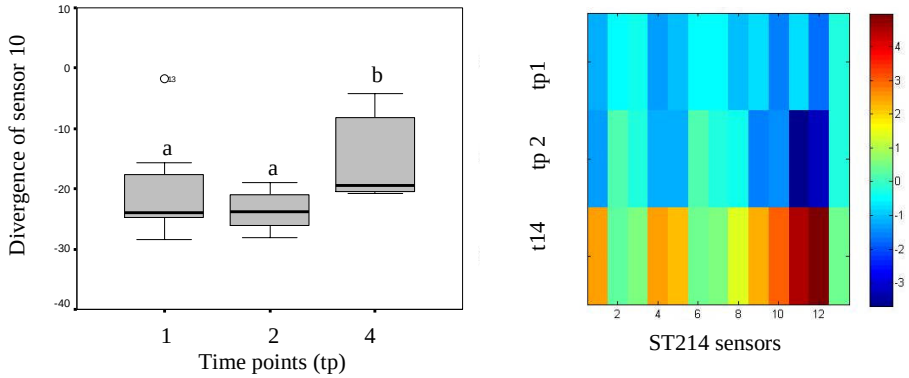

Figure 32: Divergences for sensor 10 (left) and median divergences for all sensors over time points 1 to 4 (tp, right). Significantly elevated responses were found 4 weeks post infection.

Finally, all samples before challenge obtained at time point 1 (group 1) and at time point 4 (group 2 to 4) were analysed together. Data was separated into four groups as follows: 1 = all pre-challenge samples, 2 = control group (non-vaccinated), 3 = BCG vaccinates, 4 = BCG/Ad85a vaccinates. Methodological and biological variation was assessed as before. Performing mANOVA, SPSS found no changes over all four groups. However, methodological variation affected all sensors significantly ($P \leq 0.05$). Using Statgraphics and Matlab, almost all sensors except for sensor 2, 6 and 12 were significantly changed over all groups. MRT revealed that group 4 showed generally the highest divergences while minimum responses were found for group 2 (see figure 33, left). Sensors 1 to 3, 6 and 7 were found to have highest divergences for group 4 while other groups remained at one level Sensors 5 and 9 to 13 showed lowest divergences for group 2 while other sensors remained at one level (see figure 33, right).

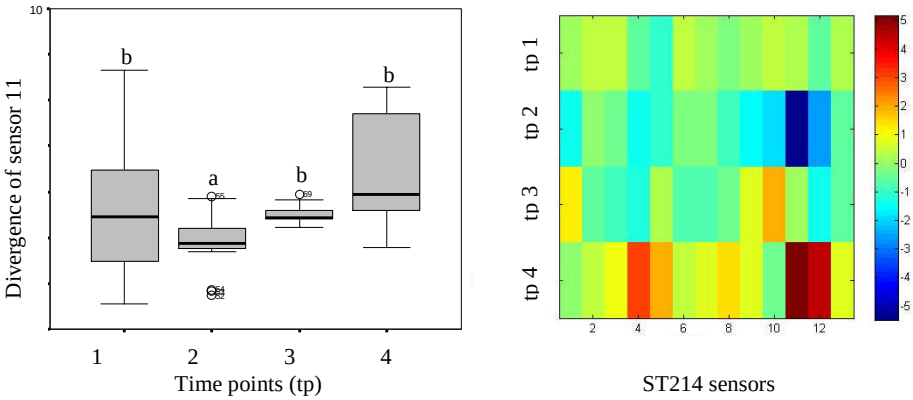

Figure 33: Divergences for sensor 11 (left) and the medians for all sensors (right). Group 4 was found to have the highest divergences while group 2 had lowest divergences (group 1 = before infection, groups 2-4 = after infection with no vaccination, BCG vaccination and Ad85a vaccination, respectively).

In conclusion, no clear results were obtained analysing all data from all time points at once. Separating data into subsets according to vaccination strategies, different temporal profiles in divergences were found. Major changes were found, in particular comparing time points 1 (just prior to infection) and 4 (4 weeks after infection). Group 2 (time point 4; no vaccination) had lowest divergences (MRT, "a", $P \leq 0.05$) while group 1 and 3 were at one level indicating no differences between pre- and post infection and BCG vaccinated samples on a group level. Responses of serum samples with Ad85a vaccination showed to have the highest divergences but were not significantly different from pre- and post infection BCG samples. Table 7 summarises the results. As explained previously, different letters indicate significantly different medians of groups with a confidence level of 95%. Groups are ranked from the lowest to the highest starting with the letter "a".

Table 7: Summarised multiple range testing (MRT) results. Group 4 was found to have the highest divergences while group 2 had lowest divergences (group 1 = before infection, groups 2-4 = after infection with no vaccination, BCG vaccination and Ad85a vaccination, respectively).

Sensors / Group	1	2	3	4	5	6	7	8	9	10	11	12	13
1	a	a	a	a	b	a	a	ab	b	b	b	ab	b
2	**a**	**a**	**a**	**a**	**a**	**a**	**a**	**a**	**a**	**a**	**a**	**a**	**a**
3	a	a	a	ab	b	a	a	ab	b	b	b	ab	b
4	b	b	b	b	b	b	b	b	b	b	b	b	b

Different letters indicate significant differences (LDS, $P \leq 0.05$)

In addition, ELISPOT or BOVIGAM test system was used to determine the γ-interferon (γ-INF) concentration in serum samples from the same individuals. Using this ELISA test kit the optical density (OD) was measured using trace

marker molecules attached to antibodies (see section 2.4.5). As a result, the optical density of the non-vaccinates control group was significantly increased indicating the presence of a high concentration of γ-INF 4 weeks after infection (experimental week 18). γ-INF were also increased for the other two groups but remained at a comparably low level (figure 34).

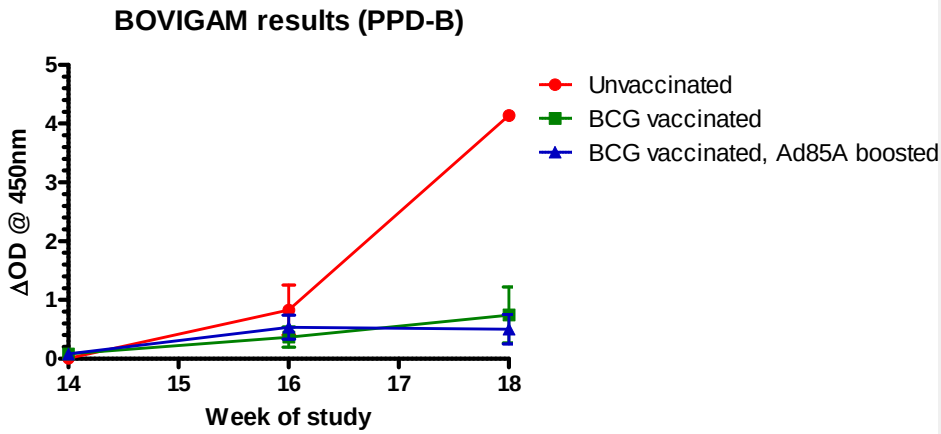

Figure 34: Optical densities (OD) at 450nm wavelength measured for all subjects and displayed as averages. The unvaccinated control group had a significantly higher γ-interferon concentration at experimental week 18 (time point 4) compared to both, the BCG- and BCG/Ad85a vaccinated group.

The pathological score was assessed at the VLA, Weybridge as described in section 2.4.5 at post-mortem. The score for the unvaccinated was highest (12.5 ± 3.5) followed by the score for the BCG vaccinated animals (5.0 ± 7.9) and the BCG/Ad85a vaccinated cattle (6.0 ± 5.9, all medians ± standard deviations). Using the non-parametric Kruskal-Wallis no differences were found between the median scores for the vaccinated individuals (ANOVA; P = 0.216, data obtained from VLA, Weybridge).

3.2.6 Variability of urine samples from *Mycobacerium bovis* infected cattle

Due to irregularities during the sampling process, data from 10 experimentally infected samples and 1 naturally infected sample were removed from the analysis. In total 33 samples were used for analysis. The main objective was to find differences in headspace comparing pre- and post infection samples applying different vaccination strategies (no vaccination and BCG vaccination).

Performing mANOVA using SPSS, a decline in divergences of sensors 2 to 4 according to the pathological score were found. Other programs could not confirm the decrease of divergences over the pathological score (data not shown).

Furthermore, responses for sensors 2, 3 and 8 to 11 decreased from the first to the second day of sample analysis. Statgraphics' mANOVA found all sensors significantly increased considering all treatment groups (samples from non-vaccinated and vaccinated animals) over time.

Testing each treatment group over time for differences in divergence using the MRT, lowest responses were found for the control group before inoculation (group 1, BCG vaccinates were slightly higher) while after inoculation, (group 5, controls at time point 3) divergences were significantly elevated for the control group but not for the corresponding BCG vaccinates. This effect was observed for sensors 1 and 8 to 13. The pathological score did not correlate with changes in sensor responses.

The changes in divergences from analysing urine samples from non-vaccinated and BCG vaccinated did not show general significant changes over time or treatment group (mANOVA). The results were inconsistent.

However, with the MRT, significantly increased responses were found at time point 3 (directly after inoculation) for the non-vaccinated samples (light grey, figure 35, left) but not for samples from the vaccinated animals (dark grey). These findings were confirmed using heat mapping (figure 35, right).

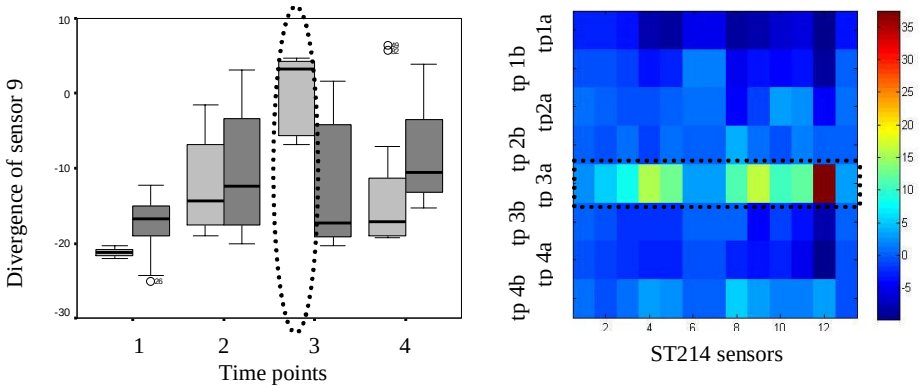

Figure 35: Divergences of sensors 9 (left) and median divergences for all sensors as a heatmap (right). Lowest divergences were found for non-vaccinated at time point 1 while highest responses were observed at time point 3 (light grey/ a = non-vaccinated, dark grey/ b = BCG vaccinated, left; dark blue and green-yellow, right).

In a second step, divergences of samples from vaccinated and non-vaccinated individuals at the group level were compared in terms their progressing changes over the course of the study before infection and at the end. Therefore, divergences were averaged for time points 1 and 2 and for both vaccination strategies. MANOVA and MRT previously found all four pre-infection groups the same. The averaged divergences for vaccinated and non-vaccinated individuals at time point 4 were related to the average of all pre-infection data. MANOVA found a significant general increase in divergences for sensors 5 and 8 to 11 from pre-infection data (group 1) to responses from

non-vaccinated individuals (group 3, figure 36, left, right) . MRT found the same tendency for all sensors except for sensors 6, 7 and 12, 13 (table 8).

Table 8: MANOVA and multiple range test (MRT) results for all sensors at the group level (significant results are shown with P ≤ 0.05). Divergences of sensors 6, and 8 to 11 showed a significant overall increase while MRT showed responses of group 3 for sensors 1 to 5, 8, 10 and 11 as significantly increase compared t groups 1 and 2.

Divergence	mANOVA f-value	mANOVA P-value	MRT Group
Sensor 1	-	-	a, a, b
Sensor 2	-	-	a, a, b
Sensor 3	-	-	a, a, b
Sensor 4	-	-	a, a, b
Sensor 5	2.178	0.033	a, a, b
Sensor 6	-	-	a, a, a
Sensor 7	-	-	a, a, a
Sensor 8	2.515	0.014	a, a, b
Sensor 9	2.480	0.015	a, ab, b
Sensor 10	2.169	0.033	a, a, b
Sensor 11	2.419	0.018	a, a, b
Sensor 12	-	-	a, a, a
Sensor 13	-	-	a, a, a

Legend: Groups 1 = time points 1 and 2, groups 2 and 3 = time points 4

Vaccinated post-infection samples were at the same level as pre-infection samples while non-vaccinated samples from the same time point showed a significant increase in divergence.

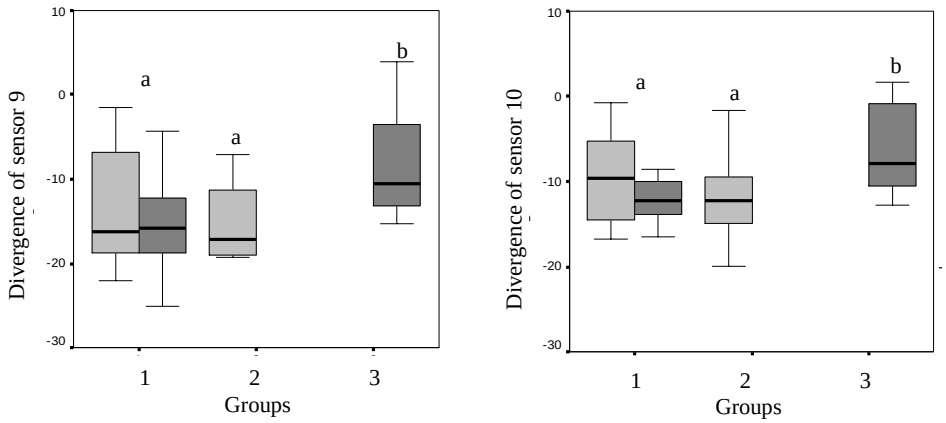

Figure 36: Responses of sensors 9 (left) and 10 (right) averaged at time points 1 and 2 (pre-infection) and time point 4. The averaged responses are split up into vaccinated and non-vaccinated. Responses for pre-infection and vaccinated sample at time point 4 are at a similar level while nonvaccinated post-infection samples showed elevated average divergences.
Legend: Groups 1 = time points 1 and 2, groups 2 and 3 = time points 4; Light grey = vaccinated, dark grey = non-vaccinated

3.3 Naturally infected individuals

3.3.1 Variability of healthy- and paraTuberculosis infected serum samples

Two sets of samples with a paraTB negative status and 19 with a positive status were deleted from analysis due to a power cut. The remaining data (43 positives, 24 negatives) obtained from e-nose headspace analysis of healthy and paraTB infected serum samples were analysed regarding their methodological and biological variation. As before, time and day of analysis significantly influenced divergences. Significant differences between paraTB positive and negative samples were found. Responses of sensors 2, 3, 6 and 7 became more positive from non-infected to infected and sensors 1 and 9 to 13 showed a decrease comparing both groups (SPSS, mANOVA, $P \leq 0.05$). Performing mANOVA using Statgraphic and Matlab, sensors 2 to 9, 12 and 13 showed significant changes between samples having a positive and a negative paraTB status. The MRT confirmed a decrease in divergence between both groups. For example, figure 37 (left) shows the decrease of sensor 9 due to paraTB infection.

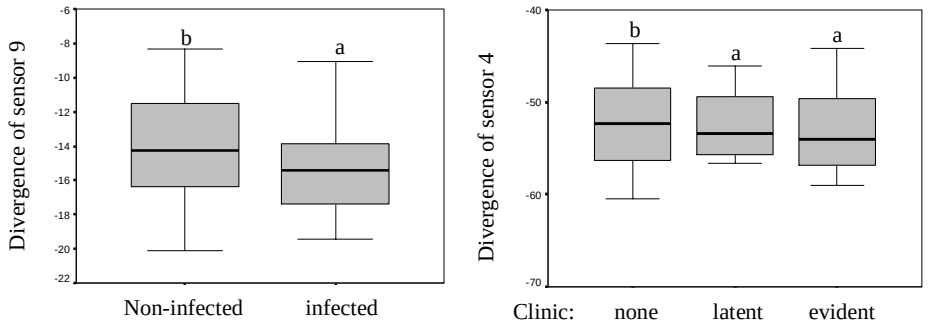

Figure 37: Divergence of sensor 9 over infection groups (left) and 4 over clinical groups (right). Responses decreased from non-infected to infected. Samples with no clinical symptoms had higher divergences than those with latent or clinically evident symptoms.

Considering the samples with a confirmed clinical and pathological status only, several changes in sensor responses were found that went along with changes in both clinical symptoms and pathology. Sensors 1, 10 and 11 increased when the clinical score and pathological score increased. Responses of sensors 1, 10 and 11 increased while sensors 6 and 7 declined when the pathological score increased (SPSS mANOVA, $P \leq 0.05$). Using Statgraphics sensors 2 to 9 and 2 to 4, 6 to 8, 12 and 13 changed according to changes in clinical and pathological score, respectively. Matlab confirmed the Statgraphics findings. The MRT confirmed decreased responses according to clinical symptoms (see figure 37, right). Regarding the pathological score, the MRT showed inconsistent tendencies over all groups ($P \leq 0.05$, data not shown).

3.3.2 Variability of healthy and Brucella infected serum samples

Before analysing data, ten samples with a Brucellosis negative- and 14 samples with a Brucellosis positive status were excluded due to unwanted

thawing following a power cut. 26 positives and 24 negatives remained for analysis. Methodological and biological variations were investigated. The time and day of analysis influenced almost all sensors significantly (mANOVA, P = 0.05; data not shown).

The main biological variation came from the differences between *Brucella* negative and positive samples. While responses of sensors 1, 6, 10, 11 13 increased, divergences decreased for sensors 2 to 4, 7, 8 using SPSS (figure 38, mANOVA, P ≤ 0.05).

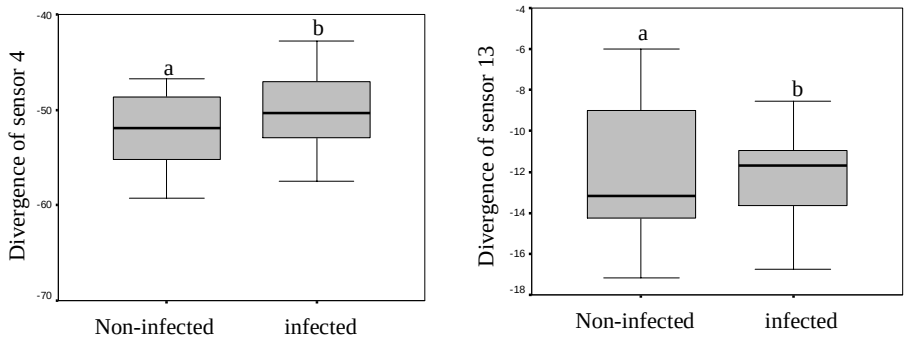

Figure 38: Divergences of sensors 4 (left) and 13 (right). Responses increased from non-infected to infected.

For Statgraphics' mANOVA, responses of sensors 1, 2, 4, 5, 8, 9, 11, 13 changed with infection status. The MRT found all changes in divergences (except for sensor 6) to increase from *Brucella* negative/ non-infected to *Brucella* positive/ infected.

3.3.3 Variability of healthy and *Mycobacterium bovis* infected serum samples from badgers

Concerning the field (wild) badgers, methodological and biological variation was found and as before, the time and day of analysis significantly influenced responses.

Before the biological variability of the headspace composition due to the infection with *Mycobacterium bovis*, all samples were ranked with a "+" or a "-" according to their infection status using culture and γ-interferon. Afterwards, samples with a "++" or a "- -"status were selected for data analysis to minimise the risk including samples with an unclear status. The number of these samples was 212 (87% of the total number) whereas 85% out of the 87% were confirmed negatives (--) and 15% out of 87% were confirmed positives (++).

Analysing data from naturally infected serum samples ("++") and samples which were supposed to be confirmed free ("- -") three clusters were observed. Using PCA, a clustering was observed according to the date of sample analysis. Each data point indicates the variance caused by all sensors over replicates 3 to 5 for one sample each. If sensors do not show changes in their response from one sample to another, there is no variance and data points will lie closely together.

The clusters which were found using PCA was clearly due to the date of analysis. Cluster A contains samples analysed on 05.01.07, cluster B contains samples from 17.01.07 and all remaining data was a part of cluster C (figure 39). Two values of the 17.01.07 and one value of the 05.01.07 have to be considered as outliers.

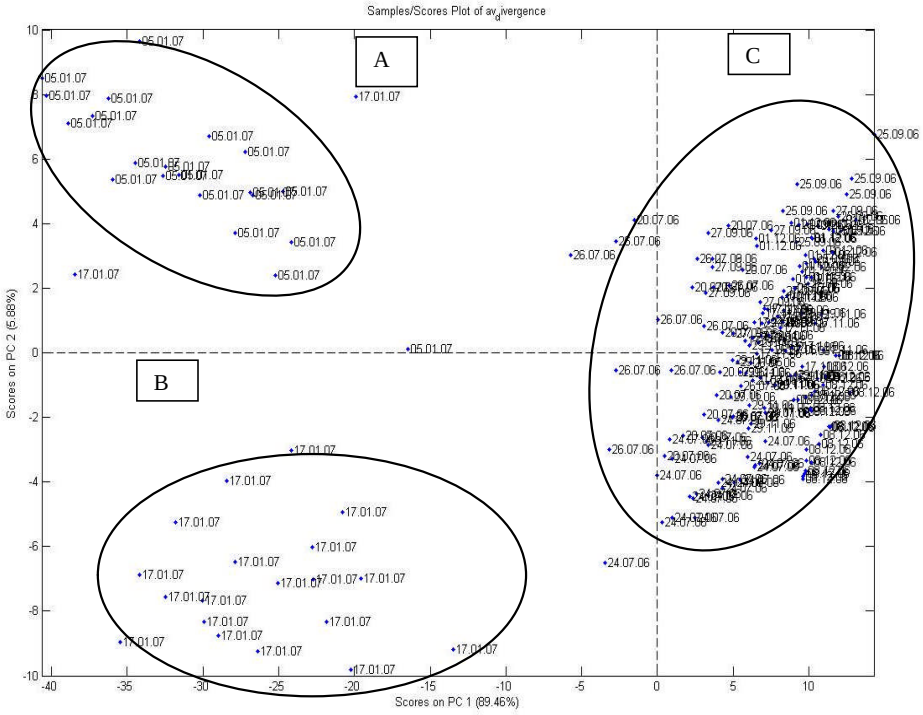

Figure 39: Clustering of values of naturally infected badger sera. Three clusters were found representing data from 05.01.07 (A), 17.01.07 (B) and all remaining data (C). The day of analysis covered more 95.34% of all variance represented by principle components 1 and 2. Single data points represent variance of a sample in comparison to other samples.

Omitting the data from 05.01.07 and 17.01.07 which caused the biggest variances regarding the whole dataset, the remaining data were re-analysed. No clustering between naturally infected and uninfected serum samples was found using SPSS (mANOVA, data not shown) and Matlab. Divergences were significantly influenced by methodological factors such as time and day of analysis. However, naturally infected samples (A) were mainly grouped into clusters on the left hand side while the majority of the average of uninfected values (B) were located on the right hand side (see figure 40). As for the PCA before, each point in the plot represents the variance caused by all 13

sensors when analysing a sample in comparison to the other samples. Replicates 3 to 5 were considered.

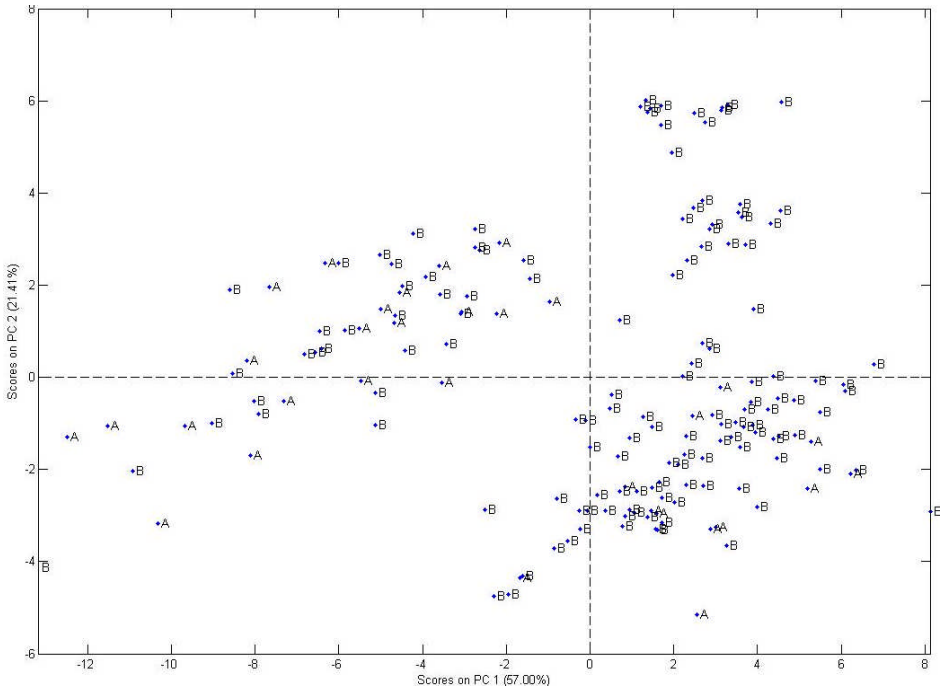

Figure 40: PCA on serum sample analysed 2006. No discrimination was found between naturally infected (A) and uninfected samples (B). Scattering of data was due to methodological factors and covered 91.41% of all variance. Single data points represent variance of a sample in comparison to other samples.

Performing the same PCA again considering the dates of e-nose analysis, a systematic change in the distribution of variation was found. Starting on the left hand side (figure 24, A) with the earliest analysed samples, a shift to the lower right corner (B) and, over the course of time into the upper right corner (C) with the latest analysed samples was investigated. According to the distribution (A-C), tree clusters could be found which grouped the values into the clusters 20.-26.07.06/ 25.09.-01.12.06 and 08.12.06 (see figure 41).

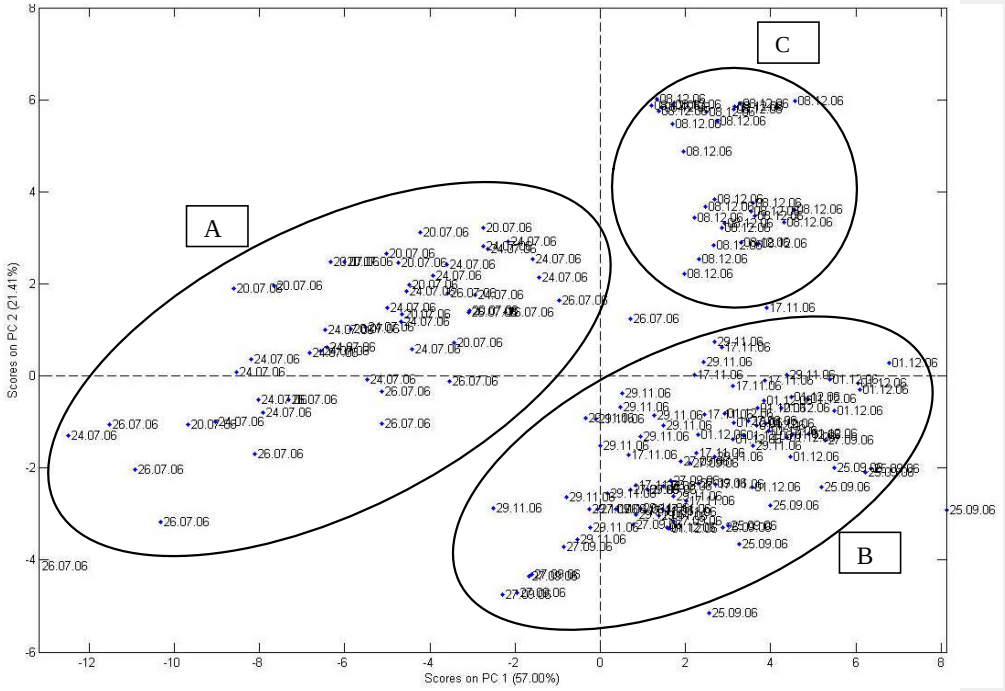

Figure 41: PCA on naturally infected serum samples. A systematic change in the distribution of the values was found. Starting on the left hand side, the values shifted over the course of time to the lower right corner and finally to the upper right corner.

Based on these findings, methodological variation clearly influenced the variation to a significant extent. The time and day of analysis covered 91.41% of all variance and no discrimination between confirmed TB positives (“+ +”) and negatives (“- -“) was found.

3.3.4 Variability of urine samples from healthy and paraTuberculosis infected cattle

29 urine samples were obtained from 3 different locations. 19 of the samples were paraTB positive and came from two locations while the remaining 10 samples classified as paraTB negative came from one location.

SPSS mANOVA revealed a significant decrease in the responses of sensors 1, 6, 7 and 9 to 11. However, the factor origin was excluded since it was co-linear with the infection status (all positive samples came from just one location). Using Statgraphics mANOVA, sensors 1, 2, 4, 5 and 9 to 13 changed significantly with infection status. Infected samples showed lower divergences than samples obtained from healthy cattle. This was also confirmed applying MRT and Matlab mANOVA. Performing Spearman's rank correlation, responses of sensors 1, 2, 4, 5 and 9 to 13 became more negative from non-infected to infected (e.g. figure 42).

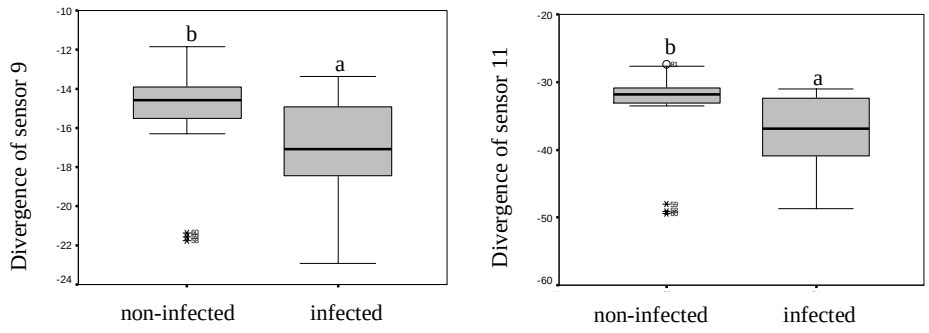

Figure 42: Divergences of sensors 9 (left) and 11 (right) over the infection status. Responses became significantly lower comparing samples from paraTB non-infected and infected individuals.

Due to the co-linearity between the *infection status* of samples and the *origin,* data were analysed taking the origin of samples into account. SPSS mANOVA showed a decrease in divergences for sensors 1, 2, 4 to 7 and 9 to 13. Samples with a paraTB positive status caused more negative responses over all three locations. Samples coming from locations 1 and 2 had a paraTB positive status while samples from location 3 were negative. Using Statgraphics' mANOVA, sensors 1, 3 to 7, 9 to 11 and 13 changed due to the parameter origin while Spearman's rank correlation found responses of sensors 1, 2, 4, 5 and 9 to 13 changed (figure 43).

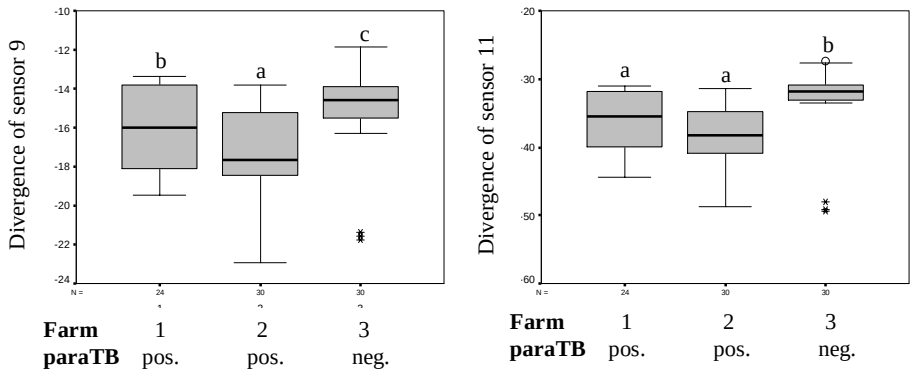

Figure 43: Divergences of sensors 9 (left) and 11 (right). Samples from farms 1 and 2 had a paraTB positive status while from farm 3 samples were paraTB negative. The negatives had a significantly higher sensor response than positives from all locations.

The MRT found significant differences in responses of sensors 6, 7, 9 and 11 according to the infection status. Differences due to sampling location were found to be less, indicating that changes in divergences were mainly due to the paraTB infection status rather than according to their origin.

3.3.5 Comparison of serum and urine samples

(I) Comparison of experimentally obtained serum samples

Before the start of analysis, all e-nose data from experimentally infected animal samples were divided into five sets 1 to 5 (1 = clinically healthy, 2 = *Mycoplasma bovis* negative, 3 = *Mycoplasma bovis* positive, 4 = *Mannheimia haemolytica* negative, 5 = *Mannheimia haemolytica* positive). Furthermore, data were reduced for set 3 due to the sub-clinical symptoms considering sampling days 28 and 35 only. Data were also reduced for set 5 considering sampling days 3 to 7 only because no clinical symptoms could be expected before this time. This reduces the number of all samples included into this consideration down to 221 (set 1 contains 91 samples; set 2 contains 61 samples; set 3 contains 2 samples; set 4 contains 37 samples; set 5 contains 30 samples; with three replicates each for a total number of 663 divergences per sensor).

Applying SPSS mANOVA, sensor 1 showed a decrease in divergence while sensors 6 to 9, 12 and 13 generally increased. For Matlab and Statgraphics' mANOVA sensors 2 to 9, 12 and 13 changed significantly. A detailed analysis of the data using the MRT revealed that for responses of sensors 2 to 5, all healthy samples were grouped the same and samples from *Mycoplasma bovis* and *Mannheimia haemolytica* positives were grouped below the healthy level (figure 44, left). Other sensors were inconsistent over all groups.

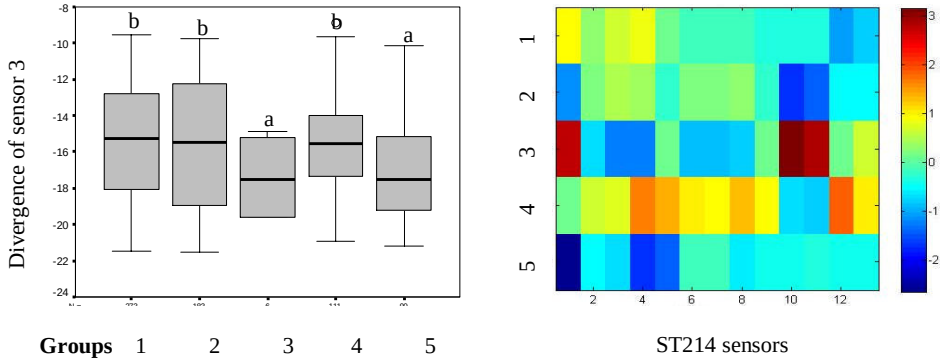

Figure 44: Divergence of sensor 3 (left) and mean-centred medians for all groups over sensors (right). Sensors 2 to 5 were found to group samples from healthy individuals as one and samples from experimentally infected animals as another group. All negative samples are represented by groups 1, 2 and 4.
Legend: 1 = clinically healthy, 2 = *Mycoplasma bovis* negative, 3 = *Mycoplasma bovis* positive, 4 = *Mannheimia haemolytica* negative, 5 = *Mannheimia haemolytica* positive i.e. sets 1, 2 and 4 were all of healthy, uninfected animals whereas 3 and 5 were of infected animals.

Heatmaps (see figure 44, right) did not completely confirm mANOVA and MRT results since it also reflects methodological variation such as time- and day of analysis that significantly influenced the results. However, dark blue representing *Mycoplasma bovis* positives and *Mannheimia heamolytica* positives, especially for sensors 2 to 5, were observed.

(II) Comparison of samples obtained from naturally infected individuals

For analysing data from samples obtained from naturally infected individuals, data sets as used for each individual study were included. All data was divided into four groups as follows: 6 = *paraTB* negative, 7 = *paraTB* positive, 8 = *Brucella* negative and 9 = *Brucella* positive.

SPSS mANOVA found divergences of sensors 2 to 9 generally increased over all 4 groups while for Statgraphics and Matlab all sensors (1 to 13) were significantly changed over all groups. Spearman's rank correlation found

increased responses of sensors 2 to 9, 12 and 13. A more detailed investigation of each group applying MRT revealed that for sensors 2, 3, 5 and 7 to 13 all groups were classified as shown in figure 45, left (b, a, c, d). The sets 6 and 8 representing healthy samples (*paraTB* negatives and *Brucella* negatives) were grouped next to each other (b, c) while sets 7 and 9 representing infected samples *(paraTB* positives and *Brucella* positives) were ranked below (a) and above (d) the level of clinically healthy groups.

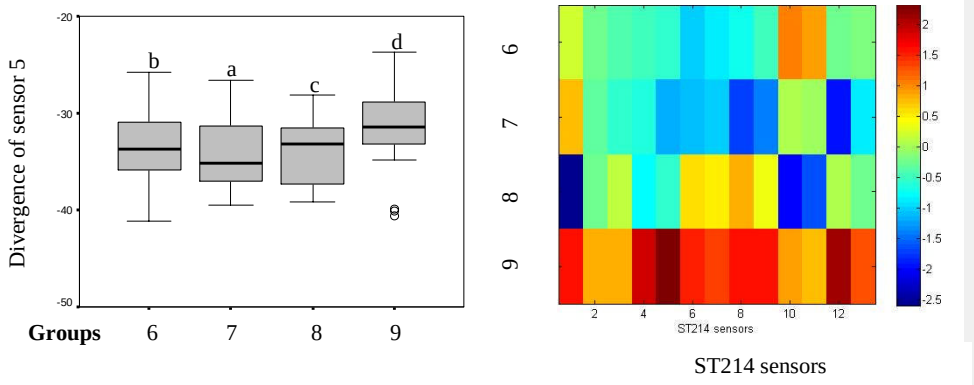

Figure 45: Divergence of sensor 5 (left) and mean-centred medians for all groups and all sensors (right). ParaTB and brucella negatives were grouped the same or similar while paraTB positives were below- and brucella positives above the negatives' level of responses.
Legend: 6 = *paraTB* negative, 7 = *paraTB* positive, 8 = *Brucella* negative and 9 = *Brucella* positive

Heatmaps did not completely confirm mANOVA and MRT results since it also reflects methodological variation such as time- and day of analysis that significantly influenced the results. However, *Brucella* positives could be observed as increased values with a red colour for almost all sensors (except for 10 and 11) while dark blue colours were observed for sensors 5 to 9 and 12 for *paraTB* positives indicating divergences below the healthy level (figure 45, right).

When analysing the averaged and auto-scaled data using (PCA), 4 clusters were found one for each disease and infection status. All data from non-diseased samples were found in the middle of the PCA plot while data from *paraTuberculosis* infected were located on the left and data from *Brucella* were located on the right. In other words, there was discrimination between infected and non-infected and between both diseases (figure 46). Most of the variation was caused by the difference between *Brucella* samples (99.87%).

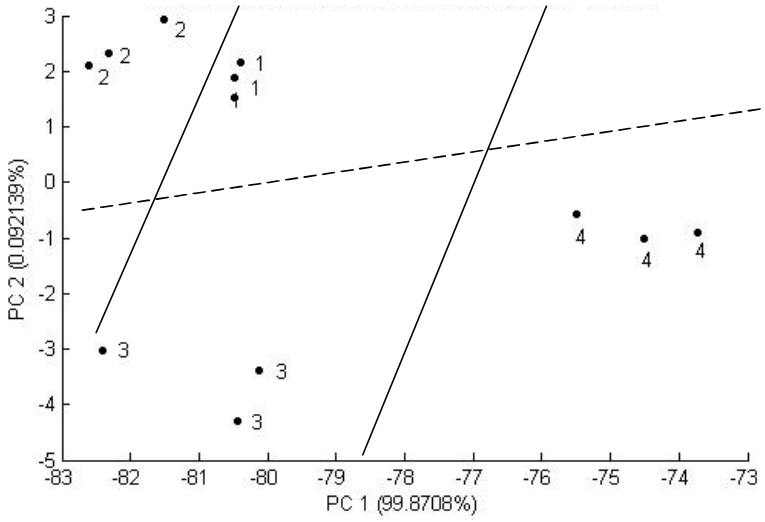

Figure 46: Averaged and auto-scaled divergences analysing serum headspace (paraTB negatives (1), positives (2) Brucella negatives (3) and positives (4)). Non-diseased data clustered in the middle (1, 3) while the cluster for the paraTB positives (2) data located on the left and the Brucella positives were located on the right.

(III) Comparison of experimentally and naturally obtained serum samples

Considering and comparing samples from both experimentally and naturally infected individuals, data as stated under 4.3.5 (I) and (II) were used for

analysis. All data were separated into nine groups as stated (1 to 5 for experimental samples and 6 to 9 for natural samples).

SPSS mANOVA found a general decrease in sensor 4 over all groups while divergences of sensor 6 to 9, 12 and 13 were found to increase. Performing mANOVA using Statgraphics and Matlab, all sensors were found to change significantly.

Considering each sensor over all groups using the MRT, a complex result was obtained.

Groups 2 vs 3 (Mycoplasma bovis negatives and positives)

Sensors 10 and 11 were able to discriminate between the infected and the healthy uninfected individuals. However, for the infected, the dataset consisted of only 6 values from 2 individuals taking replicates 3 to 5 into account. All other sensors showed no differences to the healthy individuals. Similar tendencies were observed when just analysing the groups 2/3 and when analysing all experimentally infected.

Changes in the sensor responses are based on data obtained at the end of the trial. The e-nose sensor responses indicate that perhaps the infections were not particularly severe.

Groups 4 vs 5 (*Mannheimia haemolytica* negatives and positives)

Regarding the *M.haemolytica* infection, sensors 1 to 9, 12 and 13 significantly discriminate between negatives and positive (see table 9). Significant changes in the e-nose pattern were investigated and a broad range of sensors were also found to alter when analysing the *M. haemolytica* data only (sensors 2 to 11 indicated changes across the sampling time and/ or the group).

However, in contrast to the *M. haemolytica* samples analysed separately, no difference between positives and negatives were found for sensors 10 and 11 with the reduced dataset but, instead, changes in responses for sensors 12 and 13 were significant due to the infection status. The reason for this may lie in the additional consideration of the other sets of data which caused a shift in variance and might lead also to a shift in results. Similar observations were made analysing the *Mycobacterium bovis* infected badgers (section 3.5.3). Other results are the same. When analysing data for all experimentally infected samples, the same results were found as for the whole dataset.

Groups 6 vs 7 (paraTB negatives and positives)

When analysing paraTB data, significantly changed responses of sensors 9 and 12 were found. Both sensors' divergences were also significantly changed when analysing paraTB positives and negatives only and all naturally infected. Other sensors which were altered due to the infection status (as for "paraTB only data" or the "naturally infected data") were not shown to be statistically significant.

Groups 8 vs 9 (Brucella negatives and positives)

In contrast to paraTB samples, changes in sensor response were observed for *Brucella* positive samples compared to the negatives. Significant changes were obtained for sensors 1, 2, 4, 5, 9 to 13. Except for sensors 1, 10 and 11 similar changes were observed when analysing "Brucella only" samples and all naturally infected samples. Table 9 summarises MRT results again showing significant differences between groups over all sensors indicated as different letters.

Table 9: MRT results for each sensor over groups. Brucella positives (9, "d, e, f") had the highest divergences while for sensors 1 to 5 responses were lowest for Mannheimia haemolytica infection ("a"). Non-infected samples (groups 1, 2, 4, 6 and 8) were similar to each other (e.g. sensors 2 or 3). Lowest means are indicated with "a" continuing alphabetically according to an increase in group medians.

Groups/ Sensors	1	2	3	4	5	6	7	8	9
1	c	ab	abc	bc	a	abc	bc	a	bc
2	**bc**	**b**	**abcd**	**cd**	**a**	**ab**	**ab**	**ab**	**d**
3	**cd**	**bcd**	**abcd**	**cd**	**a**	**abc**	**ab**	**abcd**	**d**
4	cd	bcd	abcd	d	a	ab	ab	abc	d
5	c	bc	abcd	d	a	abc	ab	abc	d
6	a	a	a	b	a	a	a	bc	c
7	a	a	a	b	a	a	a	bc	c
8	bc	ce	abcde	df	ab	abc	a	def	f
9	ab	ab	abcde	d	ab	bc	a	cd	e
10	c	ab	c	bc	bc	c	abc	a	c
11	bc	a	c	abc	abc	c	abc	ab	c
12	a	ab	abcd	cd	ab	bc	a	bc	d
13	a	ab	abc	c	ab	b	ab	ab	c

Legend: significant differences are indicated as different letters, LSD; $P \leq 0.05$
1 = clin. healthy, 2 = *Mycoplasma bovis* negative , 3 = *Mycoplasma bovis* positive, 4 = *Mannheimia haemolytica* negative, 5 = *Mannheimia haemolytica* positive, 6 = *paraTB* negative , 7 = *paraTB* positive, 8 = *Brucella* negative, 9 = *Brucella* positive

Healthy samples and experimentally infected

Comparing all three clinically healthy groups belonging to the experimentally infected subset, group 1 generated almost the same data compared to the healthy group 2 (sensors 2 to 7, 9, 12, 13, compare same or similar letters in table 9). Regarding group 4 only sensors 3 and 4 generated comparable results. Infected *M. haemolytica* samples were significantly different from the healthy samples of group 1 and 2 while *Mycoplasma bovis* samples generally did not change. Group 3's clinically healthy samples generated variation leading to differences between all clinically healthy samples analysed. Those findings were already confirmed when analysing the experimentally infected samples.

Healthy samples and naturally infected

Comparing the healthy samples and the naturally infected subsets, most of the sensors showed significant differences in their responses. While paraTB had significantly lower divergences than the healthy samples, Brucella had significantly higher average data. Similar tendencies were observed previously. For sensors 1 to 5, 9 and 12 showed no difference between healthy samples coming from the paraTB and Brucella groups.

Healthy, experimentally and naturally infected

Comparing all data, results were inconsistent. Sensors 2 and 3 grouped all healthy groups as the same (“cd” or “bcd”) while for data from experimentally infected individuals, the group medians were below the healthy level (“abc” and “abcd”). Data from naturally infected animals were below and above the healthy level (figures 47 and table 9). The largest differences were the significantly lowest divergences for group 5 (*Mannheimia haemolytica* positives) and the *Brucella* positives below and above the healthy level, respectively. Significant differences between groups are indicated by different letters starting with “a” for the lowest medians and continue alphabetically with increasing group medians.

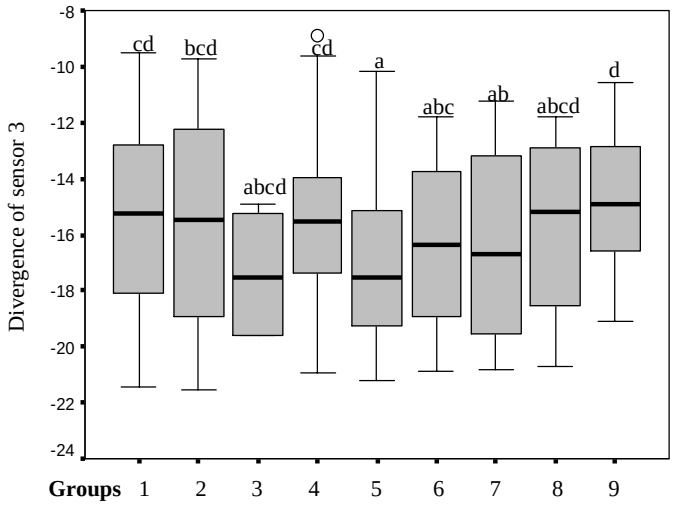

Figure 47: Divergence of sensor 3 (left) and mean-centred medians for all groups and all sensors (right), including the highlighted responses of sensor 3. Responses of groups 3 and 5 were lower comparing the experimental data only. Groups 6 and 8 are close to each other while group 7 is below and group 9 is above.

Legend: significant differences are indicated as different letters, LSD; P ≤ 0.05
1 = clin. healthy, 2 = *Mycoplsama bovis* negative , 3 = *Mycoplasma bovis* positive, 4 = *Mannheimia haemolytica* negative, 5 = *Mannheimia haemolytica* positive, 6 = *paraTB* negative, 7 = *paraTB* positive, 8 = *Brucella* negative, 9 = *Brucella* positive

Figure 48 shows the complete fingerprint of all groups over all sensors using a mean-centred heatmap. The non-covered areas represent the sensors for specific groups and diseases that show significant differences between non-infected and infected according to MRT (see figure legend). The colours of the heatmap indicated the response intensity (red = high divergences, blue = low divergences). Using the combination of means, heatmapping and MRT, the significant and specific differences for each disease and general differences due to infection can be assessed by comparing responses from diseased samples to their non-diseased equivalents.

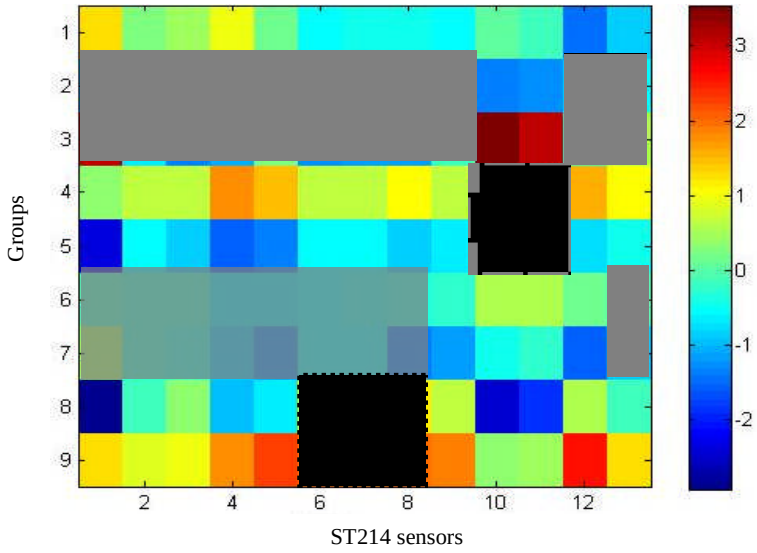

Figure 48: Mean-centred medians for all groups and all sensors. Grey covered areas represent sensors which do not show changes in divergence from non-infected to infected for the same disease. Different diseases can develop a different pattern as indicated here for two experimentally and two naturally infected cattle groups. The dashed area indicates a sensors which grouped all healthy individuals the same.

Legend: significant differences are indicated as different letters, LSD; P ≤ 0.05
1 = clin. healthy, 2 = *Mycoplsama bovis* negative , 3 = *Mycoplasma bovis* positive, 4 = *Mannheimia haemolytica* negative, 5 = *Mannheimia haemolytica* positive, 6 = *paraTB* negative, 7 = *paraTB* positive, 8 = *Brucella* negative, 9 = *Brucella* positive

(IV) Comparison of experimentally and naturally obtained urine samples

In this study, the sensor responses from urine samples from healthy cattle experimentally obtained under standardised conditions were compared to non-standardised field samples (non-infected and infected with paraTB).

Single individuals and samples as well as sample origins had no influence- or the same influence while the factor infection status significantly changed divergences of sensors 4, 5 and 9 to 13 (SPSS, mANOVA). Responses decreased from non-infected to infected based at a group level and considering the infection status only (see sensor 49, left).

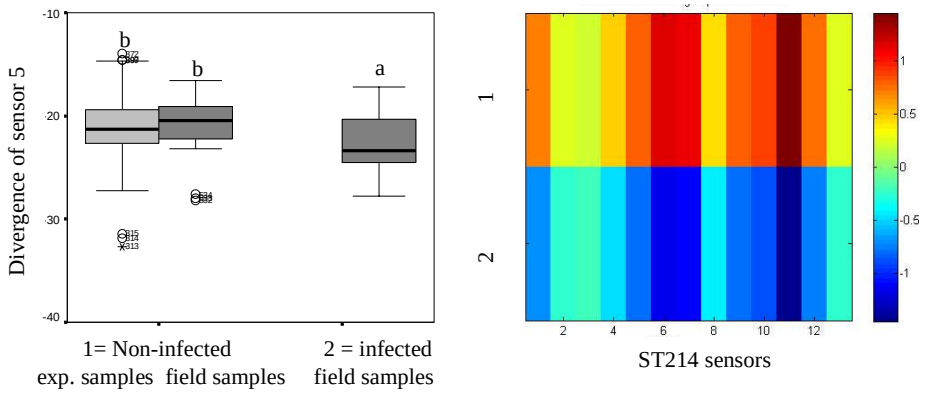

Figure 49: Divergence of sensor 3 (left) and mean-centred medians for all groups over sensors (right, 1= non-infected, 2= infected). As for sensor 3 for instance, almost all sensors showed differences between infected (lower divergences, dark grey, left) and non-infected samples (dark and brighter grey, left) independently to the origin of the sample or the way the samples were obtained.

Using Statgraphics performing multifactor ANOVA, only sensor 13 was found to change its response according to the infection status. However, the MRT confirmed for all sensors except for sensor 1, 6 and 7 that data from infected samples were significantly lower (more negative) than for clinically healthy samples. Spearman's rank correlation confirmed the significant decline in divergence due to the infection with paraTB. For Matlab multifactor ANOVA, sensors 2, 3 and 5 to 8 were found to be significantly changed because of the infection status (figure 49, right).

4. Discussion

4.1 Methodological aspects of e-nose analysis

4.1.1 Sampling methods and mass flows

Mass flow rates were very variable using two ST214 CP e-noses under different experimental setups. Firstly, mass flow rates were not constant between the two CP e-noses and varied by 17.5 % (200 and 235 ml/min, respectively). Static sampling provided constant flow rates for replicates 2 to 5 while for dynamic sampling mass flow rates changed during the sampling process which was also found by others [152]. Dynamic sampling also led to the dilution of the headspace and a non-equilibrium state. This may cause variation between replicates which was also reported by other authors [153].

In contrast, static sampling provided stable mass flow rates and equilibrium states because of the inflatable bag. The ratio of sample volume to bag volume allows comparability between analyses. However, some authors obtained the best discrimination with dynamic sampling but better sensitivity using static sampling [154]. Static sampling significantly improved e-nose responses by minimising variation over replicates. In trace gas analysis (lower ppm to ppb), stability is crucial as even small changes may lead to non-discrimination. The application of a 0.45 µm pore sized filter which was also used in other studies for sensor surface protection and to prevent contamination [42,155] led to a further drop in flow rate by one third. It represents an additional resistance to the air flow and its volatile compounds. One attempt at solving the problem of changing mass flow rates could be the

introduction of a flow cell for temperature- and flow-controlled analysis. Attempts were made to optimise the positions of the sensors on a heating block and the incoming gas so that headspace reacted in the same way with optimised sensors [156, 157].

4.1.2 Different filters and mass flow rates using static sampling

Qualitative and quantitative changes in signals were found when filters were used. The change was dependent on the pore size of the filters, which protect the conducting polymer sensing surface of the e-nose from being changed by a high extent of water vapour. Mass flow rates decreased with a decline in pore size. However, removal of water vapour will also remove other volatile compounds and leads to a change in headspace composition. This was confirmed using CP e-noses combined with PCA data analysis (clustering according to filter application) and analysing quantitative SIFT-MS data. Since most biological samples contain water (e.g. blood/serum and urine), filters have been widely used for protection of the sensors (0.45 µm PTFE, Whatman/Hepavent) [42, 152, 155, 157]. However, these results indicate that using a filter may not be a valid approach since discrimination between 2-butantol giving 10 ppm in headspace at 25°C and ROW was not possible once a 0.45 µm filter was introduced and 98% of all variation was due to the applications of different filters. The headspace was qualitatively and quantitatively changed. Results of SIFT-MS analysis showed qualitative and quantitative changes in sample composition with the addition of a filter. The claimed advantage of using a filter for sensor protection [153, 158] is highly questionable since sensor response patterns change with the use of a filter

and alter the concentration of volatiles (e.g. methanol or ammonia). Therefore, discrimination is made difficult.

4.1.3 CP e-nose characterisation

Temporal changes in sensor response have been reported by others [159, 160]. The sinewave-like changes reported here across the day are possibly due to semi-reversible changes on the sensor surface. Since this effect was observed for both CP e-noses using static bag sampling and confirmed using mANOVA and PCA, it seems to be a systematic problem which is neither associated with dilution of samples nor a non-equilibrium state. It appears to be the result of semi-reversible adsorption and incomplete desorption. Certain molecules might not be desorbed before the software determines a new baseline (offset) for acquisition. Consequently, responses cannot develop as before since binding sites may be still occupied. Since all responses are referred to the baseline signal, divergences change compared to the preceding analysis and lead to poor reproducibility. Occupation of binding sites may come from water molecules in ambient air interacting with dopants or where headspace molecules were not desorbed properly. Purging with an inert gas such as nitrogen has been used by some authors to improve desorption and repeatability [161, 162]. The reasons why responses in this study were in the form of a sine wave, however, remain unclear. This may be evidence of memory effects which have been described by several authors [152, 163, 164]. Further analyses are necessary to elucidate the cause of this effect. A comparison of sensor responses of similar CP e-noses produced by the same manufacturer was not possible due to different flow rates

(180 - 235 ml/min) and qualitatively different responses, although the same substances were analysed under identical conditions. Detailed methodological investigations were described in Knobloch *et al* (2009) [140].

4.2 Healthy and experimentally challenged individuals

4.2.1 Biological variability of serum samples obtained from healthy cattle

Serum is a biological medium with different functions and therefore reflects systemic processes of the host. Hence, physiological changes in the host will come along with a change of serum composition and with a change of the serum headspace. In contrast, urine is the excreted liquid at the end of metabolic processes of the host. For both media, it is necessary to investigate the variability arising from physiological changes of healthy subjects (e.g. over the day) and between a cohort of subjects in order to validate results and to compare them to changes in headspace due to infection.

(I) Changes in serum samples due to growth and nutrition

When serum obtained from three healthy calves (aged four months at the beginning of the trial) over a period of 40 weeks in a 2 weeks interval was headspaced and analysed (section 3.2.1) due to various methodological variations, results were only meaningful at a group level. Data from the responses from all samples were averaged so that the impact of time- and day of analysis which were the main methodological factors influencing the result, were equally distributed over all time points.

As a result, divergences remained at one level from time points 1 to 7 (weeks 0 to 13), varied from time points 8 to 14 (weeks 14 to 27) and stayed constant

again until time point 20 (week 40) but with significantly decreased averaged divergence compared to weeks 1 to 7. The total age of the calves at the variable section was 7 to 8 months which matches with the period of calves' puberty.

Calves usually reach the prepubertal period beginning after 3 months and finish puberty after approximately 9 to 10 months [165]. In this period there are massive physiological changes due to sexual maturation (e.g. proliferation of Leydig cells) including changes in hormone activity such as for testosterone, estradiol or progesterone and also the beginning of the spermatogenesis [165-168]. These systemic physiological changes mediated by hormones lead to changes in natural metabolites circulating in the host's blood stream. Consequently, the headspace of serum represents these processes and can be observed as variations in divergence for various sensors using e-nose. Responses of sensors 2 to 9, 12 and 13 showed the largest differences before and after the variable phase and indicate that a broad range of molecules are linked with this process. Physiological changes from milk fed calves to weaned adults may also affect digestion (change to ruminants, change in hormones such as for insulin, growth hormones or leptin) and could be observed in serum headspace [168, 169]. However, this may not affect the acid base status of blood but the mineral metabolism as shown by giving different diets to Holsteins Fresians [170].

A definite answer which compounds were responsible for changes in headspace is not possible since it requires GC-MS analysis. Nevertheless, the observed changes were bigger than the natural biological range and it has to be concluded that the choice of "subjects" and their physiological status

and nutrition is of major interest for a standardised VOC analysis. This has to be taken into account when looking for differences between healthy and diseased individuals.

(II) Changes in serum samples due to circadian and day to day variability

In a second trial serum samples from six clinically healthy calves were headspaced and analysed using e-nose. As a result, temporal changes were found over the day describing a profile which had the lowest divergences at 8:00 and 10:00 or 16:00, respectively. Generally, divergences were increased over the day reaching a maximum in the evening at 20:00. Furthermore, a decline in divergence was found after feeding. This may be due to systemic changes in metabolism after feeding in cattle which was also found by other authors as a diurnal variation of ammonia or urea in dairy cattle [171]. Amongst others, bile acids were also found to be increased in cattle 1 h after feeding, as well as other metabolites such as glucose, non-esterified fatty acids (NEFA), and β-hydroxybutyrate [172]. An elevated level of hydrogen peroxide (H_2O_2) as an unspecific marker of infection which is also increased during phases of increased metabolism was also found in breath condensate after food intake at exactly the same times and over the day [173]. This supports the results from this study and underlines the importance of normalised samples and precise information about what is measured.

The increase in divergence over the day may presumably not be due to the feeding process but more to general body function. Some authors indicated that there is a physiological change at the end of the day leading to an increased defecation and urination rate overnight [174].

The overall increase is supported by a significant increase at the last time point (20:00). This could be due to tiredness and the beginning of the calves' recovery. Some authors found similar changes in cattle [175] and also in humans; changes in serum composition due to exercising and recovery phases as well as food intake are already proven [176, 177]. However, blood is a strong buffer and the metabolism of food constituents may occur quite quickly and increased concentrations return to a normal physiological state. For instance, for humans the temporal blood glucose concentration were analysed by measuring the surrogate acetone in breath or emitted from skin in real time using SIFT-MS [178]. This could explain why after feeding, the sensor divergence reached the previous level again and remained constant.

As for the other trial, there are numerous sensors which changes in headspace composition indicating that there are also numerous molecules changing over the day. The results obtained are in good agreement with the literature and underline the influence of biological variability within a healthy cohort.

Nutrition, age, and physiological variability have to be taken into account for a reliable analysis. Changes in sensor responses have to be clearly separated from the natural variation of a cohort.

4.2.2 Biological variability of urine samples obtained from healthy cattle

Results from the analysis of the headspace of urine samples from juvenile and adult cattle showed no differences over all sampling days (except for sensor 10 and 11) which indicates good homogeneity and constant characteristics of excreted urine of both groups, juvenile and adult cattle.

Comparing those two groups, clear differences for various sensor responses were found, especially for sensor 4, 5 and 8 to 13. Sensors 4 and 5 showed much higher divergences for the adult cattle in comparison to juvenile cattle. Similar observations were made for sensors 8, 9, 12 and 13 which were sensitive to the same classes of compounds; alcohols, ketones and water [30].

The reasons for the discrimination between juvenile and adult cattle may be a different physiological status comparable to the serum composition discussed in the previous section which will not be considered in detail again. Even more important is the fact that these two groups of animals were fed differently and that urine reflects metabolic processes rather than the physiological status of the individual. Different nutrition therefore leads to a different VOC pattern in urine headspace. Juvenile cattle receive milk replacer with a high energy content and have a generally lower dry matter intake (DMI) resulting in a higher concentration of blood glucose, lactate, pyruvate, β-hydroxybutyrate or NEFA (also see 4.2.1) [179]. All of them have hydroxyl- (-OH), carbonyl (-C=O) or carboxyl groups (-COOH) which are characteristic features of alcohols, ketones/ aldehydes or organic acids. Since e-nose exploits these features and since higher concentrations of these groups trend to cause more negative divergences, urine from juvenile cattle produces more negative divergences when analysed. The impact of nutrition on the urine composition is well known since urea or ammonia was directly correlated to the protein intake, for example [180-182]. Other authors state that the DMI percentage is of much greater importance than the protein concentration for urine composition [183]. Additionally, also ruminant digestion is an issue producing

metabolic products with less hydroxyl- and carbonyl groups but higher amine concentration.

Considering all four time points over the day, a distinct profile for most of the sensors was observed. There was no general trend over the day but divergences of sensors 2 to 8, 12 and 13 changed after eating and became more negative, especially after morning feeding. Similar results were also observed for these sensors analysing serum headspace. In particular sensors 6 and 7 which are supposed to react to alcohols or hydroxyl groups showed a decrease in divergences after feeding. Molecules with hydroxyl- or keto groups originate from various sources but it is believed that there is a direct linkage to feeding. However, since no GC-MS studies have been carried out, this hypothesis remains unproven.

Nevertheless, it has to be underlined that VOC composition of headspace from urine changes comparing young and adult cattle. Feeding is a factor which significantly influences the results of headspace analysis of urine as well as serum.

4.2.3 Variability of serum samples after *Mycoplasma bovis* infection

Similar to the studies carried out before, methodological variation (time and day of analyses) significantly influenced the sensor responses resulting in large variation over sampling days. This explains the large range of responses in the Box and Whisker plots. Hence, results were meaningful only at a group level and did not allow conclusions based on single observations.

The aim of this study was to compare sensor divergences over the course of the disease for both serum headspace from animals given a phosphate

buffered saline (PBS) placebo and headspace from animals experimentally infected with *Mycoplasma bovis*. However, the infection with this pathogen led to only a mild respiratory tract infection with sub-clinical symptoms. Rectal temperature, respiratory rate antibody concentrations and macroscopic and histological analyses revealed some symptoms with a maximum approximately 7 days after infection.

For e-nose divergences, only minor changes over time were observed. At the end of the study (around day 21 after infection) divergences started to decrease for both the placebo treated group and the infection group but changes for the latter group were slightly larger. Nevertheless, decreases in divergence were within the biological range and could not be statistically confirmed using the multiple range test (MRT).

In the international literature it was reported that the detection of the pathogen was mainly performed using PCR [184] but no test system is known for field detection including serum headspace analysis. This could indicate that it is not possible to detect changes in headspace of serum samples due to *Mycoplasma bovis* infection but results from other studies carried out during this project did show differences according to host responses after infection or directly to infections, nutrition or ageing. But in this case, *Mycoplasma bovis* as an infection with sub-clinical symptoms is said to be not very pathogenic. *Mycoplasma bovis* in general does not have a great pathogenicity but *Mycoplasma bovis* may cause sub-clinical symptoms [185] so that it finally becomes only severe if additional factors (e.g. co-infection or bad housing conditions) compromise the immune system. This also explains the large variety of other disease manifestations which are obviously associated with

this pathogen [186]. Nonetheless, the importance of this pathogen today for bovine domestic animals as a causative agent for mastitis [187], arthritis [188, 189] and pneumonia [190, 191] remains unquestioned.

4.2.4 Variability of serum samples after Mannheimia heamolytica infection

The purpose of this study was to assess the potential of the e-nose to detect differences in sensor responses when analysing VOCs in serum headspace from calves with an acute respiratory infection and to evaluate e-nose signals in comparison with the acute host response and rectal temperature; both known biomarkers of disease.

The experimentally induced *Mannheimia haemolytica* (*M. haemolytica*) challenge used in this study represents a severe bacterial infection for cattle as an animal model. Lipopolysaccharides (LPS) were most likely involved in the pathogenesis of acute host response and spontaneous deaths of animals. *Mannheimia* species belong to the group of gram-negative bacteria producing LPS and LPS binding protein (i.e. Lipopolysaccharide binding protein; LBP) increased significantly after challenge (see section 3.2.4). Calves are able to tolerate LPS only to a limited extend and show hyperresponsitivity to LPS as an endotoxin [192].

The systemic host response to infection also included the acute phase response (APR) which is a highly conserved, complex, and non-specific series of immunological reactions mediated by pro-inflammatory cytokines and resulting in an entire array of metabolic and physiologic changes. One characteristic feature of APR after bacterial infection is a remarkable change in concentration of acute phase proteins (APPs) [193]. The origin, importance

and role of these molecules in the host response are reviewed elsewhere and both APP concentrations measured in this study, LBP and haptoglobin (Hp) are accepted as major APPs in cattle [99, 100, 142, 194-196] describing the severity and progress of the disease.

With the e-nose used in this experiment, clinically healthy cattle could be discriminated from challenged individuals with severe clinical symptoms. Significant differences in divergences in e-nose sensor array responses were found at the group level considering the median of groups per day. These differences obtained with sensors 3, 6 and 7 allowed discrimination between infected and non-infected individuals. Discrimination based on individual samples was again not possible because of large variation across all sensors due to methodological factors and inconsistencies of the sensor surface associated with them [140].

Discrimination was also made difficult by the temporal changes in divergences over the course of the infection. Many sensors (e.g. 2 to 8) showed a significant decline at days 2 and 3 after challenge while responses obtained from other time points after infection were similar to pre-infection divergences. This minimised the total differences between all pre- and post challenge samples but on the other hand, this temporal profile reflected the progression of the infection.

The fact that e-nose sensor signals were reduced (i.e. decreasing reactions in e-nose response) after challenge is in good agreement with data reported from human medicine showing the ability of an electronic nose to detect changes in the human body odour as a result of renal dysfunction by reducing multivariate sensor signals [41, 197].

However, the biochemical background for both the discrimination between infection and non-infection and the temporal profile after infection still remains unclear since it could not be elucidated in this study which molecules were responsible for the changes. To clarify this point, further analytical options and techniques are required (e.g. GC-MS).

In this study, the severity of the experimentally induced bacterial infection was confirmed and characterised by clinical illness and spontaneous deaths. Body temperature and concentrations of APPs measurable in the peripheral blood provided additional quantitative assessment of the host response. Different APPs may show either an increase or a decrease in concentration following infection [99].

The two APPs included in this study, LBP and Hp, increased significantly after exposure to *M. haem*. A1. These findings confirm results from previous studies reporting an increased concentration of many APPs, including Hp and LBP, following an infection of the respiratory tract of calves with gram-negative bacteria (*Pasteurella multocida* or Mannheimia haemolytica) [197, 198]. LBP and Hp were positively correlated in this study and expressed similar temporal profiles over the experimental period. Interestingly, the correlation between LBP and Hp was stronger using Spearman's rank correlation ($r_{SP} > 0.7$) compared to the correlations between body temperature and each of the APPs ($r_{SP} \sim 0.5$). Nevertheless all three parameters reflected the APR in calves after bacterial infection with *M. haem*. A1, thus providing a good basis for the evaluation of responses of e-nose sensors.

The divergence of multiple sensors as a part of the e-nose array changed significantly over time comparing pre- and post challenge samples.

Comparing the temporal profile of the e-nose responses with rectal temperature and APP concentrations revealed general correlations of several sensors and the surrogate markers for infection. Correlations between e-nose responses and LBP or Hp were more prominent compared to correlations between e-nose sensors and rectal temperature. However, correlation coefficients were low ($r_{SP} \leq 0.20$). This might be due to the fact that the temporal profile observed for each of e-nose signal, rectal temperature and APP concentrations were sometimes out of phase with one another, even though they were comparable in shape. Nevertheless, the correlation between the concentration of APPs as surrogate markers of infection and e-nose sensor responses demonstrate the potential for VOC analysis by e-nose or other methods for monitoring and diagnosing infection and/or host response.

4.2.5 Variability of serum samples from *Mycobacterium bovis* infected cattle

The objective of this study was to assess the potential of e-nose to detect differences in headspace of serum samples after animals were infected with *Mycobacterium bovis*. Different vaccination strategies (no vaccination, BCG vaccination and BCG/ Ad85a vaccination) were applied to the animals and the changes in headspace were analysed over time and according to vaccinations.

Samples for all three groups were collected on 4 time points, 1 prior to infection but when the subjects were already vaccinated and 3 time points (weeks 2 to 4 post infection). The BCG/ Ad85a vaccinated animals were not sampled at time point 3.

As for the studies before, methodology caused most of the variation. Accordingly, data analysis was performed on the basis of medians and means rather than on individual data. Based on the averaged data, different patterns of e-nose responses were obtained.

The unvaccinated control animals showed a significant decrease in divergence mainly for sensors 8 to 13 which were sensitive mainly to alcohols and ketones (sensor 8, 9, 12 and 13) or aldehydes (sensors 10, 11). The BCG vaccinated animals had constant divergences except for time point 3 (3 weeks after infection). Some sensors showed also lower divergences before infection. For the BCG/ Ad85a vaccination group, highest divergences were found at time point 4 (4 weeks after infection). For both groups almost the same sensors as for the first group were sensitive to changes in headspace. In order to compare all three groups to each other and to changes over the study, only time points 1 and 4 were considered. Samples from all groups at time point 1 (non-vaccinated, BCG vaccinated and BCG/ Ad85a vaccinated) were regarded as one group because they were all taken prior to infection and samples and were not statistically different due to vaccination. These samples were compared to each differently vaccinated group after infection at time point 4. The BCG vaccinated- and BCG/ Ad85a vaccinated had more positive divergences compared to the pre-infection data but without any statistical relevance. Both groups were classified the same using the MRT. This result was observed in particular for sensors 5 (alcohols, ketones), 9 (alcohols, ketones), 10 (aldehydes), 11 (aldehydes), 13 (alcohols, ketones; see table 1 in the introduction section). The group responses for the control animals were classified as “a” while all other groups were classified as “b”. In other words,

the control group could have a higher quantity of polar molecules as mentioned above.

Interestingly, when comparing e-nose and Bovigam results, similar trends were observed. γ-Interferon (γ-INF) was increased at time point 4 (experimental week 18, see section 3.2.5) for the non-vaccinated controls and divergences for the same group were lowest.

Using both techniques, no differences were found between both vaccinated groups (BCG and BCG/Ad85a) which further support the e-nose results. The pathological score was highest for the non-vaccinated group and no statistical difference was found between vaccinated groups. Altogether, results using all three groups independently indicate the ability to discriminate between *Mycobacterium bovis* positives and negatives in an experimental infection and underline the potential of e-nose as a rapid detection system. However, as for the previous studies, it remains unclear whether changes in headspace are due to the infection with *Mycobacterium bovis* or just a result of the animals' host response since no GC-MS study was carried our in parallel. Additionally, it would be interesting to see if different results could be obtained using similar pathogens (e.g. infections with other *Mycobacteria* sp.), but this remains future work. Also, since the type of e-nose showed huge methodological variation this study can only show the potential under optimised circumstances and is not suitable for field detection of single animals. But previous studies have already proven the potential (see introduction section 1.4.3 (III)). Nevertheless, this is to the best of my knowledge, the first study dealing with the analysis of serum headspace from *Mycobacterium bovis* infected cattle and the comparison of results from immunological and

pathological investigations which draw the same conclusion. Latest results from other groups also demonstrated the ability of using a differential mobility spectrometer (DMS) for tuberculosis detection [199, 200] underlining the possibility of detecting tuberculosis for both veterinary and human medicine as an alternative to the various immunological tests that are currently used. Results obtained so far with these immunological tests are in most cases inconsistent so that alternatives are urgently required [201]. Current ELISA tests exploit the detection of different antibodies with different specificities and selectivities [202-204] and different biomarkers for different tuberculosis infections are under discussion for various immune-based screening systems. However, none of these tests are as inexpensive, portable and requiring as few laboratory personnel as a well engineered e-nose for headspace analysis for screening purpose which could contribute to a better rapid field testing adding independent information

4.2.6 Variability of urine samples from *Mycobacerium bovis* infected cattle

In this study, serum samples were analysed from the same individuals as in the previous study. Samples were collected and analysed from control animals and BCG vaccinated individuals but the first two time points in this study were prior to infection while the remaining two were after infection.

As a result, large variations due to methodological issues (e.g. time and day of analysis) were found. This allowed only a consideration at a group level. Under these circumstances, divergences for each group (time points 1 to 4 over vaccination strategies) remained almost the same and were not statistically different with one exception. There was a significant peak for the

control animals at time point 3. Divergences were much more positive than compared to those from all other groups. The results clearly indicate that shortly after infection urine from the control animals were different than urine from the vaccinated subjects. No correlation was found between the pathological scores and e-noses responses.

After averaging all data before infection at time points 1 and 2, averaged pre-infection data was compared with the data at time point 4 for the non-vaccinated control group and the BCG vaccinated group. An increase in divergences for the non-vaccinated control group was observed while the vaccinated group remained constant. This result was not confirmed considering the each group at single time points. But interestingly, the same sensors as for the serum samples showed significant changes over time (sensors 5 and 9 to 11). However, responses for urine samples increased while for the serum samples divergences were decreased. The reason for this effect will remain unknown since no GC-MS analysis was carried out.

Diurnal changes in urine headspace of healthy cattle or due to nutrition were already found in previous studies (section 3.2.2) and results in the literature [205] showed the potential of using the same type of electronic nose for the headspace analysis of urine samples from human dialysis patents. Some authors found changes in urine from humans and were able to correlate those with the presence of pulmonary tuberculosis using a polymerase chain reaction (PCR) test [206, 207] while others analysed VOCs from human urine samples to screen for different types of bacteria [208]. Based on these results reported in literature and the presented study results it appears that changes in urine headspace VOC can be caused by the *Mycobacteria* ssp. entering the

host or by the immune system responding to the infection. The results from this study indicate that the latter may be the case since in the course of the experimental infection no further changes could be observed. However, since no GC-MS analysis was carried out, the exact headspace composition remains unclear. E-nose results just indicate a reduced concentration of molecules with dipole moments as reactive groups (keto- and hydroxyl groups) immediately following the infection.

4.3 Naturally infected individuals

4.3.1 Variability of healthy- and paraTuberculosis infected serum samples

The objective of this study was to investigate the possibility of differentiating between serum samples from *paraTuberculosis* positive and negative animals. The analysis of variance revealed large variation due to the time and day of analysis which, as in previous studies, allowed only a consideration of data on a group level. Based on the group divergences significant differences expressed as lower divergences were found.

Including the pathology and clinical signs of infection into the analysis and comparing these parameters with changes in divergence, significant changes in sensor responses were found. Responses decreased with increasing severity of clinical symptoms while the correlations between sensor responses and the pathological scores were inconsistent.

The sensors which showed differences between the infection statuses were susceptible to amines, alcohols and ketones. Again, this suggests that the

changes are not due to a single compound changed, but rather a mixture of molecules which are altered due to infection or host response. The sampled animals came from different regions in Germany, had a different gender and were fed differently. This non-standardisation leads to large biological variation which makes it more difficult to detect differences in serum headspace composition. However, discrimination at a group level between *paraTuberculosis* positives and negatives was possible and, thus, showed the potential of VOC analysis of serum samples using e-noses. This could be a useful tool for screening herds and give additional information due to a poor sensitivity and selectivity of existing immunological tests [204] (also section 1.6.4).

4.3.2 Variability of healthy and Brucella infected serum samples

Apart from methodological variation, a general increase in divergence from healthy to *Brucella* infected samples was investigated. Various sensors were found to show differences after infection of non-standardised cattle. Number and type of sensors (sensitivity towards amines, alcohols and ketones) suggest complex changes in the VOC composition of serum headspace on a group level due to infection. The impact of these results and the relation to the other infections will be discussed under 4.3.5 (II/ III). As for the *paraTuberculosis* infected samples, e-nose showed the potential for *Brucella* detection using serum headspace analysis.

4.3.3 Variability of healthy and *Mycobacterium bovis* infected serum samples from badgers

Similar to the studies in sections 3.3.1 and 3.3.2 non-standardised serum samples were headspaced and analysed using e-nose. But in contrast serum was sampled from wildlife badgers, which represent a natural reservoir of *Mycobacteria* and in particular of *Mycobacterium bovis*. The badgers are proven to continuously re-infect cattle herds which lead to serious health and economic problems [209].

In this study, data analysis showed the day of analysis as having the largest impact on the data set. Samples could be clearly discriminated according to day but no discrimination was found between samples with a confirmed tuberculosis positive and negative status. Since samples came from non-standardised subjects the range of biological variation (e.g. gender, nutrition, health status or living conditions) was high. But in addition to other studies, changes in serum headspace may also be due to the presence of various anaesthetics which had been given to the badgers prior to the blood samples being taken. In total, these reasons lead, from the statistical point of view, to variation which cannot be eliminated (also due to a lack of information about samples) and which cover the differences in headspace due to the infection with *Mycobacterium bovis*. Under these circumstances there is no way of using this e-nose for rapid field detection or even just for screening. Accordingly, some authors critically state that electronic noses need to qualify specific states which require exact information about the analysed samples. Furthermore they need to be more sensitive and specific [210]. But specificity is not the problem since (i) e-noses exploit the overlapping specificities of

different sensors to generate a pattern or fingerprint and (ii) it loses its universal applicability. An increase in specificity will lead to single biosensors, again. Other authors state that electronic noses are already sensitive enough, for instance for on the field detection of fruit infections using quartz resonator based e-noses [211]. But it is believed that by making sensor responses more consistent and reliable much better results could be obtained also using conducting polymer bases e-noses (also see section 3.1 and [140]). However, it will not reach sensitivities of MS systems. In comparison to alternative systems, there is also insufficient sensitivity using immunological test systems [212] and the problem with cross reactivities of different antigens. In a similar vein to the GC-MS validation of e-nose data, immunological tests need to be validated using cultures [213]. Finally, electronic nose may have some potential in screening for infections even for non-standardised field samples as section 3.3.5 shows.

4.3.4 Variability of healthy and paraTuberculosis infected urine samples

In addition to serum headspace analysis (section 3.3.1), urine samples were headspaced and VOC composition was analysed using e-nose. The objective was to assess the potential ability to discriminate between *paraTuberculosis* positives and negatives. As a result, the averaged divergences were decreased from non-infected to infected samples. However, since all negatives came from one farm in Germany the relation the impact of the origin of samples was assessed. The MRT proved that all samples with a positive *paraTuberculosis* status had significantly lower averaged divergences independent of the animal's location. In other words, the variation of the

'origin' (potentially different nutrition and housing) was lower than differences caused by the infection. The best of my knowledge, this is the first study using electronic noses for field detection of *paraTuberculosis* in urine and illustrates that screening urine samples for this disease can be a potential application of e-nose together with immunological tests improve sensitivity and selectivity.

4.3.5 Comparison of serum and urine samples

(I) Comparison of experimentally obtained serum samples

For the comparison of all experimentally obtained serum samples all data was divided into 5 groups (section 3.3.5) and the averaged divergences were compared to each other. The result for sensors 2 to 5 showed a significant decrease in sensor responses for groups 3 and 5 which represented the groups of *Mycoplasma bovis* positives (a disease with subclinical symptoms) and *Mannheimia haemoytica* positives (a disease with obvious clinical symptom and spontaneous deaths). All other groups representing samples from clinically healthy individuals had an averaged divergence at about one level. These results indicate that discrimination was possible when analysing serum samples from animals under nearly identical and controlled ambient-, biological and feeding conditions.

The overall pattern furthermore indicated that discrimination was possible for different reasons. While sensors 2 to 5 grouped divergences according to the infection status (positive or negative), different sensors were able to discriminate between positives and negatives for each disease. This effect matches with the theoretical principle of e–noses; to differentiate based on different 'fingerprints' which is in particular important since e-nose seemed to

pick up responses due to infection (e.g. immune response) and more specific responses according to the particular disease. In case methodological variation can be significantly reduced and a robust sampling methodology can be included (temperature- and flow control) e-nose may potentially be used as a screening tool for serum samples obtained under standardised experimental conditions. A complex dataset is vital for e-nose analysis since statistics have to deal with variation than can be associated to a disease. This was not proven to specifically detect one of the diseases but it was to illustrate differences to healthy equivalents and therefore the prove-of-concept as a screening tool.

(II) Comparison of samples obtained from naturally infected individuals

Comparing the averaged sensor responses from the analysis of all naturally obtained samples, divergences for healthy samples were found to be at one level or next to each other while samples from paraTuberculosis positive animals had more negative divergences- and from Brucellosis positive animals, more positive divergences. These results were confirmed using PCA. Samples from healthy individuals were all between *paraTuberculosis* positives and *Brucella* positives. The main variance (99.9% of all covered variance) for averaged divergences was caused by the disease status for both positive groups followed by their origin (0.1% of all covered variance, *Brucella* samples came from the UK, *paraTuberculosis* samples came from Germany). These results demonstrate that in case methodological variation can be reduced (as mentioned in the section before) there is a potential of even differentiating between non-standardised field samples. This is the first study that was successfully able to discriminate non-standardised field samples

under limited circumstances (averaging samples resulting in unwanted variance elimination). The future objective is to achieve discrimination without averaging and using techniques like partial least squares discriminant analysis (PLS-DA) to match unknown samples to an infection status using a database. The remaining question will then be how large the biological variation of the field samples will be (apart from the methodological variation); but this will be an objective for future projects. A data base and the application of discriminant analysis (DA) will have to cope with these difficulties.

(III) Comparison of experimentally and naturally obtained serum samples

Grouping all samples (nine groups) according to the disease and infection state, a complex fingerprint was obtained. This is probably the most comprehensive VOC analysis study for different experimental infection studies and naturally obtained samples using e-noses.

There was one sensor (sensor 3) which showed to have averaged divergences of all samples from healthy individuals at one level, *Mycoplasma bovis* positives, *Mannheimia haemolytica* positives at a level below and *Brucella* an averaged response above this level (results for *Mycoplasma bovis* were not significantly different using the MRT. A second sensor (sensor 2) showed a similar, but slightly less clear-cut trend. Other observations for the remaining sensors resulted in a complex pattern or fingerprint. This suggests that e-nose picks up a range of substances which are either released by the bacteria (disease specific) or a result of the infection with pathogens (e.g. immune response). Similar responses in comparison to the samples from healthy individuals can be interpreted as the detection changes in VOC composition due to the immune response while the different patterns following

the ability to discriminated between particular diseases seems rather disease specific. Accordingly a complete fingerprint was obtained which was specific for the diseases including three experimental studies and naturally obtained samples from non-diseased- and infected individuals with two different diseases (see section 3.3.5 (III)).

In the future, this way of displaying data may be a useful alternative to PCA plots especially for field applications showing changes in sensor responses in a simple and understandable way to farmers or medicines (human or veterinarians) immediately after screening individuals.

(IV) Comparison of experimentally and naturally obtained urine samples

The comparison of the urine studies showed that urine from experimentally and naturally obtained samples from non-infected cattle were not significantly different from each other. However there were large differences in divergence for almost all sensors showing that due to infection, the headspace of urine significantly changed. These changes due to a natural infection with *Mycobacterium avium* ssp. *paratuberculosis* were bigger than the changes between non-infected experimentally and naturally obtained urine samples.

However, it remains unknown whether in the *paraTuberculosis* infected animals, co-infections can be excluded. This could also change e-nose responses. *ParaTuberculosis*, as almost all infections with *Mycobacteria* spp., waits until the hosts' immune defence is compromised by a co-infection and enters the subject more easily (section 1.6.4). However, no obvious co-infection was found by veterinarians in Germany and, additionally, the pathogenic nature of the disease indicates that the differences may be due to infection. *ParaTuberculosis* develops in the gastro-intestinal tract which is

closely linked to kidneys and urine excretion. This could be the reason why changes in urine headspace are obvious. But since no GC-MS study was performed, this hypothesis remains unproven.

The experimental infection with *Mycobacterium bovis* (section 3.2.6) did not show large variation in urine headspace composition due to infection considering data for each time point. However, directly after infection, divergences were elevated for almost all sensors. A consideration of all pre-infection data and data obtained at the end of the study (time point 4) showed a significant increase in divergences for several sensors but only for the non-vaccinated control animals while responses from vaccinated subjects remained at the pre-infection level. A very low pathological score for the vaccinated subjects and a significantly higher score for the non-vaccinated individuals supported the findings applying an alternative γ-INF assay. However, it is not entirely clear why this result could not be obtained for the averaged data of each time point but there were two effects which ocurred with the second consideration: (i) elimination of pre-infection variation by averaging all data after statistical analysis found non-vaccinated and vaccinated groups the same and (ii) the elimination of variation at time point 3 (after infection). It seems that variation directly after the infection which may be associated to the host response, was too large and covered the variance due to the disease progress for the non-vaccinated individuals.

Altogether, it can be concluded that in this study sensor responses change more due the the host response following the infection than to the infection itself. However, both effects could be observed eliminating disturbing variance.

4.6 Statistical analysis

As shown on the previous pages, there are various reasons which can cause variation. Biological variation can be caused by different ages, nutrition, housing or different infection states. Methodological variation can occur due to uncontrolled sampling process (filter application, unstable mass flow rates) or inconsistent sensor response generation (e.g. changes in temperature, semi-reversible adsorption).

In most studies, the main objective is to see whether one can use an e-nose to differentiate between non-infected and infected individuals. In other words, there are two groups of data which should be different enough for discrimination. Other types of variation than the 'infection status' can be interpreted as disturbing factors and make discrimination much more difficult.

In this case, methodological weaknesses of this particular e-nose cause largely overlapping datasets. Different studies additionally add variation (e.g. naturally obtained/ non-standardised samples) and therefore reduce the probability to see differences due to infection. For this reason the status of the samples was encoded, and univariate multifactor analysis of variance (mANOVA) was performed in combination with the multiple range test (MRT). Both techniques calculate significant results for separate factors which influence the complete dataset and need to be defined before. There was no possibility using multivariate principle component analysis (PCA) for raw data since PCA picks up only the factors which cause the largest changes in divergence for the complete dataset; and this was clearly not due to the infection state which covers only a small fraction of variation.

Also the analysis of raw data using discriminant function analysis (DA) or partial least square discriminant function analysis (PLSDA) is not valid for the following reasons:

(I) PLSDA/ DA requires a stable system since it uses a dataset to train a model first (equation) which is then validated with a second dataset to predict for instance the disease status with a certain accuracy. As already mentioned, there was unpredictable methodological (e.g. no controlled temperature) and biological variation (inter/ intraindividual variation). Since this type of variation is much bigger than for instance the 'disease status' it will only be possible in the best case to generate a model with a low accuracy rate. This is not useful for diagnostic purposes or screening.

(II) For training and validation a large amount of data is required for each separate disease and infection- and vaccination state considering the remaining influencing parameters as constant. Although a lot of samples with a lot of different 'disease statuses' the remaining parameters were all varying, in particular the methodological ones.

(III) For most of the studies a progressing infection was observed rather than a clearly different disease status such as 'infected/ non-infected'. Statistically, the 'disease status' was not a constant over time and therefore cannot clearly be discriminated using PLSDA/ DA. Differences between consecutive time points are too small. However, in case the remaining variation can be eliminated, PCA can be used for graphical discrimination to show the 'migration' of data points following the progressing disease, which was done for the *Mannheimia haemolytica* infection (section 3.2.4) or the paraTB and Brucella data (section 3.3.5 (II)). But PCA required the reduction of disturbing

variance which was achieved by randomly analysing and averaging data. Under these circumstances, unwanted variation was equally distributed on each group and discrimination was achieved. Alternatively, data for relevant sensors was displayed as Box and Whisker plots which allowed the illustration of temporal profiles of divergences but Boxes and Whiskers also indicated a large overlapping due to different biological and methodological variation. MRT identified whether the averaged divergences were significantly different or not. Responses of all mean and median divergences were normalised and displayed as heatmaps and gave a complete fingerprint. This was accomplished by the Matlab script.

5. Conclusion & future work

Methodological

- Under the given circumstances, the conducting polymer type of e-nose described here is not ready to be used as a tool for detection of diseases, in particular field detection, or even for screening.

- The methodology of the device needs to be improved in terms of a flow- and temperature control. Their absence complicates analysis especially in on-field environments by generating large methodological variation which overlaps with the biological variation.

- Filter use cannot be recommended for protecting the sensor surface against contamination or destruction since filter change the sample composition and makes the sensor responses inconsistent.

- Incomplete desorption from sensors affects conducting polymer sensors. Longer purging with inert gases may solve this problem and lead to more consistent responses over time.

- Methodological variation leads to an inconsistent system for headspace analysis and therefore multivariate data such as discriminant analysis (DA) is not applicable since variation cannot be predicted.

- Randomised analysis of samples and the consideration of group averaged data to were used instead to eliminate disturbing variation and to perform univariate statistics and principle components analysis (PCA). Under these circumstances meaningful results can be obtained and displayed as Box and Whisker plots, heatmaps or PCA plots.

- An automated program for data analysis was created which enables the usage of various uni- and multivariate techniques and allows multiple ways of displaying and analysing data.
- In future, data should be analysed without averaging since large databases will be required for DA.
- The combination of heatmaps and MRT results can be used as alternatives for PCA plots.

Biological

- The ability of e-nose to discriminate biological media was demonstrated. Methodological variation made discrimination difficult. Meaningful results were only obtained at a group level.
- E-nose responses showed diurnal changes analysing serum and urine samples from clinically healthy cattle. Changes were mostly due to food intake but also over the day.
- Serum and urine samples from clinically healthy cattle show changing headspace composition with the ageing of the individuals (hormonal and physiological changes) and nutrition.
- Good results were obtained for the experimental infection with strong clinical symptoms (*Mannheimia haemolytica* A1). Results were confirmed using alternative immunological methods (ELISA testing of acute phase proteins) and other clinical symptoms (rectal temperature). A progressive change in VOC composition following clinical signs was observed. For sub-clinical infections (*Mycoplasma bovis*) results were less clear. Infections with *Mycobacterium avium* ssp. *paraTuberculosis* and *Mycobacterium bovis*

showed also correlations between e-nose responses and immunological results.

- Discrimination of urine headspace samples between non-diseased and diseased cattle after infection with *Mycobacterium bovis* and *Mycobacterium avium* ssp. *paraTuberculosis* was possible at a group level. Changes in sensor responses detecting host responses were larger than changed due to infection of *Mycobacterium bovis*.

- Naturally infected individuals with strong clinical symptoms could be discriminated at a group level. All healthy samples could be grouped as one. Clinical signs were correlated with e-nose results underlining the principal ability of e-nose to detect and screen for diseases in serum and urine headspace also under field conditions.

- Finally, comprehensive studies including controls- and differently infected animals, nutrition, housing and gender need to be conducted in order to establish a well defined database for the prediction of diseases under different circumstances. CG-MS need to be applied for validation and to identify biomarkers.

List of abbreviations (in alphabetic order)

Chemical elements are not listed but described in the text. Variables of equations and are not included since they are also explained in the text.

A			
	Ad85a	genetically modified adeno virus for vaccination enhancement	
	AG	arabinogalactan	
	a.i.	*ante infectionem*, before infection	
	APP	acute phase proteins	
	APR	acute phase response	
B			
	BAW	bulk acoustic wave	
	BCG	Bacillus Calmette-Guérin	
C			
	cfu	colony forming units	
	CP	conducting polymer	
D			
	d	day	
	DA	discriminant (function) analysis	
	DEFRA	Department for Environment, Food and Rural Affairs	
	DMI	dry matter intake	
	DMS	differential (ion) mobility spectrometer	
E			
	ECD	electron capture detector (for GC-MS analysis)	
	ELISA	enzyme linked immuno-sorbent assay	
	e-nose	electronic nose	
	eV	electron volts	SI unit of energy
F			
	FID	flame ionisation detector (for GC-MS analysis)	
	FLI	'Friedrich-Loeffler-Institut', institute for molecular pathogenesis	
	FPA	fluorescence polarisation assays	
	FSM	full scan mode	
G			
	γ-INF	γ-interferon	
	g	gram	SI unit of mass
	GC-MS	gas chromatography-mass spectrometry	
	Glom	glomeruli	
H			
	Hp	haptoglobin	
	HWD	hot wire detector (for GC-MS analysis)	
I			
	i.d.	internal diameter	
	Ig	immune globuline	
	IR	infra red	
L			
	(n, µ, m) L	(nano, mycro, milli) liter	(SI unit of volume)
	LC	liquid chromatographic	

LPB	lipopolysaccharide binding protein	
LPS	lipopolysaccharide	
Ltd.	Limited	

M

(n, µ, m) m	(nano, mycro, milli)meter	SI unit of distance
MAC	*Mycobacterium avium* complex	
mANOVA	multifactor analysis of variance	
MAP	*Mycobacterium avium* ssp *paratuberculosis*	
MAPc	mycolyl-arabinogalactan-peptidoglycan complex	
MAPIA	multi-antigen print immunoassays	
M.haem A1	*Mannheimia haemolytica* serotype A1	
MHz	(Mega)Hertz	SI unit of frequency
MIM	multiple ion mode	
MRT	multiple range test	
MS	mass spectrometry	

N

NEFA	non-esterified fatty acids	
NMR	nuclear magnetic resonance	

O

OB	olfactory bulb	
OE	olfactory epithelium	

P

p	pressure	
Pa	Pascal	SI unit of pressure
PA	proton affinity	
PBS	phosphate buffered saline	
PCA	principle component analysis	
PCR	polymerase chain reaction	
PID	photo ionisation detector (for GC-MS analysis)	
PIM	phosphatidylinositol mannosides	
p.i.	*post infectionem*, after infection	
PLSDA	partial least squares discriminant (function) analysis	
ppb	parts-per-billion,	gas molecule concentration
PPD	purified protein derivate	
ppm	parts-per-million,	gas molecule concentration
ppt	parts-per-trillion,	gas molecule concentration

Q

QCM	quartz crystal mycrobalance	

R

r_{SP}	Spearman's rank correlation coefficient	
RT-PCR	real-time polymerase chain reaction	

S

s	second	SI unit of time
SAW	surface acoustic wave	
SDS-PAGE	sodium dodecylsulphate-polyacrylamide gel electrophoresis	
SIFT-MS	Selected Ion Flow Tube-Mass Spectrometry	
sp.	species	
SPME	solid phase micro extraction	
ssp.	subspecies.	

T

TB	tuberculosis	
TCD	thermal conductivity detector (for GC-MS application)	

	TLC	thin layer chromatography
	TSA	tuberculostearic acid
U		
	UK	United Kingdom
V		
	υ	velocity
	VOC	volatile organic compounds

List of references

1 Pearce, T.C. (1997). Computational parallels between the biological olfactory pathway and its analogue 'the electronic nose': Part I. Biological olfaction. Biosystems 41(1). 43-67.

2 Shepherd, G.M. (1991). Sensory transduction: entering the mainstream of membrane signalling, Cell 67(5), 845-851.

3 Gesteland, R.C., J.Y. Lettvin, and W.H. Pitts. (1965). Chemical transmission in the nose of the frog. Journal of Physiology 181(3), 525-559.

4 Breer, H., (2003). Olfactory receptors: molecular basis for recognition and discrimination of odors. Analytical and Bioanalytical Chemistry 377(3), 427-433.

5 Duchamp, A., Revial, M.F., Holley, A. MacLeod, P. (1974). Odor Discrimination by Frog Olfactory Receptors. Chemical Senses & Flavour 1(2), 213-233.

6 Mathews, D.F., (1972). Response patterns of single neurons in the tortoise olfactory epithelium and olfactory bulb. Journal of Genetics and Physiology 60(2), 166-180.

7 Mombaerts, P., Wang, F., Dulac, C., Chao, S.K., Nemes, A., Mendelsohn, M., Edmondson, J., Axel, R. (1996). Visualizing an olfactory sensory map. Cell 87(4), 675-686.

8 Kauer, S., Hamilton, K.A., (1987). Odor Information Processing in the Olfactory Bulb. Evidence from Extracellular and Intracellular Recordings and from 2-Deoxyglucose Activity Mapping. Annals of the New York Academy of Sciences 510(1), 400-402.

9 Hauptmann, P., Borngraeber, R. and Schroeder, J. (2000). Artificial electronic tongue in comparison to the electronic nose- state of the art and trends, In 2000 IEEUEIA International Frequency Control Symposium and Exhibition.

10 Snopok, B.A. and Kruglenko, I.V., (2002). Multisensor systems for chemical analysis: state-of-the-art in Electronic Nose technology and new trends in machine olfaction. Thin Solid Films 418(1), 21-41.

11 Capone, S., Forleo, A., Francioso, L., Rella, R., Siciliano, P., Spadavecchia, J., Presicce, D.S., Taurino, A.M. (2003). Solid state gas sensors: State of the art and future activities. Journal of Optoelectronics and Advanced Materials 5(5), 1335-1348.

12 James, D., Scott, S.M., Ali, Z., O'Hare, W.T. (2005). Chemical sensors for electronic nose systems. Microchimica Acta, 149(1-2) 1-17.

13 Wu, T.Z. (1999). A piezoelectric biosensor as an olfactory receptor for odour detection: electronic nose. Biosensors & Bioelectronics 14(1), 9-18.

14 Gopel, W., (2000). From electronic to bioelectronic olfaction, or: from artificial "moses" to real noses. Sensors and Actuators B-Chemical 65(1-3), 70-72.

15 Spanel, P. Diskin, A.M., Abbott, S.M., Wang, T., Smith, D. (2002). Quantification of volatile compounds in the headspace of aqueous liquids using selected ion flow tube mass spectrometry. Rapid Communication in Mass Spectrometry 16(22), 2148-2153.

16 Sander, R. (1999). Compilation of Henry's Law Constants for Inorganic and Organic Species of Potential Importance in Environmental Chemistry (Version 3).

17 Snider, J.R. and Dawson, N.S., (1985). Tropospheric Light Alcohols, Carbonyls, and Acetonitrile- Concentrations in Southwestern United-States and Henry Law Data. Journal of Geophysical Research-Atmospheres 90(2), 3797-3805.

18 Walt, D.R. (1998). Optical sensor arrays for odour recognition. Biosensors & Bioelectronics 13, 697-699.

19 Spadavecchia, J., Ciccarella, G., Rella, R., Capone, S., Siciliano, P., (2003). Metallophthalocyanines thin films in array configuration for electronic optical nose applications. Sensors and Actuators B-Chemical 96(3), 489-497.

20 Suslick, K.S., Rakow, N.A., Sen, A. (2004). Colorimetric sensor arrays for molecular recognition, Tetrahedron 60, 11133–11138

21 Christie, S., Scorsone, E., Persaud, K., Kvasnik, F. (2003). Remote detection of gaseous ammonia using the near infrared transmission properties of polyaniline. Sensors and Actuators B-Chemical 90(1-3), 163-169.

22 Bailey, R.C., Parpia, M.; Hupp, J.T. (2005). Bibliographic Page Sensing via optical interference. Materials Today 8(4), 46-52.

23 Lee, S.M., Dyer, D.C., Gardner, J.W., (2003). Design and optimisation of a high-temperature silicon micro-hotplate for nanoporous palladium pellistors. Microelectronics Journal 34(2), 115-126.

24 Gall, M. (1991). The Si Planar Pellistor - a Low-Power Pellistor Sensor in Si Thin-Film Technology. Sensors and Actuators B-Chemical 4(3-4), 533-538.

25 Li, Y.F. and Y.F. Fan (1996). Doping competition of anions during the electropolymerization of pyrrole in aqueous solutions. Synthetic Metals 79(3), 225-227.

26 Gibson, T.D., Prosser, O., Hulbert, J.N., Marshall, R.W., Corcoran, P., Lowery, P., Ruck-Keene, E.A., Heron, S., (1997). Detection and simultaneous identification of microorganisms from headspace samples using an electronic nose. Sensors and Actuators B-Chemical 44(1-3) 413-422.

27 Ampuero, S. and Bosset, J.O., (2003). The electronic nose applied to dairy products: a review. Sensors and Actuators B-Chemical 94(1), 1-12.

28 Gardner, J.W. and Bartlett, P.N. (1995). Application of conducting polymer technology in microsystems. Sensors and Actuators A-Physical 51(1), 57-66.

29 De Melo, C.P., Neto, B.B., De Lima, E.G., De Lira, L.F.B., De Souza, J.E.G.. (2005). Use of conducting polypyrrole blends as gas sensors. Sensors and Actuators B-Chemical 109(2), 348-354.

30 Gibson, T.D., personal communication, Sciensive Inc., Leeds (UK)

31 Hodgins, D. (1995). The Development of an Electronic Nose for Industrial and Environmental Applications. Sensors and Actuators B-Chemical 27(1-3), 255-258.

32 Hamilton, S., Hepher, M. , Sommerville, J., (2005). Polypyrrole materials for detection and discrimination of volatile organic compounds. Sensors and Actuators B-Chemical 107(1), 424-432.

33 Freund, M.S. and Lewis, N.S., (1995). Chemically Diverse Conducting Polymer-Based Electronic Nose. Proceedings of the National Academy of Sciences of the United States of America 92(7) 2652-2656.

34 Quaranta, F., Rella, R., Siciliano, P., Capone, S., Distante, C., Epifani, M., Taurino, A. (2002). Preparation and characterization of nanostructured materials for an artificial olfactory sensing system. Sensors and Actuators B-Chemical 84(1), 55-59.

35 Siciliano, P. (2000). Preparation, characterisation and applications of thin films for gas sensors prepared by cheap chemical method. Sensors and Actuators B-Chemical 70(1-3), 153-164.

36 Wolfrum, E.J., Meglen, R.M., Peterson, D., Sluiter, J. (2006). Metal oxide sensor arrays for the detection, differentiation, and quantification of volatile organic compounds at sub-parts-per-million concentration levels. Sensors and Actuators B-Chemical 115(1), 322-329.

37 Pavlou, A., Magan, N., Jones, J.M., Brown, J., Klatser P., Turner, A.P.F., (2004). Detection of Mycobacterium tuberculosis (TB) in vitro and in situ using an electronic nose in combination with a neural network system. Biosensors & Bioelectronics 20, 538–544.

38 Pavlou, A., Magan, N., Sharp, D., Brown, J., Barr, H., Turner, A.P.F., (2000). An intelligent rapid odour recognition model in discrimination of *Helicobacter pylori* and other gastroesophageal isolates in vitro. Biosensors & Bioelectronics 15, 333–342.

39 Thaler, E.R., Hanson, C.W., (2006). Use of an electronic nose to diagnose bacterial sinusitis. American Journal of Rhinology 20(2): 170-172.

40 Voss, A., Baier, V., Reisch, R., von Roda, K., Elsner, P., Ahlers, H., Stein, G., (2005). Smelling renal dysfunction via electronic nose. Annals Biomedical Engineering 33(5), 656-660.

41 Magan, N., McNulty, C., Jones, J., Sharp, D., Brown, J., Turner, A.P.F., (2002). Use of an electronic nose system for diagnoses of urinary tract infections. Biosensors & Bioelectronics 17, 893-899.

42 Fend, R., Geddes, R., Lesellier, S., Vordermeier, H.M., Corner, L.A.L., Gormley, E., Costello, E., Hewinson, R.G., Woodman, A.C., Chambers, M.A., (2005). The use of an electronic nose to detect Mycobacterium bovis infection in badgers and cattle. Journal of Clinical Microbiology 43(4), 1745-1751.

43 Wang, P.T.Y., Xie H., Shen F, (1997). A novel method for diabetes diagnose based on electronic nose. Biosensors & Bioelectronics 12(9-10), 1032-1036.

44 Meyer, R.L., Larsen, L.H., Revsbech, N.P., (2002). Microscale biosensor for measurement of volatile fatty acids in anoxic environments. Applied and Environmental Microbiology 68(3), 1204-1210.

45 Stetter, J.R., Strathmann, S., McEntegart, C., Decastro, M., Penrose, W.R. (2000). New sensor arrays and sampling systems for a modular electronic nose. Sensors and Actuators B-Chemical 69(3), 410-419.

46 Brunink, J.A.J., Di Natale, C., Bungaro, F., Davide, F.A.M., D'Amico, A., Paolesse, R., Boschi, T., Faccio, M., Ferri, G., (1996). The application of metalloporphyrins as coating material for quartz microbalance-based chemical sensors. Analytica Chimica Acta 325(1-2), 53-64.

47 Paolesse, R., Di Natale, C., Macagnano, A., Davide, F., Boschi, T., D'Amico, A., (1998). Self-assembled monolayers of mercaptoporphyrins as sensing material for quartz crystal microbalance chemical sensors. Sensors and Actuators B-Chemical 47(1-3), 70-76.

48 Di Natale, C., Olafsdottir, G., Einarsson, S., Martinelli, E., Paolesse, R., D'Amico, A., (2001). Comparison and integration of different electronic noses for freshness evaluation of cod-fish fillets. Sensors and Actuators B-Chemical 77(1-2), 572-578.

49 Lin, C.-F., Wu, T.-Z., Hao, O.J., Lin, Y.-C., Rau, Y.-R. (2000). Biosensor for Detecting Odorous Compounds. Journal of Environmental Engeneering 126(5), 446-450.

50 Casalinuovo, I.A., Di Pierro, D., Bruno, E., Di Francesco, P., Coletta, M. (2006). Experimental use of a new surface acoustic wave sensor for the rapid identification of bacteria and yeasts. Letters in Applied Microbiology 42(1), 24-29.

51 Battiston, F.M, Ramseyer, J.-P., Lang, H.P, Baller, M.K, Gerber, C., Gimzewski, J.K, Meyer, E., Gu□ntherodt, H.-J. (2001). A chemical sensor based on a microfabricated cantilever array with simultaneous resonance-frequency and bending readout. Sensors and Actuators B-Chemical 77(1-2), 122-131.

52 Sun, A., Yang, Y., Jiang, Y., Fan, Z., Liu, Q., Zhou, Q., (2000). Electro-mass olfactory multi-sensor (EMMS). Sensors and Actuators B-Chemical 66(1-3), 88-93.

53 Smith, D. and S□pane□l, P., (1996). The novel selected-ion flow tube approach to trace gas analysis of air and breath. Rapid Communications in Mass Spectrometry 10(10), 1183-1198.

54 Smith, D. and S□pane□l, P.(2005). Selected ion flow tube mass spectrometry (SIFT-MS) for on-line trace gas analysis. Mass Spectrometry Reviews 24(5), 661-700.

55 S□pane□l, P., Hall, E.F.H., Workman, C.T., Smith, D. (2004). A directly coupled monolithic rectangular resonator forming a robust microwave plasma ion source for SIFT-MS. Plasma Sources Science & Technology 13(2), 282-284.

56 S□pane□l, P.and Smith, D., (2000). Influence of water vapour on selected ion flow tube mass spectrometric analyses of trace gases in humid air and breath. Rapid Communications in Mass Spectrometry 14(20), 1898-1906.

57 Smith, D., Diskin, A.M., Ji, Y., S□pane□l, P. (2001). Concurrent use of H_3O^+, NO^+ and O_2^+ precursor ions for the detection and quantification of diverse trace gases in the presence of air and breath by selected ion-flow tube mass spectrometry. International Journal of Mass Spectrometry 209(1), 81-97.

58 Turner, C., Spanel, P., Smith, D., (2006). A longitudinal study of methanol in the exhaled breath of 30 healthy volunteers using selected ion flow tube mass spectrometry, SIFT-MS. Physiological Measurement 27(7), 637-648.

59 Wang, T.S., Spanel, P., Smith, D. (2003). Selected ion flow tube, SIFT, studies of the reactions of H_3O^+, NO^+ and O_2^+ with eleven $C_{10}H_{16}$ monoterpenes. International Journal of Mass Spectrometry 228(1), 117-126.

60 Wang, T.S., Spanel, P., Smith, D., (2004). A selected ion flow tube study of the reactions of H_3O^+, NO^+ and O_2^+ with some phenols, phenyl alcohols and cyclic carbonyl compounds in support of SIFT-MS and PTR-MS. International Journal of Mass Spectrometry 239(2-3), 139-146.

61 Turner, C., Spanel, P., Smith, D., (2006). A longitudinal study of breath isoprene in healthy volunteers using selected ion flow tube mass spectrometry (SIFT-MS). Physiological Measurement 27(1), 13-22.

62 Karl, T., Prazeller, P., Mayr, D., Jordan, A., Rieder, J., Fall, R., Lindinger, W., (2001). Human breath isoprene and its relation to blood cholesterol levels: new measurements and modeling. Journal of Applied Physiology 91(2), 762-770.

63 Spanel, P., Davies, S., D. Smith (1999). Quantification of breath isoprene using the selected ion flow tube mass spectrometric analytical method. Rapid Communications in Mass Spectrometry 13(17) 1733-1738.

64 Wilson, P.F., Freeman, C.G., McEwan, M.J., Allardyce, R.A., Shaw, G.M. (2003). SIFT-MS measurement of VOC distribution coefficients in human blood constituents and urine. Applied, Occupational and Environmental Hygene 18(10), 759-763.

65 Carrol, W., Lenney, W., Wang, T., S□pane□l, P., Alcock, A., Smith, D., (2005). Detection of volatile compounds emitted by Pseudomonas aeruginosa using selected ion flow tube mass spectrometry. Pediatric Pulmonology 39(5), 452-456.

66 Allardyce, R.A., Langford, V.S., Hill, A.L., Murdoch, D.R. (2006). Detection of volatile metabolites produced by bacterial growth in blood culture media by selected ion flow tube mass spectrometry (SIFT-MS). Journal of Microbiological Methods 65(2), 361-365.

67 Scotter, J..M., Langford, V.S., Wilson, P.F., McEwan, M.J., Chambers, S.T., (2005). Real-time detection of common microbial volatile organic compounds from medically important fungi by Selected Ion Flow Tube-Mass Spectrometry (SIFT-MS). Journal of Microbiological Methods 63(2), 127-134.

68 Julák, J., Stránská, E., Rosová, V., Geppert, H., S□pane□l, P., Smith, D., (2006). Bronchoalveolar lavage examined by solid phase microextraction, gas chromatography-mass spectrometry and selected ion flow tube mass spectrometry. Journal of Microbiological Methods 65(1), 76-86.

69 Syhre, M., Chambers, S.T. (2008). The scent of Mycobacterium tuberculosis. Tuberculosis 88, 317-323.

70 Pauling, L., Robinson, A.B., Teranishi, R., Cary, P., (1971). Quantitative Analysis of Urine Vapor and Breath by Gas-Liquid Partition Chromatography. Proceedings of the National Academy of Sciences of the United States of America 68(10), 2374-2379.

71 Teranishi, R., Mon, T.R., Robinson, A.B., Gary, P., Pauling, L., (1972). Gas-Chromatography of Volatiles from Breath and Urine. Analytical Chemistry 44(1), 18-22.

72 Sanchez, J.M. and Sacks, R.D., (2006). Development of a multibed sorption trap, comprehensive two-dimensional gas chromatography, and time-of-flight mass spectrometry system for the analysis of volatile organic compounds in human breath. Analytical Chemistry 78(9), 3046-3054.

73 Marsili, R.T. (1999). SPME-MS-MVA as an electronic nose for the study of off-flavors in milk. Journal of Agricultural and Food Chemistry 47(2), 648-654.

74 Pillonel, L., Bossett, J.O., Tabacchi, R., (2002). Rapid preconcentration and enrichment techniques for the analysis of food volatile. A review. Lebensmittel-Wissenschaft Und-Technologie-Food Science and Technology 35(1), 1-14.

75 Ciccioli, P., Bertoni, G., Brancaleoni, E. (1976). Evaluation of Organic Pollutants in Open Air and Atmospheres in Industrial Sites Using Graphitized Carbon-Black Traps and Gas Chromatographic-Mass Spectrometric Analysis with Specific Detectors. Journal of Chromatography 126, 757-770.

76 Helmig, D., Vierling, L. (1995). Water-Adsorption Capacity of the Solid Adsorbents Tenax-Ta, Tenax-Gr, Carbotrap, Carbotrap-C, Carbosieve-Siii, and Carboxen-569 and Water Management-Techniques for the Atmospheric Sampling of Volatile Organic Trace Gases. Analytical Chemistry 67(23), 4380-4386.

77 Cope, K.A. World Scientific Publishing Inc., (2005), Breath ethane in disease: Methods for analysis based on room air correction, in Breath Analysis: For clinical Diagnosis and therapeutic monitoring, World Scientific Publishing Inc., 237-248.

78 Janovsky, U. (2005), Breath gas analysis in patients suffering from propionic acidaemia, in Breath Analysis: For clinical Diagnosis and therapeutic monitoring, World Scientific Publishing Inc., 401-408.

79 Cavalli, J.F., Fernandez, X., Lizzani-Cuvelier, L., Loiseau, A.-M., (2003). Comparison of Static Headspace, Headspace Solid Phase Microextraction, Headspace Sorptive Extraction,

and Direct Thermal Desorption Techniques on Chemical Composition of French Olive Oils. Journal of Agricultural and Food Chemistry 51 (26), 7709-7716.

80 Pfannkoch, E., Whitecavage, J., (2004). Analysis of Volatiles, in Solid Matrices: Comparison of the Sensitivities of Static Headspace GC, Solid Phase Microextraction, and Direct Thermal Extraction. LC-GC North America 22, 62-63

81 Phillips, M., How to analyse breath and make sense of the data: a personal view, in Breath Analysis: For clinical Diagnosis and therapeutic monitoring, World Scientific Publishing Inc., 293-304.

82 Phillips, M., Cataneo, R.N., Condos, R., Ring Erickson, G.A., Greenberg, J., La Bombardi, V., Munawar, M.I., Tietje, O., (2007). Volatile biomarkers of pulmonary tuberculosis in the breath. Tuberculosis 87(1), 44-52.

83 Syhre, M., Manning, L., Phuanukoonnon, S., Harino, P., Chambers, S. (2009). The scent of Mycobacterium tuberculosis – Part II breath. Tuberculosis xxx 1–4.

84 Sachse, K., Pfützner, H., Hotzel, H., Demuth, B., Heller, M., Berthold, E., (1993). Comparison of various diagnostic methods for the detection of Mycoplasma bovis. OIE Revue Scientifique et Technique 12(2), 571-580.

85 Bashiruddin, J.B., Frey, J., Königsson, M.H., Johansson, K.-E., Hotzel, H., Diller, R., de Santis, P., Botelho, A., Ayling, R.D., Nicholas, R.A.J., Thiaucourt, F., Sachse, K., (2005). Evaluation of PCR systems for the identification and differentiation of *Mycoplasma agalactiae* and *Mycoplasma bovis*: A collaborative trial. Veterinary Journal 169(2), 268-275.

86 Ewers, C., Lübke-Becker, A., Wieler, L.H., (2004). Mannheimia haemolytica und die Pathogenese der Enzootischen, Bronchopneumonie. Berl. Münch. Tierärztl. Wschr. 117, 97-115.

87 Rice, J.A., Carrasco-Medina, L., Hodgins, D.C., Shewen, P.E., (2007). Mannheimia haemolytica and bovine respiratory disease. Animal Health and Research Reviews 8(2), 117-128.

88 Linden, A., Desmecht, D., Amory, H., Daube, G., Lecomte, S., Lekeux, P., (1995). Pulmonary ventilation, mechanics, gas exchange and haemodynamics in calves following intratracheal inoculation of Pasteurella haemolytica. Zentralblatt der Veterinarmedizin 42(8), 531-544.

89 Desmecht, D., Linden, A., Amory, H., Lekeux, P., (1996a). Hemodynamic responses to Pasteurella haemolytica inoculation in calves given type 2 serotonergic antagonist. Canadian Journal of Physiology and Pharmacology 74(5), 572-579.

90 Desmecht, D., Linden A., Lekeux, P. 1996b (1996b). The relation of ventilatory failure to pulmonary, respiratory muscle and central nervous system disturbances in calves with an experimentally produced pneumonia. Journal of Comparative Pathology 115(3), 203-219.

91 Jeyaseelan, S., Sreevatsan, S., Maheswaran, S.K., (2002). Role of *Mannheimia haemolytica* leukotoxin in the pathogenesis of bovine pneumonic pasteurellosis. Animal Health and Research Reviews 3(2), 69-82.

92 Zecchinon L., Fett T., Desmecht, D., (2005). How Mannheimia haemolytica defeats host defence through a kiss of death mechanism. Veterinaty Research 36(2), 133-156.

93 TerHune, T.N., Skogerboe, T.L., Shostrom, V.K., Weigel, D.J., (2005). Comparison of pharmacokinetics of danofloxacin and enrofloxacin in calves challenged with Mannheimia haemolytica. American Journal of Veterinary Research 66(2), 342-349.

94 Corrigan, M.E., Drouillard, J.S., Spire, M.F., Mosier, D.A., Minton, J.E., Higgins, J.J., Loe, E.R., Depenbusch, B.E., Fox, J.T., (2007). Effects of melengestrol acetate on the inflammatory

response in heifers challenged with *Mannheimia haemolytica*. Journal of Animal Science 85(7), 1770-1779.

95 Lubbers, B.V., Apley, M.D., Coetzee, J.F., Mosier, D.A., Biller, D.S., Mason, D.E., Henao-Guerrero, P.N., (2007). Use of computed tomography to evaluate pathologic changes in the lungs of calves with experimentally induced respiratory tract disease. American Journal of Veterinary Research 68(11), 1259-1264.

96 Schimmel, D., Erler, W., Feist, H., (1992). Results of experimental immunization of calves with different Pasteurella antigens [Article in German]. Dtsch Tierarztl Wochenschrift 99(5), 204-206.

97 Confer, A.W., Ayalew, S., Panciera, R.J., Montelongo, M., Wray, J.H., (2006). Recombinant Mannheimia haemolytica serotype 1 outer membrane protein PlpE enhances commercial M. haemolytica vaccine-induced resistance against serotype 6 challenge. Vaccine 24(13), 2248-2255.

98 Confer, A.W., Ayalew, S., Montelongo, M., Step, D.L., Wray, J.H., Hansen, R.D., Panciera, R.J. (2009). Immunity of cattle following vaccination with a Mannheimia haemolytica chimeric PlpE-LKT (SAC89) protein. Vaccine 27 (11), 1771-1776

99 Shewen, P.E., Carrasco-Medina, L., McBey, B.A., Hodgins, D.C., (2008). Challenges in mucosal vaccination of cattle. Veterinary Immunology and Immunopathology 128 (1-3), 192-198

100 Murata, H., Shimida, N., Yoshioka, M., (2004). Current research on acute phase proteins in veterirary diagnosis: an overview. The Veterinary Journal 168, 28-40.

101 Eckershall, P.D., (2004). The time is right for acute phase protein assays. The Veterinary Journal 168, 3-5.

102 Eckershall, P.D., (2000). Recent advances and future prospects for the use of acute phase proteins as markers of disease in animals. Revue de Medicine Veterinaire 151, 577-584

103 Kaufmann, S.H.E., Schaible, Ulrich E.,et al. (2002). Schlaglicht Impfstoffentwicklung gegen Tuberkulose, in BIOspektrum. Max Planck Institute: Berlin.
Available at: http://www.biospektrum.de/artikel/929813 and http://www.biospektrum.de/blatt/

104 Kretschmer, H. *Geschichte der Tuberkulose (german)* (2000). Available at: http://www.medicalpicture.de/cont_88.tuberkulose.php
http://lepra-tuberkulose.de/tub/tinfkt_01.html.

105 Amanfu, W., *The situation of tuberculosis and tuberculosis control in animals of economic interest.* Tuberculosis (Edinb), 2006. **86**(3-4): p. 330-5.

106 Lewin, A., *Pathogenitätsmechanismen intrazellulär persistierender Bakterien*. 2005, Robert Koch Institute: Berlin. Officially published information. Available at: http://www.rki.de/DE/Content/Forsch/Projektgruppen/PG2/P22/P22__AL__IPB__D.html

107 Nicklin, J., Graeme-Cook, K. et Killington, R., *Instant Notes- Microbiology*. Second Edition ed. 2002: Bios Scientific Publishers Limited p. 130-145

108 Precsott, Harley, Klein, *Microbiology*. 6th ed. 2005: McGraw-Hill, p. 507-509

109 de la Rua-Domenech, R. (2006), *Human Mycobacterium bovis infection in the United Kingdom: Incidence, risks, control measures and review of the zoonotic aspects of bovine tuberculosis.* Tuberculosis, 86(2), p. 77-109.

110 Thoen, C., P. Lobue, and I. de Kantor, *The importance of Mycobacterium bovis as a zoonosis.* Vet Microbiol, 2006. **112**(2-4): p. 339-45.

111 Khoo, K.-H., Dell, A., Morris, H.R., Brennan, P.J., Chatterjee, D., (1995). Structural definition of acylated phosphatidylinositol mannosides from Mycobacterium tuberculosis: definition of a common anchor for lipomannan and lipoarabinomannan. Glycobiology 5(1), 117-127.

112 Hermon-Taylor, J. (2001). Protagonist. Mycobacterium avium subspecies paratuberculosis is a cause of Crohn's disease. Gut 49(6), 755-756.

113 Image available at: http://www.cyberlipid.org/

114 Röse, L., (2004). Role of Undecaprenyl Phosphokinase in mycobacteria: impact on biofilm formation, growth, properties, persistence, and virulence. Ph.D. Thesis, Humboldt University: Berlin.

115 Snow, G.A., (1970). Mycobactins: iron-chelating growth factors from mycobacteria. Bacteriology Reviews 34(2), 99-125.

116 Cousins, D.V., Florisson, N., (2005). A review of tests available for use in the diagnosis of tuberculosis in non-bovine species. Review in Science and Techniques, 24(3), 1039-1059.

117 de la Rua-Domenech, R., Goodchild, A.T., Vordermeier, H.M., Hewinson, R.G., Christiansen, K.H., Clifton-Hadley, R.S., (2006). Ante mortem diagnosis of tuberculosis in cattle: a review of the tuberculin tests, gamma-interferon assay and other ancillary diagnostic techniques. Research and Veterinary Science 81(2), 190-210.

118 Vordermeier, H.M., Chambers, M.A., Cockle, P.J., Whelan, A.O., Simmons, J., Hewinson, R.G. (2002). Correlation of ESAT-6-specific gamma interferon production with pathology in cattle following Mycobacterium bovis BCG vaccination against experimental bovine tuberculosis. Infection and Immunology 70(6), 3026-2032.

119 Dalley, D.J., Hogarth, P. J. , Hughes, S. , Hewinson R. G. , Chambers, M.A., (2004). Cloning and sequencing of badger (Meles meles) interferon-γ and its detection in badger lymphocytes. Veterinary immunology and immunopathology 101(1-2), 19-30.

120 Holland, D.D., Pierre, S.D., Claude, E., (2005). Fluorescence Polarisation assay (FP) test-Field Trial and Testing Results for Validation of the FP Test in Cattle, Bison, and Swine. Report of the committee on Brucellosis Nashville, TN, USA.

121 Torkko, P., Katila, M.L., Kontro, M., (2003). Gas-chromatographic lipid profiles in identification of currently known slowly growing environmental mycobacteria. Journal of Medical Microbiology 52(4) 315-323.

122 Alugupalli, S., Sikka, M.K., Larsson, L., White, D.C., (1998). Gas chromatography mass spectrometry methods for the analysis of mycocerosic acids present in Mycobacterium tuberculosis. Journal of Microbiological Methods 31(3), 143-150.

123 Brooks, J.B., Edman, D.C., Alley, C.C., (1980). Frequency-Pulsed Electron-Capture Gas-Liquid-Chromatography and the Tryptophan Color Test for Rapid Diagnosis of Tuberculous and Other Forms of Lymphocytic Meningitis. Journal of Clinical Microbiology 12(2), 208-215.

124 Minnikin, D.E., Minnikin, S.M., Parlett, J.H. (1984). Mycolic Acid Patterns of Some Species of Mycobacterium. Archives of Microbiology 139(2-3), 225-231.

125 Barclay, R. and Ratledge, C., (1988). Mycobactins and exochelins of Mycobacterium tuberculosis, M. bovis, M. africanum and other related species. Journal of Genetics and Microbiology 134(3), 771-776.

126 Rhoades, E., Hsu, F.-F., Torrelles, J.B., Turk, J., Chatterjee, D., Russell, D.G., (2003). Identification and macrophage-activating activity of glycolipids released from intracellular Mycobacterium bovis BCG. Molecular Microbiology 48(4), 875-888.

127 Madigan, M.T.e.M.J.M., *Brock Biology of Microorganisms*. 10th Edition ed. 2003: Pearson international Education, pp. 413-417, 761-769.

128 Armstrong, J.A. and P.D. Hart (1975). *Phagosome-lysosome interactions in cultured macrophages infected with virulent tubercle bacilli. Reversal of the usual nonfusion pattern and observations on bacterial survival.* J Exp Med, 142(1), 1-16.

129 Russell, D.G., J. Dant, and S. Sturgill-Koszycki (1996). *Mycobacterium avium- and Mycobacterium tuberculosis-containing vacuoles are dynamic, fusion-competent vesicles that are accessible to glycosphingolipids from the host cell plasmalemma.* J Immunol, **156**(12), 4764-73.

130 Harth, G. and M.A. Horwitz (1999). *An inhibitor of exported Mycobacterium tuberculosis glutamine synthetase selectively blocks the growth of pathogenic mycobacteria in axenic culture and in human monocytes: extracellular proteins as potential novel drug targets.* J Exp Med,. 189(9), 1425-36.

131 Ferrari, G. (1999). *A coat protein on phagosomes involved in the intracellular survival of mycobacteria.* Cell, 97(4), 435-47.

132 Gilleron, M., (2001). *Acylation state of the phosphatidylinositol mannosides from Mycobacterium bovis bacillus Calmette Guerin and ability to induce granuloma and recruit natural killer T cells.* J Biol Chem, 276(37), 34896-904.

133 Venisse, A., J.J. Fournie, and G. Puzo (1995). *Mannosylated lipoarabinomannan interacts with phagocytes.* Eur J Biochem, 231(2), 440-7.

134 Quirke, P. (2001).Antagonist. Mycobacterium avium subspecies paratuberculosis is a cause of Crohn's disease. Gut 49(6), 757-760.

135 Mo□bius, P., Luyven, G., Hotzel, H., Ko□hler, H., (2008). High genetic diversity among Mycobacterium avium subsp. paratuberculosis strains from German cattle herds shown by combination of IS900 restriction fragment length polymorphism analysis and mycobacterial interspersed repetitive unit-variable-number tandem-repeat typing. Journal of Clinical Microbiology 46 (3), 972-981.

136 Möbius, P., Hotzel, H., Raßbach, A., Köhler, H., (2008). Comparison of 13 single-round and nested PCR assays targeting IS900, ISMav2, f57 and locus 255 for detection of Mycobacterium avium subsp. Paratuberculosis. Veterinary Microbiology 126 (4), 324-333.

137 Koehler, H. (2009), personal communication, Friedrich Loeffler Institute, Jena, Germany

138 McGiven, J.A., Sawyer, J., Perrett, L.L., Brew, S.D., Commander, N.J., Fisher, A., McLarnon, S., Harper, K., Stack, J.A., (2008). A new homogeneous assay for high throughput serological diagnosis of brucellosis in ruminants. Journal of Immunological Methods 337, 7-15.

139 Commander, N.J., (2009) personal communication, Brucella Research Group, Statutory and Exotic Bacteria, Veterinary Laboratories Agency Weybridge, New Haw, Addlestone, Surrey, KT15 3NB, United Kingdom

140 Knobloch, H., Turner, C., Spooner, A., Chambers, M.A., (2009) Methodological variation in headspace analysis of liquid samples using electronic nose. , Sensors and Actuators B-Chemical 139, 353-360.

141 Schimmel, D. (1987). Results of experimental infection of calves with Pasteurella multocida and Pasteurella haemolytica | [Ergebnisse experimenteller Infektionen von Ka□lbern mit Pasteurella multocida und Pasteurella haemolytica.]. Archiv für Experimentelle Veterinärmedizin 41, 463-472.

142 Schroedl, W., Fuerll, B., Reinhold, P., Krueger, M., Schuett, C., (2001) A novel acute phase marker in cattle: lipopolysaccharide binding protein (LBP). Journal of Endotoxical Research 7(1), 49-52.

143 Schroedl, W., Jaekel, L., Krueger, M., (2003). C-reactive protein and antibacterial activity in blood plasma of colostrum-fed calves and the effect of lactulose. Journal of Dairy Science 86, 3313-3320.

144 Dean, G.S., Rhodes, S.G., Coad, M., Whelan, A.O., Cockle, P.J., Clifford, D.J., Hewinson, R.G., Vordermeier, H.M., (2005). Minimum infective dose of Mycobacterium bovis in cattle. Infection and Immunity 73(10), 6467-6471.

145 Vordermeier, H.M., Huygen, K., Singh, M., Hewinson, R.G., Xing, Z. (2006). Immune responses induced in cattle by vaccination with a recombinant adenovirus expressing Mycobacterial antigen 85A and Mycobacterium bovis BCG. Infection and Immunity 74(2), 1416-1418.

146 Whelan, A.O., Wright, D.C., Chambers, M.A., Singh, M., Hewinson, R.G., Vordermeier, H.M., (2008). Evidence for enhanced central memory priming by live Mycobacterium bovis BCG vaccine in comparison with killed BCG formulations. Vaccine 26(2), 166-173.

147 Vordermeier, H.M. Rhodes, S.G., Dean, G., Goonetilleke, N., Huygen, K., Hill, A.V.S., Hewinson, R.G., Gilbert, S.C. (2004). Cellular immune responses induced in cattle by heterologous prime-boost vaccination using recombinant viruses and bacille Calmette-Guerin. Immunology 112(3), 461-470.

148 Rhodes, S.G. Gavier-Widen, D., Buddle, B.M., Whelan, A.O., Singh, M., Hewinson, R.G., Vordermeier, H.M. l. (2000). Antigen specificity in experimental bovine tuberculosis. Infection and Immunity 68(5), 2573-2578.

149 Riollet, C. Mutuel, D., Duonor-Cérutti, M., Rainard, P., (2006). Determination and characterization of bovine interleukin-17 cDNA. Journal of Interferon and Cytokine Research 26(3), 141-149.

150 Thacker, T.C. Palmer, M.V., Waters, W.R., (2007). Associations between cytokine gene expression and pathology in Mycobacterium bovis infected cattle. Veterinary Immunology and Immunopathology 119(3-4), 204-213.

151 Waters, W.R. Palmer, M.V., Nonnecke, B.J., Thacker, T.C., Scherer, C.F.C., Estes, D.M., Jacobs Jr., W.R., Glatman-Freedman, A., Larsen, M.H., (2007). Failure of a Mycobacterium tuberculosis DeltaRD1 DeltapanCD double deletion mutant in a neonatal calf aerosol M. bovis challenge model: comparisons to responses elicited by M. bovis bacille Calmette Guerin. Vaccine 25(45), 7832-7840.

152 Ampuero, S., Bogdanov, S., Bosset, J.O., (2004). Classification of unifloral honeys with an MS-based electronic nose using different sampling modes: SHS, SPME and INDEX. European Food Research and Technolology 218, 198–207.

153 Misselbrook, T.H.H, Hobbs, J.P., Persaud, K.C., (1997). Use of an electronic nose to measure odour concentration following application of cattle slurry to grassland. Journal of Agricultural Engineering and Research 66, 213–220.

154 Lozano, J., Santos, J.P., Gutierrez, J., Horrillo, M.C., (2007). Comparative study of sampling systems combined with gas sensors for wine discrimination. Sensors and Actuators B: Chem. 126, 616–623.

155 Magan, N., Pavlou, A.K., Chrysanthakisa, I., (2001). Milk-sense: a volatile sensing system recognises spoilage bacteria and yeasts in milk. Sensors and Actuators B: Chem. 72, 28–34.

156 Facitelli M., Benassi, A., Di Francesco, F., Domenici, C., Marano, L., Pioggia, G., (2002). Fluid dynamic for simulation of a measurement chamber for electronic noses, Sensors and Actuators B: Chem. 85, 166–174.

157 Di Francesco, F., Facitelli, M., Marano, L., Pioggia, G., (2005). A radially symmetric measurement chamber for electronic noses. Sensors and Actuators B: Chem. 105, 295–303.

158 Wilson, A.D., Lester, D.G., Oberle, C.S., (2004). Development of conductive polymer analysis for the rapid detection and identification of phytopathogenic microbes. Techniques 94, 419–431.

159 Nake, A., Dubreuil, B., Raynaud, C., Talou, T., (2005). Outdoor in situ monitoring of volatile emissions from treatment plants with two portable technologies of electronic Noses. Sensors and Actuators B: Chem. 106, 36–39.

160 Kashwan, K.R., Bhuyan, M., (2005). Robust electronic-nose system with temperature and humidity drift compensation for tea and spice flavour discrimination. IEEE- Asian Conference on Sensors and International Conference on New Techniques and Biomedical Research

161 Chimenti, M., De Rossi, D., Di Francesco, F., Domenici, C., Pieri, G., Pioggia, G., Salvetti, O., (2003). A neural approach for improving the measurement capability of an electronic nose. Measasurent Science and Technology 14, 815–821.

162 Bourgeois, W. and Stuetz, R.M., (2002). Use of a chemical sensor array for detecting pollutants in domestic wastewater. Water Research 36, 4505-4512.

163 Kukla, A.L., Shirshov, Y.M., Piletsky, S.A., (1996). Ammonia sensors based on sensitive polyaniline films. Sensors and Actuators B: Chem. 37, 135–140.

164 Partridge, A.C., Harris, Y.P., Andrews, M.K., (1996). High sensitivity conducting polymer sensors. Analyst 121, 1349–1353.

165 Amann, R.P., (1983). Endocrine changes associated with onset of spermatogenesis in Holstein bulls. Journal of dairy science 66 (12), 2606-2622.

166 Schillo, K.K., Hansen, P.J., Kamwanja, L.A., (1983). Influence of season on sexual development in heifers: Age at puberty as related to growth and serum concentrations of gonadotropins, prolactin, thyroxine and progesterone. Biology of Reproduction 28 (2), 329-341.

167 Devkota, B., Koseki, T., Matsui, M., Sasaki, M., Kaneko, E., Miyamoto, A., Amaya Montoya, C., Miyake, Y.-I., (2008). Relationships among age, body weight, scrotal circumference, semen quality and peripheral testosterone and estradiol concentrations in pubertal and postpubertal Holstein bulls. Journal of Veterinary Medical Science 70(1), 119-121

168 Chelikani, P.K., Ambrose, D.J., Keisler, D.H., Kennelly, J.J., (2009). Effects of dietary energy and protein density on plasma concentrations of leptin and metabolic hormones in dairy heifers. Journal of dairy Science 92(4), 1430-1441.

169 Armstrong, D.G., Gong, J.G., Webb, R., (2003). Interactions between nutrition and ovarian activity in cattle: physiological, cellular and molecular mechanisms. Reproduction (Cambridge, England) Supplement 61, 403-414.

170 Delaquis, A.M., Block, E., (1995). The effects of changing ration ingredients on acid-base status, renal function, and macromineral metabolism. Journal of dairy Science 78(9), 2024-2039.

171 Gustafsson, A.H., Palmquist, D.L. (1993). Diurnal variation of rumen ammonia, serum urea, and milk urea in dairy cows at high and low yields. Journal of dairy Science 76(2), 475-484.

172 Eicher, R., Liesegang, A., Bouchard, E., Tremblay, A., (1999). Effect of cow-specific factors and feeding frequency of concentrate on diurnal variations of blood metabolites in dairy cows. American Journal of Veterinary Research 60(2), 1493-1499.

173 Knobloch, H., Becher, G., Decker, M., Reinhold, P., (2008). Evaluation of H_2O_2 and pH in exhaled breath condensate samples: Methodical and physiological aspects. Biomarkers 13(3), 319-341.

174 Aland, A., Lidfors, L., Ekesbo, I., (2002). Diurnal distribution of dairy cow defecation and urination Applied Animal Behaviour Science 78(1), 43-54.

175 Gombe, S., Hall, W.C., McEntee, K., (1973). Regulation of blood levels of LH in bulls: Influence of age, breed, sexual stimulation and temporal fluctuations. Journal of Reproduction and Fertility 35(3), 493-503.

176 Romon, M., Fur, C.L., Lebel, P., Edmé, J.-L., Fruchart, J.-C., Dallongeville, J., (1997), Circadian variation of postprandial lipemia. American Journal of Clinical Nutrition 65(4), 934-940.

177 Coleman, R.A., Herrmann, T.S., (1999). Nutritional regulation of leptin in humans. Diabetologia 42(6), 639-646.

178 Turner, C., Parekh, B., Walton, C., Španěl, P., Smith, D., Evans, M., (2008). An exploratory comparative study of volatile compounds in exhaled breath and emitted by skin using selected ion flow tube mass spectrometry. Rapid Communications in Mass Spectrometry 22(4), 526-532.

179 Klotz, J.L., Heitmann, R.N., (2006). Effects of weaning and ionophore supplementation on selected blood metabolites and growth in dairy calves, Journal of dairy Science 89(9), 3587-3598.

180 James, T., Meyer, D., Esparza, E., Depeters, E.J., Perez-Monti, H., (1999). Nutrition, feeding, and calves: Effects of dietary nitrogen manipulation on ammonia volatilization from manure from Holstein heifers. Journal of dairy Science, 82(11), 2430-2439

181 Smits, M.C.J, Valk, H., Elzing, A., Keen, A., (1995). Effect of protein nutrition on ammonia emission from a cubicle house for dairy cattle. Livestock Production Science 44(2), 147-156.

182 Groff, E.B., Wu, Z., (2005). Milk production and nitrogen excretion of dairy cows fed different amounts of protein and varying proportions of alfalfa and corn silage. Journal of dairy Science 88(10), 3619-3632.

183 Thomas, J.W., Tinnimit, P., (1976). Amounts and sources of protein for dairy calves. Journal of dairy Science 59(11), 1967-1984.

184 Hotzel, H., Demuth, B., Sachse, K., Pflitsch, A., Pfuïzner, H., (1993). Detection of Mycoplasma bovis using in vitro deoxyribonucleic acid amplification. OIE Revue Scientifique et Technique 12 (2), pp. 581-591

185 Douart, A., (2002). Bacterial agents implicated in infectious bronchopneumonias of cattle. Point Veterinaire 33(231), 26-30.

186 Caswell, J.L., Archambault, M., (2007). Mycoplasma bovis pneumonia in cattle. Animal health research reviews / Conference of Research Workers in Animal Diseases 8(2), 61-186.

187 Filioussis, G., Christodoulopoulos, G., Thatcher, A., Petridou, V., Bourtzi-Chatzopoulou, E., (1997). Isolation of Mycoplasma bovis from bovine clinical mastitis cases in Northern Greece. Veterinary Journal (London, England) 173 (1), 215-218.

188 Gagea, M.I., Bateman, K.G., Shanahan, R.A., Van Dreumel, T., McEwen, B.J., Carman, S., Archambault, M., Caswell, J.L., (2006). Naturally occurring Mycoplasma bovis-associated pneumonia and polyarthritis in feedlot beef calves. Journal of Veterinary Diagnostic Investigation 18(1), 29-40.

189 Wilson, D.J., Skirpstunas, R.T., Trujillo, J.D., Cavender, K.B., Bagley, C.V., Harding, R.L., (2007). Unusual history and initial clinical signs of Mycoplasma bovis mastitis and arthritis in first-lactation cows in a closed commercial dairy herd. Journal of the American Veterinary Medical Association 230(10), 1519-1523.

190 Radaelli, E., Luini, M., Domeneghini, C., Loria, G.R., Recordati, C., Radaelli, P., Scanziani, E., (2009). Expression of Class II Major Histocompatibility Complex Molecules in Chronic Pulmonary Mycoplasma bovis Infection in Cattle. Journal of Comparative Pathology 140 (2-3), 198-202.

191 Radaelli, E., Luini, M., Loria, G.R., Nicholas, R.A.J., Scanziani, E., (2008). Bacteriological, serological, pathological and immunohistochemical studies of Mycoplasma bovis respiratory infection in veal calves and adult cattle at slaughter. Research in Veterinary Science 85(2), 282-290.

192 Elsasser, T.H., Blum, J.W., Kahl, S., (2005). Characterization of calves exhibiting a novel inheritable TNF-alpha hyperresponsiveness to endotoxin: associations with increased pathophysiological complications. Journal of Applied Physiology 98(6), 2045-2055.

193 Baumann, H., Gauldie, J., (1994). The acute phase response. Immunolgy Today 5, 74-80.

194 Bannerman, D.D., Paape, M.J., Hare W.R., Sohn, E.J., (2003). Increased levels of LPS-binding protein in bovine blood and milk following bacterial lipopolysaccharide challenge. Journal of dairy Science 86, 3128–3137.

195 Sachse, K., Grossmann, E., Berndt, A., Schütt, Ch., Henning, K., Theegarten, D., Anhenn, O., Reinhold, P., (2004). Respiratory chlamydial infection based on experimental aerosol challenge of pigs with Chlamydia suis. Comparative Immunology, Microbiology and Infectious Diseases 27, 7-23.

196 Angen, O., Thomsen, J., Larsen, L.E., Larsen, J., Kokotovic, B., Heegaard, P.M., Enemark, J.M., (2009). Microbiological investigations on trans-tracheally aspirated bronchoalveolar fluid and acute phase protein response. Veterinary Microbiology, Jan 4. [Epub ahead of print]

197 Kodogiannis, V. and Wadge, E., (2005) The use of gas-sensor arrays to diagnose urinary tract infections. International Journal of Neural Systems 15, 363-376.

198 Cheryk, L.A., Hooper-McGrevy, K.E., Gentry, P.A., (1998). Alterations in bovine platelet function and acute phase proteins induced by Pasteurella haemolytica A1. Canadian Journal of Veterinary Research 62(1), 1-8.

199 Gerber, M., Keshava, N., Robles, A.C., Rearden, P., Trevejo, J. Analysis of biomarker features from a differential mobility spectrometer for the detection of tuberculosis. 2007 IEEE/NIH

Life Science Systems and Applications Workshop 2008, LISA, Article number 4400894, 100-103.

200 Cunha, M.G., Hoenigman, S., Kanchagar, C., Rearden, P., Sassetti, C.S., Trevejo, J.M., Keshava, N. Joint analysis of differential mobility spectrometer and mass spectrometer features for tuberculosis biomarkers. Proceedings of the 30th Annual International Conference of the IEEE Engineering in Medicine and Biology Society, EMBS'08 - "Personalized Healthcare through Technology", Article number 4649164, 359-362.

201 Nol, P..Lyashchenko, K.P., Greenwald, R., Esfandiari, J., Waters, W.R., Palmer, M.V., Nonnecke, B.J., Keefe, T.J., Thacker, T.C., Rhyan, J.C., Aldwell, F.E., Salman, M.D., (2009). Humoral immune responses of white-tailed deer (Odocoileus virginianus) to Mycobacterium bovis BCG vaccination and experimental challenge with M. bovis. Clinical and Vaccine Immunology 16(3), 323-329.

202 Waters, W.R., Palmer, M.V., Thacker, T.C., Bannantine, J.P., Vordermeier, H.M., Hewinson, R.G., Greenwald, R., Esfandiari, J., McNair, J., Pollock, J.M., Andersen, P., Lyashchenko, K.P., (2006). Early antibody responses to experimental Mycobacterium bovis infection of cattle. Clinical and Vaccine Immunology 13(6), 648-654

203 Whelan, C., Shuralev, E., O'Keeffe, G., Hyland, P., Hang, F.K., Snoddy, P., O'Brien, A., Connolly, M., Quinn, P., Groll, M., Watterson, T., Call, S., Kenny, K., Duignan, A., Hamilton, M.J., Buddle, B.M., Johnston, J.A., Davis, W.C., Olwill, S.A., Clarke, J., (2008). Multiplex immunoassay for serological diagnosis of Mycobacterium bovis infection in cattle. Clinical and Vaccine Immunology 15(12), 1834-1838

204 Seth, M., Lamont, E.A., Janagama, H.K., Widdel, A., Vulchanova, L., Stabel, J.R., Waters, W.R., Palmer, M.V., Sreevatsan, S., (2009), Biomarker discovery in subclinical mycobacterial infections of cattle. Public Library of Science ONE 4 (5) Article number e5478

205 Fend, R., Bessant, C., Williams, A.J., Woodman, A.C., (2004). Monitoring haemodialysis using electronic nose and chemometrics. Biosensors and Bioelectronics 19(12), 1581-1590.

206 Gopinath, K. and Singh, S., (2009). Urine as an adjunct specimen for the diagnosis of active pulmonary tuberculosis. International Journal of Infectious Diseases 13(3), 374-379

207 Torrea, G., Van de Perre, P., Quedraogo, M., Zougba, A., Sawadogo, A., Dingtoumda, B., Diallo, B., Defer, M.C., Sombié, I., Zanetti, S., Sechi, L.A. (2005). PCR-based detection of the Mycobacterium tuberculosis complex in urine of HIV-infected and uninfected pulmonary and extrapulmonary tuberculosis patients in Burkina Faso. Journal of Medical Microbiology 54, 39-44.

208 Aathithan, S., Plant, J.C., Chaudry, A.N., French1, G.L., (2001). Diagnosis of Bacteriuria by Detection of Volatile Organic Compounds in Urine Using an Automated Headspace Analyzer with Multiple Conducting Polymer Sensors. Journal of Clinical Microbiology 39, 2590-2593.

209 Woodroffe, R., Donnelly, C., Johnston, W., Bourne, F., Cheeseman, C., (2005). Spatial association of Mycobacterium bovis infection in cattle and badgers Meles meles. Journal of Applied Ecology 42, 852–862.

210 Thaler, E.R., Hanson, C.W., (2005). Medical applications of electronic nose technology. Expert Review of Medical Devices. 2(5), 559-566.

211 Di Natale, C., Macagnano, A., Martinelli, E., Paolesse, R., Proietti, E., D'Amico, A., (2001). The evaluation of quality of post-harvest oranges and apples by means of an electronic nose. Sensors and Actuators, B: Chem 78(1-3), 26-31.

212 Michel, A.L, and Simões, M., (2009). Comparative field evaluation of two rapid immunochromatographic tests for the diagnosis of bovine tuberculosis in African buffaloes (Syncerus caffer). Veterinary Immunology and Immunopathology 127(1-2), 186-189.

213 Lyashchenko, K.P., Greenwald, R., Esfandiari, J., Chambers, M.A., Vicente, J., Gortazar, C., Santos, N., Correia-Neves, M., Buddle, B.M., Jackson, R., O'Brien, D.J., Schmitt, S., Palmer, M.V., Delahay, R.J., Waters, W.R., (2008). Animal-side serologic assay for rapid detection of Mycobacterium bovis infection in multiple species of free-ranging wildlife. Veterinary Microbiology 132(3-4), 283-292.

Appendices

Uni and multivariate Data analysis

MATLAB 2006 including PLS toolbox version 3.5

The following sections explain the modular built Matlab script used in this project.
In this particular case, it “re-analyses” the urine data from clinically healthy individuals (see section 2.2.2) but was modified and applied for almost all studies which are described. The reader is guided through the script step by step in section A.
Green letters are comments to allow a better understanding while boxes on the right indicate when a plot is generated or relevant information can be obtained from the Matlab workspace. The relevant plots are shown in section B.

Section A

```
%Script by Henri Knobloch, June 2008, modified Feb 2009
%many thanks to Andrew Spooner for assistance
%HELP see index "anovan"

%0. Clearing workspace and importing data
%----------------------------------------
tic;
clear all
close all
clc

%Import data set one. Give path of the new *.txt file
newData = importdata('urine_expclin healthy.txt');


%1. Defining matrices
%--------------------
    %1.1 Defining column headings and data matrix
        paraheader = newData.textdata(1,1:7);
        dataheader = newData.textdata(1,8:end);

    %1.2 Defining non-normalised, autoscaled and mean-centred matrix
      %for Principle Component Analyis (PCA)
        matrixNON = newData.data(1:474,8:20);
        matrixAUTO = auto(newData.data(1:474,8:20));
        matrixMNCN = mncn(newData.data(1:474,8:20));

    %1.3 Defining impact factors
        para.repl = newData.data(1:end,1);
        para.body_temp = newData.data(1:end,2);
        para.age = newData.data(1:end,3);
        para.smpl_day = newData.data(1:end,4);
        para.smpl_time = newData.data(1:end,5);
        para.anal_day = newData.data(1:end,6);
        para.anal_time = newData.data(1:end,7);


%2. Starting ANOVA+ MEAN, MEDIAN and STD DEVIATION calculation
%-------------------------------------------------------------
%COMMENT: variable names = paraheaders

%2.0 Creating a loop starting with column 8= Divergence sensor 1
finishing

%at column 20= Divergence sensor 13: calculating Skewness and
%Kurtosis to check for normal distribution. Gives histograms and a
%table containing both parameters for all sensors.
        i = 8;
        for i = 8:20
            data.divi = newData.data(1:end,i);
            ploti = data.divi;
        if i == 8
            plot = ploti;
        else
            plot = horzcat (plot, ploti);
        end
            l = i-7;
            sk = skewness(plot);
```

Can be copied from Matlab workspace

1_example histogram

```
        ku = kurtosis(plot);
            figure();
            hist(ploti);
            title(['Distribution for sensor ', num2str(l)]);
            ylabel('Frequency');
            xlabel('Distribution');

%2.1 ANOVA + Box- and Whisker Plots
%2.1 Performing ANOVA
%uses the mANOVA function to calculate the variance for each
%parameter given in brackets.

        [p, table,stats,terms] = anovan(data.divi,{para.repl
        para.body_temp, para.age para.smpl_day para.smpl_time
        para.anal_day para.anal_time}, 'model', 'linear',
        'varname', paraheader);
```

2_example mANOVA (sensor 5)

```
  %2.1.1 Summarising all p/F values for the significance and
  extent of
    %the influence ofa parameter and generating a big new for
  each sensor
    %1 to 13
         if i == 8
            sump = (p);
          else
            sump = horzcat(sump, p);
          end
          clear p
```

Can be copied from Matlab workspace

```
    %2.1.2 Summarising all tables and generating a big new table
  + erasing
    %tables 1 to 13
         if i == 8
            sumtable = (table);
          else
            sumtable = vertcat(sumtable, table);
          end
          clear table
          clear stats
          clear terms

    %2.1.3 Generating Box and Whisker- Plots for sensor responses
    1-13
    %in dependence to parameters e.g. {para.age}/ 'young',
    'adult'
            k = i-7;
                scrsz = get(0,'ScreenSize');
                figure('Position',[1 scrsz(4)/2 scrsz(3)/2
              scrsz(4)/2])
                %COMMENT: [left, bottom, width, height]
            h = BOXPLOT(data.divi, {para.age }, 'notch','on');
                title(['Responses of sensor: ', num2str(k)]);
                %Repositioning x-axis
                   temp1 = get(gca,'Position');
                   temp1(2) = temp1(2)+ 0.03;
                   set(gca,'Position',temp1)
                %Labelling x-/y-axis
```

3_example Boxplot (sensor 5)

```
                    ylabel('Divergence in %');
                    legend('1= young','2= adult');

                clear temp1
                clear scrsz
                clear h

%2.2 Calculating MEANs, MEDIANs and STD. DEVIATIONS for sensors
  Returning its tables
    % 2.2.1 Calculating the column mean and returns the coloumns
    %mean for each group for each sensor

                m1 = mean(data.divi(1:195,1));
                m2 = mean(data.divi(196:474,1));
            m = vertcat(m1, m2);
            if i == 8
                mtable = (m);
            else
                mtable = horzcat(mtable, m);
            end
                clear m1
                clear m2
                clear m

    %2.2.2 Calculating the MEDIAN and returns the coloumns mean
    % for each group for each sensor
                n1 = median(data.divi(1:195,1));
                n2 = median(data.divi(196:474,1));
            n = vertcat(n1, n2);
            if i == 8
                ntable = (n);
            else
                ntable = horzcat(ntable, n);
            end
                clear n1
                clear n2
                clear n

    %2.2.3 Calculating the column STD. DEVIATION and returns the
        Coloumns mean for each group for each sensor
                o1 = std(data.divi(1:195,1));
                o2 = std(data.divi(196:474,1));
            o = vertcat(o1, o2);
            if i == 8
                otable = (o);
            else
                otable = horzcat(otable, o);
            end
                clear o1
                clear o2
                clear o

   %end of all calculation
    end
```

Can be copied from Matlab workspace

Can be copied from Matlab workspace

Can be copied from Matlab workspace

```
      %2.2.4 Summarising all MEANs, MEDIANs and STD. DEVIATIONs
         % a) Barchart including MEAN and MEDIAN for all sensors
         % b) MEAN including errorbars (STD. DEVIATIONS)
                    figure();
                a = errorbar(mtable',otable');
                    %Labelling + formatting
                    title('MEAN and STANDARD DEVIATION for ST214
                        sensors');
                    xlabel('ST214 sensors');
                    ylabel('Divergence in %');
         %legend('','');  (allows further figure description)
                    axis([1 13 -80 0])
                    set(gca,'YDir','reverse')

                %MEAN compared to MEDIAN
                    temp2 = horzcat(mtable, ntable);
                    figure();
                b = bar(temp2);

                       %determines the colour of the bars for mtable
                       and n table based on RGB
                    colormap([0 0 1; 1 0 0])

                    set(gca,'YDir','reverse')
                    %Labelling+ formatting
                    title('MEAN and MEDIAN for ST214 Sensors');
                    xlabel('mean(blue)/median(red) for "age", 1=
                              young, 2=
                              adult');
                    ylabel('Divergence in %');
               %legend('','');  (allows further figure description)
                        set(gca,'ZDir','reverse');
                        %Repositioning x-axis
                        temp1 = get(gca,'Position');
                        temp1(1) = temp1(1)- 0.05;
                        set(gca,'Position',temp1)

                    clear temp1
                    clear temp2
                    clear a
                    clear b

      %2.3 Creating heatmaps as an alternative way of displaying data
          %displays all group status versus all sensors and gives
colour
          %patterns for ...

           %2.3.1 RAW data MEANS per group

                  figure();
                      imagesc (mtable);
           %colormap (gray); if uncomment figure turns into b/w

                      title('raw MEAN of all groups over sensors')
                      xlabel('ST214 sensors');
                      set(gca,'YTick',[1 2]);
                      set(gca, 'YTickLabel','Young cattle | Adult
                          cattle|');
                      colorbar;
```

4_example MEAN and STD overview

5_example MEAN and MEDIAN barchart

6_example raw MEAN

```
%2.3.2 RAW data MEDIANS per group

        figure();
            imagesc (ntable);
          %colormap (gray); if uncomment figure turns into b/w

            title('raw MEDIAN of all groups over sensors')
            xlabel('ST214 sensors');
            set(gca,'YTick',[1 2]);
            set(gca, 'YTickLabel','Young cattle|Adult
                cattle|');
            colorbar;

    %2.3.3 MEAN-centered MEANS per group
        figure();
            tempmtable= mncn(mtable);
            imagesc (tempmtable);
          %colormap (gray); if uncomment figure turns into b/w

            title('mncn MEAN of all groups over sensors')
            xlabel('ST214 sensors');
            %ylabel('groups');
            set(gca,'YTick',[1 2]);
            set(gca, 'YTickLabel','Young cattle|Adult
                cattle|');
            colorbar;

    %2.3.4 MEAN-centered MEDIANS per group

         figure();
            tempntable= mncn(ntable);
            imagesc (tempntable);
          %colormap (gray); if uncomment figure turns into b/w

            title('mncn MEDIAN of all groups over sensors')
            xlabel('ST214 sensors');
            %ylabel('groups');
            set(gca,'YTick',[1 2]);
            set(gca, 'YTickLabel','Young cattle|Adult
                cattle|');
            colorbar;

        clear tempmtable
        clear tempntable

%2.4 Performing Principle component analysis
    %2.4.1 Returns 4 windows (for 5 components) for diplaying
    %LOADINGS and SCORES as PCA results and a Plot control
     panel
        options.plots = 'final';
        options.display = 'off';
        model = pca(matrixNON,5,options);
        pred = pca(matrixNON,5,options);

        options.plots = 'final';
        options.display = 'off';
        model = pca(matrixAUTO,5,options);
        pred = pca(matrixAUTO,5,options);

        options.plots = 'final';
        options.display = 'off';
```

7_example raw MEDIAN

8_example mean-centred MEAN

9_example mean- centred MEDIAN

10A/B_example 2D/3D PCA plots

```
            model = pca(matrixMNCN,5,options);
            pred = pca(matrixMNCN,5,options);

            clear pred
            clear options

        %2.4.1 Returns for non-normalised, autoscaled and mean-
               centred
        %data a 'Principle Component Visualization Tool' as an
        %alternative to 2.4.1

            Label = newData.data(1:474,3);
            mapcaplot(matrixNON, Label);
            mapcaplot(matrixAUTO, Label);
            mapcaplot(matrixMNCN, Label);

  %2.5 Deleting remaining temporary variables
clear newData
clear data
```

11A/B/C_example
Visualisation tool
MEDIAN

Section B

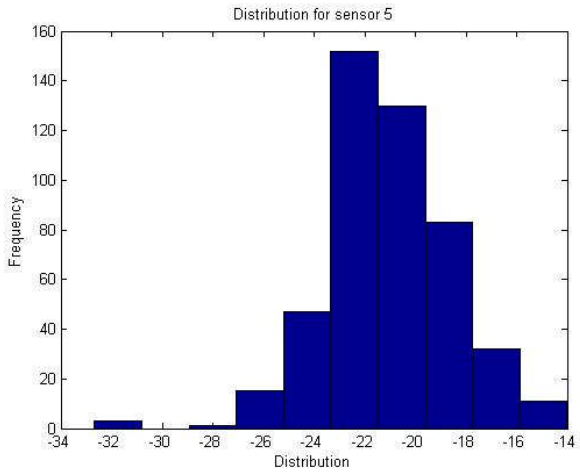

Figure 50: Histogram showing the distribution of data and indication whether data is normally distributed or not.

Analysis of Variance

Source	Sum Sq.	d.f.	Mean Sq.	F	Prob>F
repl	6.56	2	3.279	1.47	0.2315
body_temp	163.99	16	10.25	4.59	0
age	34.72	1	34.722	15.55	0.0001
smpl_day	72.01	5	14.402	6.45	0
smpl_time	54.29	3	18.097	8.1	0
anal_day	837.27	6	139.544	62.48	0
anal_time	668.03	29	23.036	10.31	0
Error	918	411	2.234		
Total	3051.94	473			

Constrained (Type III) sums of squares.

Figure 51: Gives a mANOVA table of factors which may influence the divergences for each sensor. "Probability>F" (least significant difference) is 95% or ≤0.05 is showing the probability that response of a sensors is significantly changed due to one factor. The F-value indicates the impact.

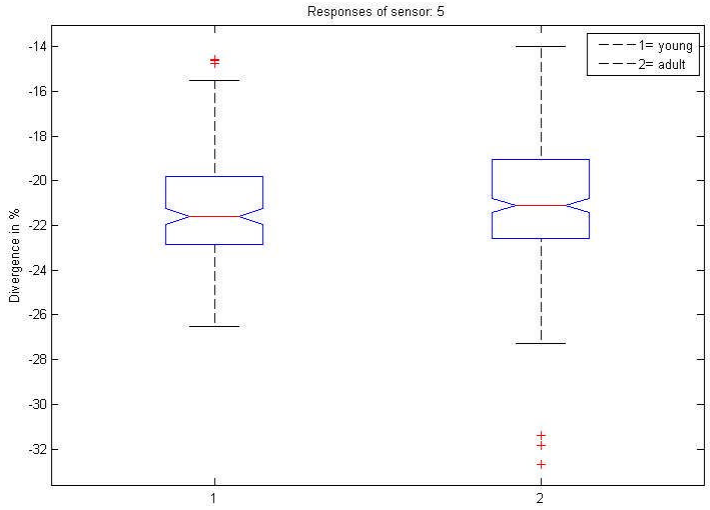

Figure 52: Notched Box and Whisker plot. Gives for each sensor a 25% to 75 percentile interquartile ranged box with a median (red line). Red crosses are outliers and are further than 1.5 lengths of the boxes away from the mean.

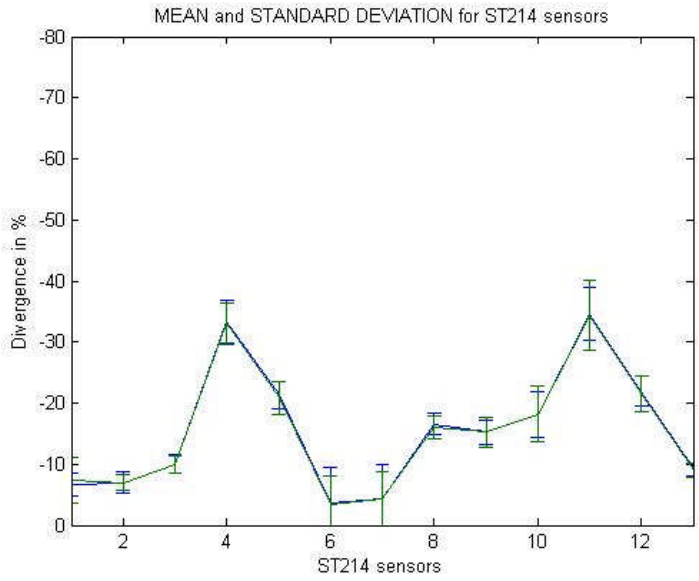

Figure 53: Gives one chart which displays the means and standard deviations for all sensors. This figure gives information about divergences for each sensor and its variability over all analyses.

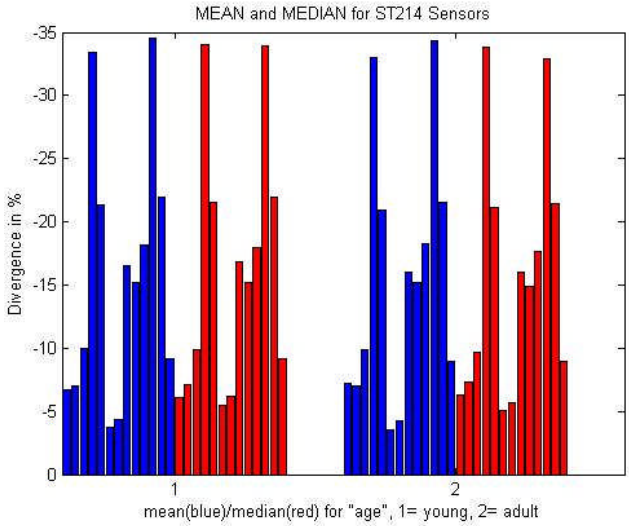

Figure 54: Gives one chart showing the means and medians for all sensors. With this comparison of divergences for each sensor, obvious non-normal distributed data for each sensor may be found.

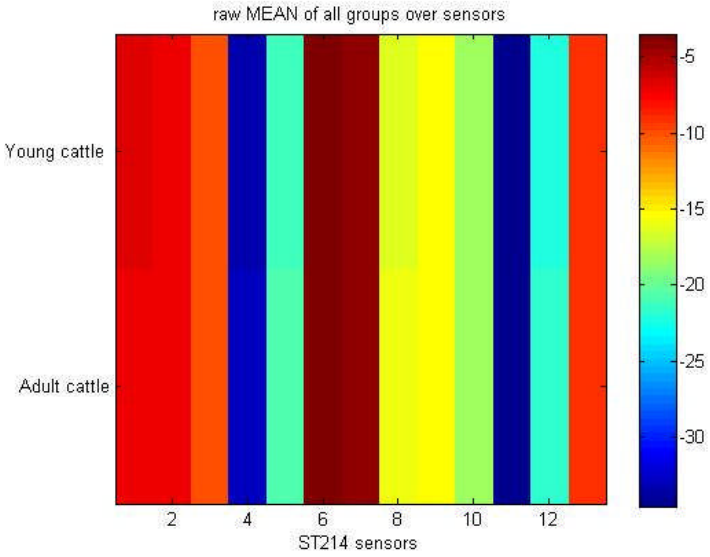

Figure 55: Illustrates the means of raw data over all sensors and for specified groups. It shows the range of divergences on a scale.

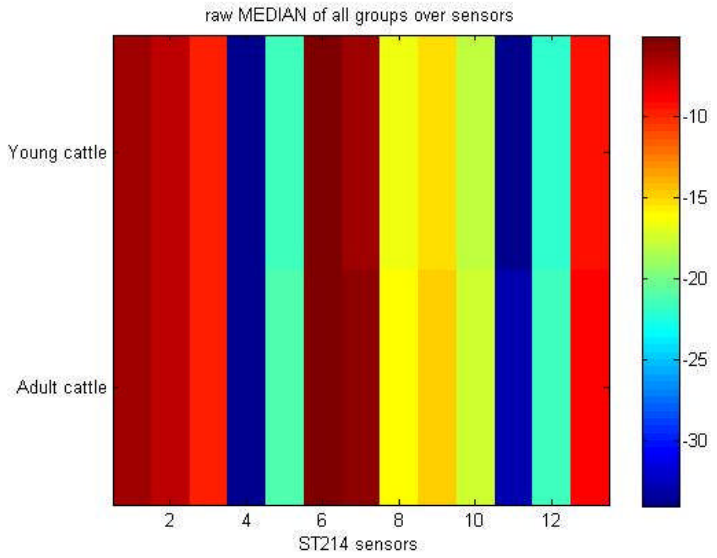

Figure 56: Illustrates the medians of raw data over all sensors and for specified groups. It shows the range of divergences on a scale.

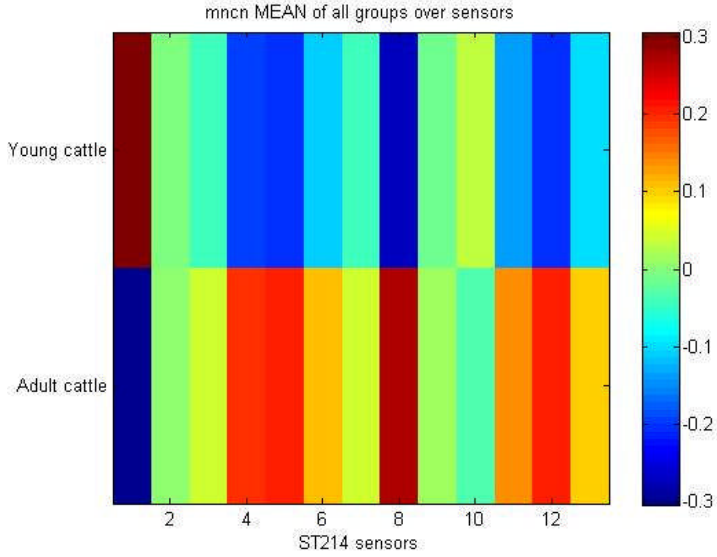

Figure 57: Illustrates the mean-centred means of data over all sensors and for specified groups. It shows the range of divergences on a scale. Data was mean-centred for each sensor to see differences to reduce magnitudes between different ranges in sensor responses ant to show the differences between groups.

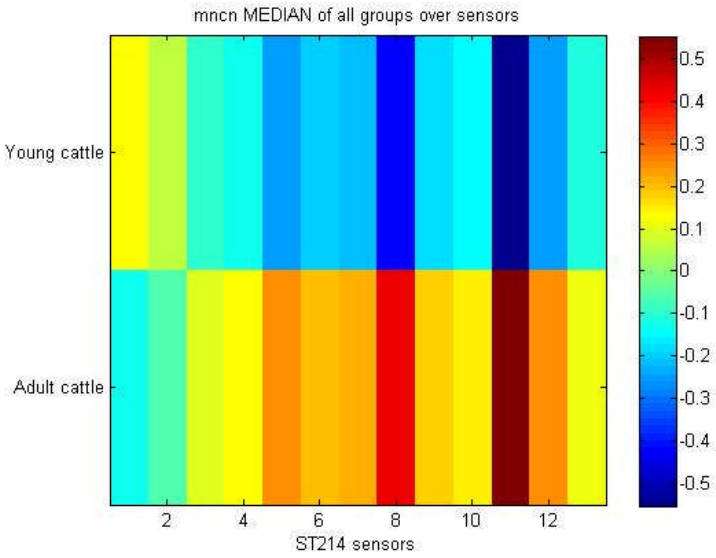

Figure 58: Illustrates the mean-centred medians of data over all sensors and for specified groups. It shows the range of divergences on a scale. Data was mean-centred for each sensor to see differences to reduce magnitudes between different ranges in sensor responses ant to show the differences between groups.

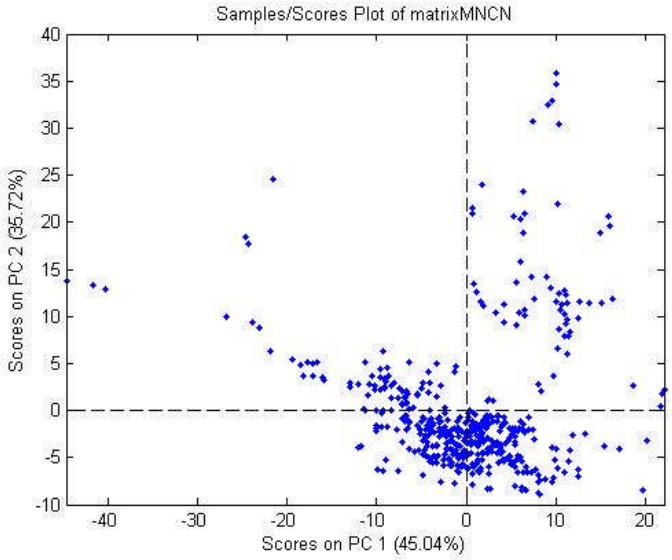

Figure 59A: Illustrates principle component 1 against 2 (2D, others possible) and illustrates variation due to both PCs as a scatter plot. Loadings can be obtained as well (not shown).

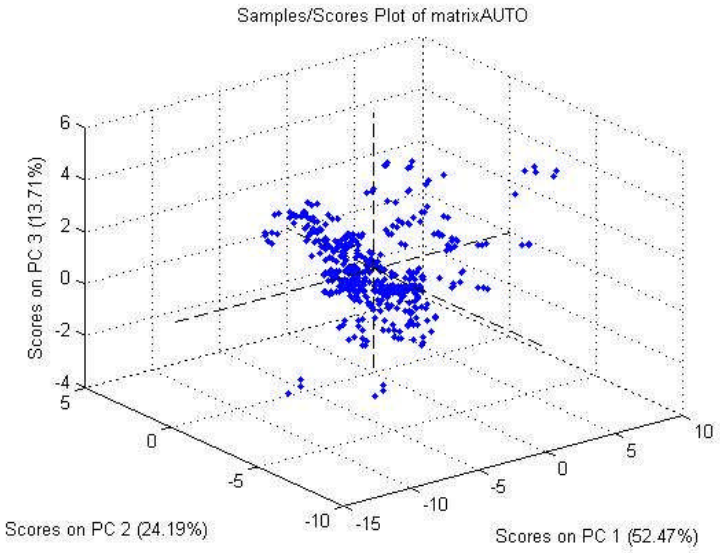

Figure 59B: Illustrates principle component 1 against 2 against 3 (PC 1 to 3, others possible) and illustrates variation due to both PCs as a scatter plot. Loadings can be obtained as well (not shown).

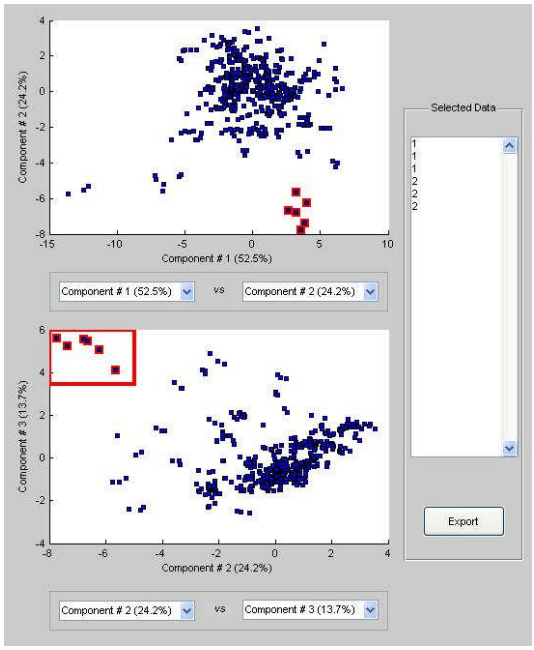

Figure 60: 2D PCA tool for a fast identification of data points in a scatter plot and an overview and comparison of PCA-scatter plots.

Papers published as a first author